United States Department of Agriculture

# Historical Forest Structure, Composition, and Spatial Pattern in Dry Conifer Forests of the Western Blue Mountains, Oregon

Derek J. Churchill, Gunnar C. Carnwath, Andrew J. Larson, and Sean A. Jeronimo

Forest Service

Pacific Northwest Research Station

General Technical Report PNW-GTR-956

November 2017

## Authors

**Derek J. Churchill** is a research scientist and **Sean A. Jeronimo** is a Ph.D. candidate, School of Environmental and Forest Sciences, College of the Environment, University of Washington, Seattle, WA 98195; **Gunnar C. Carnwath** is a vegetation specialist, U.S. Department of Agriculture, Forest Service, Pacific Northwest Region, Custer Gallatin National Forest, Bozeman, MT, 59715 and **Andrew J. Larson** is an associate professor, Department of Forest Management, College of Forestry and Conservation, University of Montana, Missoula, MT 59812.

Cover photo: Snag at Umatilla Breaks in Oregon on the Umatilla National Forest, USDA Forest Service.

## Abstract

**Churchill, Derek J.; Carnwath, Gunnar C.; Larson, Andrew J.; Jeronimo, Sean A. 2017.** Historical forest structure, composition, and spatial pattern in dry conifer forests of the western Blue Mountains, Oregon. Gen. Tech. Rep. PNW-GTR-956. Portland, OR: U.S. Department of Agriculture, Forest Service, Pacific Northwest Research Station. 93 p.

In frequent-fire forests of the interior Western United States, historical (prefire suppression) conditions are often used as a reference to set management objectives, guide prescriptions, and monitor treatment effectiveness. We quantified the historical size, density, composition, and spatial patterns of dry mixed-conifer forests in the Blue Mountains of Oregon to establish reference conditions that could be used for ongoing forest-restoration efforts. In total, 14 reconstruction plots ranging from 2.3 to 5.0 ha were established, with plots located on ponderosa pine (*Pinus ponderosa* Lawson & C. Lawson), Douglas-fir (*Pseudotsuga menziesii* (Mirb.) Franco), and grand fir (*Abies grandis* (Douglas ex D. Don) Lindl.) potential vegetation sites. Within each plot, all historical structures—live trees, snags, and logs that were alive in 1890—were mapped, and 1890 diameters were reconstructed. Historical structure and composition on the 14 plots consisted of an open canopy, uneven-aged mosaic of widely spaced individual trees, tree clumps, and openings dominated by large trees. Mean values for historical tree density of trees greater than 15 cm diameter at breast height (d.b.h.) ranged from 53 to 197 trees per hectare, and basal area ranged from 11 to 24 $m^2 \cdot ha^{-1}$. Basal area varied widely across each plot, and the mean value was not representative of the density in the majority of the plot in almost all cases. Mean tree diameter ranged from 35.2 to 57.8 cm, with over 50 percent of the basal area composed of trees greater than 50 cm d.b.h. Species composition was dominated by ponderosa pine on plots within the ponderosa pine and Douglas-fir series. Grand fir was abundant on three of the four plots within the grand fir series, comprising 44 to 48 percent of the basal area on these three plots. The proportion of historical trees occurring as widely spaced individuals (no neighbors within 6 m) ranged from 0.53 to 0.10. Ten of 14 plots had large tree clumps (10 to 15 trees) or very large clumps (16 to 30 trees), with the proportion of trees in these clumps ranging from 0.05 to 0.43. The proportion of the plot area in large openings ranged from 0.15 to 0.72, with most openings being sinuous and linear in shape and ranging from 18 to 45 m across. The range of conditions presented in this reference dataset provides managers flexible targets that can be used to guide restoration of variable conditions within and across treatment units. When using the dataset to inform prescription development, we recommend first determining the target stem density appropriate for the site and then selecting a clumping level to help guide the spatial pattern to be created through restoration treatment. Management objectives, current conditions, biophysical conditions, and anticipated future disturbance and climate change can then be considered when setting targets for density and clumping. This reference information can also be used to monitor the extent to which treated stands are within the ranges of size, density, composition, and pattern quantified in this study.

Keywords: Restoration, dry forests, spatial pattern, reference conditions.

# Contents

# Chapter 1: Introduction and Background

Three essential elements of forest ecosystems are structure, composition, and function. Structure includes the size, density, and spatial arrangement of live and dead vegetation. Structure and composition interact to regulate ecosystem function (Franklin et al. 2002), including feedbacks with disturbance processes such as fire (Noss et al. 2006). Presently, management objectives for dry, mixed-conifer forests on federal lands in the interior Western United States emphasize restoration of structure and composition consistent with the historical range of variability (HRV), promotion of resilience and adaptive capacity, and forest conditions that foster primarily low-severity fire effects (CFLRP 2012; USDA FS 2012, 2014). To meet these objectives, managers often use reference conditions, such as those provided by estimates of HRV, to develop understanding of system functioning and to guide development and evaluation of treatments (Hagmann et al. 2014, Moore et al. 1999, Reynolds et al. 2013, Stine et al. 2014) The HRV concept applies to contemporary management aimed not only at ecosystem restoration, but also at increasing resilience and climate change adaptation (Keane et al. 2009, Seidl et al. 2015, Stephens et al. 2010). When used in the framework of climate analog conditions or the future range of variability (Gärnter et al. 2008, Stine et al. 2014)—reference sites with climate conditions similar to the projected future climate regime of the project area—historical reference conditions provide defensible, transparent data that can be used to inform treatment design and monitoring (Churchill et al. 2013, Hessburg et al. 2013).

The rationale for using reference conditions to guide management targets in dry forests is that historical forest conditions persisted through centuries of frequent disturbances and significant climatic fluctuation while sustaining native biodiversity and other ecosystem services (Fule 2008, Hessburg et al. 2015, Jackson and Hobbs 2009, Keane et al. 2009, Swetnam et al. 1999). The mechanistic links between the structure and composition of historical forest conditions and their resilience have been the topic of much recent research (Agee 2005, Peterson et al. 2011, Reynolds et al. 2013, Stephens et al. 2010). The importance of structure dominated by large and old trees, and composition dominated by fire and drought-tolerant species has been well established (Agee and Skinner 2005, Franklin et al. 2013, Jain et al. 2012, Lutz et al. 2012, Powell 2014, Stine et al. 2014). Here we highlight a number of the mechanisms in which the spatial pattern of these forests engenders resilience:

- The complex network of openings in frequent-fire forests is thought to inhibit the spread of crown fires by forcing crown fires back to the ground when flareups occur (Beaty and Taylor 2007, Parisien et al. 2010, Pimont et al. 2011, Stephens et al. 2010, Thaxton and Platt 2006). These openings also impede the buildup of epidemic insect outbreaks by disrupting pheromone plumes (Fettig et al. 2007).
- Large openings and dense patches create variability in light, moisture, and soil nutrient environments that increases understory plant abundance and diversity (Dodson et al. 2008, Gundale et al. 2006, North et al. 2005).
- The contrast of dense patches of tree clumps and openings provides the diversity of habitat conditions needed by many species of birds and small mammals (Buchanan et al. 2003, Dodd et al. 2006, Latif et al. 2015, Long and Smith 2000).
- A variable spatial pattern facilitates frequent and patchy regeneration that creates a multiaged tree structure and a continuing flow of replacement trees. Frequent pulses of regeneration may contribute to high levels of within-stand genetic diversity of trees found in dry forests (Hamrick et al. 1989, Linhart et al. 1981).
- Variable overstory tree arrangements generate variation in litter accumulation that, in combination with a patchy understory of tree seedlings, saplings, herbs, forb, and shrubs, creates variability in surface fuel beds conditions (Fry et al. 2014, Fry and Stephens 2010, Gundale et al. 2006, Hiers et al. 2009, Thaxton and Platt 2006).

Reference information and guiding principles have been established for ecosystem restoration of many frequent-fire forest systems in the Western United States (Allen et al. 2002, Franklin et al. 2013, Hessburg et al. 2005, Jain et al. 2008, Kaufmann et al. 2007, Peterson et al. 2005, Powell 2014, Reynolds et al. 2013, Stine et al. 2014). However, the availability of reference information for spatial pattern was limited until relatively recently, and in some regions, still is. Larson and Churchill (2012) conducted a comprehensive literature review and found only 25 studies reporting reference spatial information, with most data coming from sites in southwestern ponderosa pine forests, Sierra Nevada mixed-conifer forests, and Cascadian mixed-conifer forests in central Oregon and Washington. Reference spatial information was conspicuously limited for dry mixed-conifer forests of the Rocky Mountain region and the Blue Mountains of eastern Oregon and southeastern Washington (Larson and Churchill 2012). Several new studies have begun to fill these gaps (Churchill 2013, Fry et al. 2014, Hopkins et al. 2014, Lydersen et al. 2013, Schneider et al. 2015), but spatial reference information specific to the Blue Mountains is not available.

The purpose of this study is to quantify the historical structure and composition of dry mixed-conifer forests in the Blue Mountains of Oregon. Addressing the absence of historical spatial pattern information is a primary objective. The analyses and results reported here were designed to facilitate the use of reference information in guiding development of silvicultural prescriptions, marking guidelines, and treatment monitoring. We sought to define and report ranges of conditions in order to provide managers with flexible targets that can be used to guide restoration treatments within and across treatment units.

The reference information can be incorporated into a variety of implementation approaches (e.g., Graham et al. 2007, Knapp et al. 2012, North and Sherlock 2012, Powell 2012). The results are especially suited to using the individuals, clumps, and openings (ICO) silvicultural and monitoring approach to quantifying spatial pattern developed by Churchill et al. (2013). Detailed implementation guidelines for using the ICO method are provided in Churchill et al. (2014), including examples of how to use the reference data presented in this report.

We also wanted to improve understanding of the factors that shaped and maintained forest development and patterns on these sites. Specifically, we sought to determine if tree density and tree spatial patterns differed along a gradient of moisture and productivity as indicated by potential vegetation series (the ponderosa pine, Douglas-fir, and grand fir potential vegetation series) within the warm dry upland forest plant association group (sensu Powell et al. 2007). In earlier work and review of the literature, we noticed that historical tree density and spatial pattern seemed to vary systematically across environmental (e.g., moisture) gradients, with moister sites supporting higher tree densities, and a greater proportion of trees occurring as members of closely spaced tree clumps (Churchill 2013, Larson et al. 2012). However, higher tree densities and greater clumping have not been found on more productive sites in other studies of historical conditions in dry mixed-conifer forests (Hagmann et al. 2014, Merschel et al. 2014, Reynolds et al. 2013, Schneider et al. 2015) We hypothesized that grand fir sites historically supported higher tree densities with more, larger tree clumps, and that ponderosa pine series sites historically had the lowest stem densities with fewer, smaller clumps.

A secondary objective of this study was to compare current to historical density and composition. Although increases in density relative to historical conditions have been widely reported for dry forests (Covington and Moore 1994, Hagmann et al. 2013, Harrod et al. 1999, Hessburg et al. 1999, Lydersen et al. 2013, Reynolds et al. 2013, Sánchez Meador et al. 2009, Stine et al. 2014) some recent studies claim that forest density has not increased in the Blue Mountains and other portions of the West (Williams and Baker 2012).

# Chapter 2: Methods

## Study Area Description

This study was conducted on the southern Malheur National Forest within the Blue Mountains physiographic province of eastern Oregon. The climate is characterized by warm summers and cold winters. The majority of precipitation falls as snow with significant rain in the spring. Summers are generally very dry, though thunderstorms are common in July and August. The closest recording National Climate Data Center station in Seneca, Oregon, shows an average of 35 cm a year of precipitation between 1981 and 2010. Mean maximum temperature for July and August during this period was 27 °C, while mean minimum temperature during January and December was -11.5 °C. Because of its proximity to the Blue Mountains, climate conditions in Seneca should be a fair approximation for the study area.

Sampling occurred in two primary areas: Dugout Creek Research Natural Area (RNA) and Canyon Creek RNA (fig. 2.1). These sites were chosen because they contain large, contiguous patches of the desired plant communities that have experienced little to no commercial logging or other management actions. Environmental information for RNA study sites is based on the Natural Area Establishment Reports (http://www.fsl.orst.edu/rna).

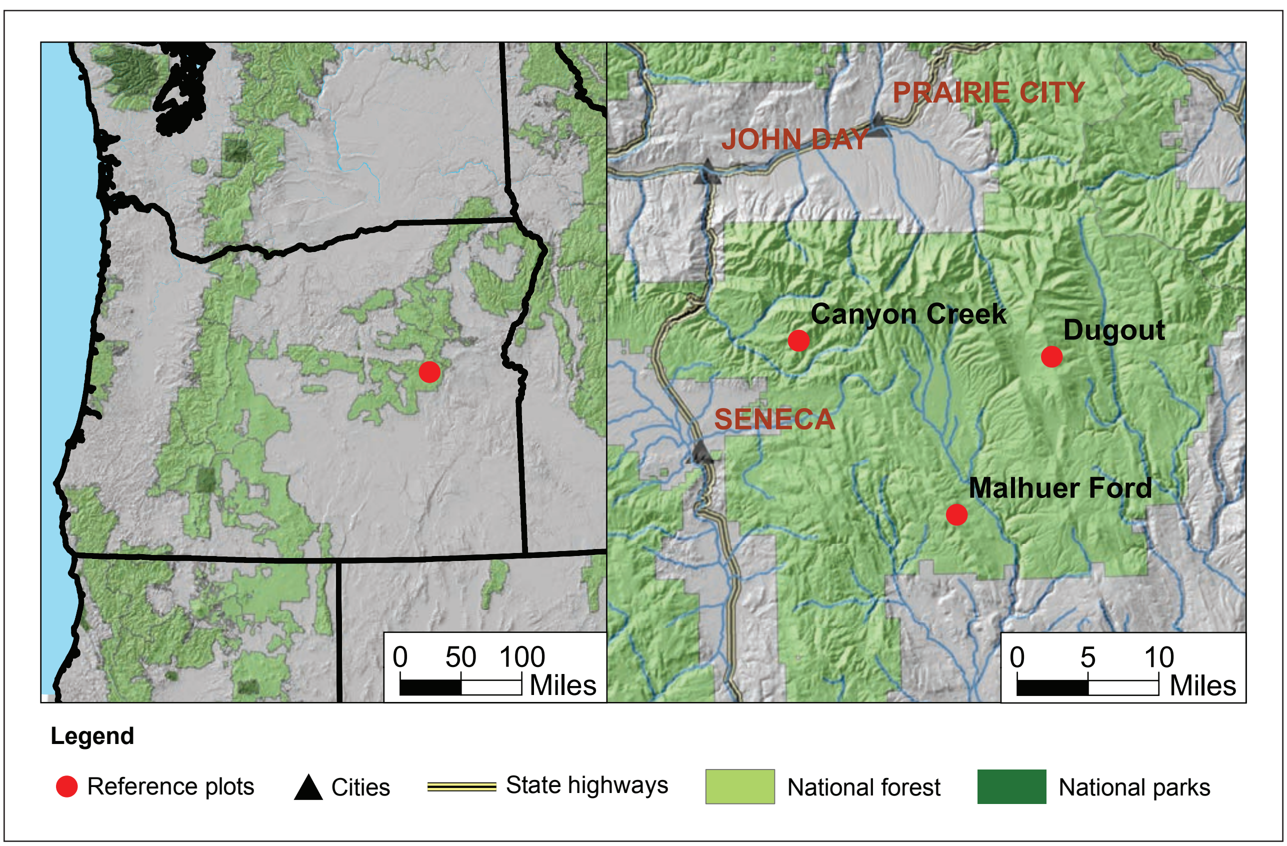


Figure 2.1—Reference plots in the Malheur National Forest.

The 350-ha Dugout Creek RNA was established to represent a ponderosa pine (*Pinus ponderosa* Lawson & C. Lawson) community with pinegrass (*Calamagrostis rubescens* Buckley) and elk sedge (*Carex geyeri* Boott), and a grand fir (*Abies grandis* (Douglas ex D. Don) Lindl.) community with pinegrass. The elevation of Dugout RNA ranges from about 1500 to 1750 m with moderately steep, west-facing slopes reaching down to the North Fork Malheur River. There are several small drainages within the RNA that flow in shallow ravines, including Dugout Creek and Stink Creek. The upper portion of the RNA consists of a large bench with generally open scablands. The undulating terrain of the lower slope is covered with deep soils and ponderosa pine/elk sedge, ponderosa pine/pinegrass, and grand fir/pinegrass communities. The area is broken by several ancillary ridges with generally shallow soils and stands of mountain mahogany (*Cercocarpus* spp.). The overstory of the forested area is generally dominated by large-diameter (up to 1.5 m) ponderosa pines with a mixture of ponderosa pine, grand fir, and Douglas-fir (*Pseudotsuga menziesii* (Mirb.) Franco)) in the understory. Western larch (*Larix occidentalis* Nutt.) occurs as a minor overstory component, primarily in the grand fir communities. The herbaceous vegetation is usually dominated by either elk sedge or pinegrass, indicating different plant associations (sensu Johnson and Clausnitzer 1992).

The 283-ha Canyon Creek RNA was established to represent unmanaged dry forest ecosystems in the Blue Mountains of central and northeastern Oregon. The Canyon Creek RNA is located within the southwestern corner of the Strawberry Wilderness Area. The RNA is generally south and east facing with a gentle slope rising from 1400 m at Canyon Creek to moderately steep ridges on the northern and western edges at approximately 1800 m. Ponderosa pine is the most common tree species throughout the RNA. Douglas-fir and grand fir become increasingly dominant with increasing elevation. Soils are variable but generally consist of residual andesitic soils with patches of colluvial and residual granitic soils. Strawberry (*Fragaria* spp.), heartleaf arnica (*Arnica cordifolia* Hook.), and grouseberry (*Vaccinium scoparium* Leiberg ex Coville) are common understory species at higher elevations with pinegrass and elk sedge dominating closer to Canyon Creek. On more open areas of the RNA, western juniper (*Juniperus grandis* R.P. Adams) and mountain mahogany are found along with bluebunch wheatgrass (*Pseudoroegneria spicata* (Pursh) Á. Löve ), and Sandberg bluegrass (*Poa secunda* J. Presl).

## Site Selection

This study focused on describing historical conditions within the warm-dry upland forest (UF) plant association group (PAG) as defined by Powell et al. (2007). The warm dry UF PAG represents a collection of finer scale potential vegetation types (PVTs) that are similar to each other within a temperature-moisture matrix. The biophysical environments delineated by the individual plant associations within the warm dry PAG are described in Johnson and Clausnitzer (1992).

To capture the full range of environmental conditions that occur within the warm dry UF PAG, we stratified our sampling design based on the potential vegetation series. The series indicates the dominant climax plant species within a particular PVT (sensu Johnson and Claustnitzer 1992). For example, the grand fir series includes every PVT where grand fir is presumed to be the dominant tree species at climax. Within the warm dry UF PAG, there are three primary climax series: ponderosa pine, Douglas-fir, and grand fir.

Within each potential vegetation series, we selected five plots to characterize historical conditions. Plot locations were determined by overlaying a modeled potential vegetation layer over the boundaries of Dugout and Canyon Creek RNAs using ArcGIS 10.1. The Create Random Points Tool was used to generate coordinates for 15 random points in each of the three potential vegetation series within the warm-dry UF PAG. Each point was numbered sequentially within each potential vegetation series (e.g., DF01-DF15, GF01-GF15, and PP01-PP15).

Random points were visited in the field in sequential order to determine their suitability for sampling. Criteria for site selection included (1) desired PAG and potential vegetation series (as determined in the field), (2) no or minimal evidence of previous management, (3) fairly homogenous slope and aspect with no major edaphic or topographic variation, and (4) no evidence of fire or other major disturbances since 1890. If a site was deemed suitable, it was accepted and subsequently sampled. If a site was deemed unsuitable because the potential vegetation series was incorrect but all other criteria were met (i.e., an error in the PVT map), it was designated as an alternate site for the series to which it actually belonged. For example, if "GF01" was a suitable sampling site but was actually a Douglas-fir climax area, it would become the first alternate site to sample in the event that a Douglas-fir site had to be rejected.

Owing to a lack of suitable sites within the ponderosa pine series at Dugout and Canyon Creek RNAs, we added one additional sampling site in a nearby area known as the Malheur Ford. The Malheur Ford sampling area is located at the confluence of Black Canyon Creek and the Malheur River (fig. 2.1), and contains significant areas of unlogged, pure ponderosa pine forests. Two of the ponderosa pine series plots were located in this area using the protocol described above.

In total, 14 plots were established, with 8 in the Dugout Creek RNA, 4 in the Canyon Creek RNA, and 2 at Malheur Ford (table 2.1). Target plot size was 4 ha, as past reconstructions in dry forests have shown that 4 ha is a good threshold to capture gaps (Churchill 2013) in open canopy dry forests. Plots were square except where short slopes or complex topography required rectangular plots. Plot size was expanded where possible to capture additional area and to account for additional edge in rectangular plots. Actual plot size ranged from 3.8 to 5.0 ha for 13 of the 14 plots. The size of the 14$^{th}$ plot was reduced to 2.3 ha owing to very high density and time constraints. In total, five plots totaling 21.6 ha were located on ponderosa pine series, five plots totaling 20.6 ha on Douglas-fir series, and four plots totaling 15.6 ha on grand fir series. A fifth plot in the grand fir series was not installed owing to time constraints. Historical structures within a 10-m buffer around each plot were included in the mapping to reduce edge effects on spatial pattern analysis results.

**Table 2.1—Biophysical and location data for 14 plots**

| Plot | Location[a] | Plant association[b] | Plot size | Elevation | Aspect | Avg. slope | Plot type |
|---|---|---|---|---|---|---|---|
| | | | *Hectares* | *Meters* | | *- Percent -* | |
| P1 | Dugout RNA | PIPO/CAGE | 4.7 | 1699 | SW | 25 | Stem map |
| P2 | Dugout RNA | PIPO/CARU | 4.4 | 1760 | SW | 3 | Stem map |
| P3 | Canyon Creek RNA | PIPO/CARU | 4.1 | 1561 | SW | 30 | Quick map |
| P4 | Malheur Ford | PIPO/CARU | 4.4 | 1545 | SW | 4 | Stem map |
| P5 | Malheur Ford | PIPO/CARU | 4.0 | 1561 | SW | 15 | Stem map |
| D1 | Dugout RNA | PSME/CARU | 3.8 | 1649 | W | 30 | Stem map |
| D2 | Dugout RNA | PSME/CAGE | 4.2 | 1579 | NW | 30 | Stem map |
| D3 | Canyon Creek RNA | PSME/CARU-VASC | 4.1 | 1490 | SE | 15 | Stem map |
| D4 | Dugout RNA - North | PSME/CARU | 4.3 | 1615 | W | 25 | Quick map |
| D5 | Dugout RNA - North | PSME/CAGE | 4.1 | 1689 | W | 25 | Stem map |
| G1 | Dugout RNA | ABGR/CARU | 5.0 | 1740 | N | 20 | Stem map |
| G2 | Dugout RNA | ABGR/CARU | 4.0 | 1675 | N | 30 | Stem map |
| G3 | Canyon Creek RNA | ABGR/CARU | 2.3 | 1661 | E | 20 | Stem map |
| G4 | Canyon Creek RNA | ABGR/CAGE-VASC | 4.3 | 1704 | E & S | 15 | Quick map |

[a] RNA = research natural area.
[b] PIPO = *Pinus ponderosa*, CAGE = *Carex geyeri,* CARU = *Calamagrostis rubescens*, PSME = *Pseudotsuga menziesii*, VASC = *Vaccinium scoparium*, ABGR = *Abies grandis*.

Tree clumps that extended past the buffer were also noted. The four corners of each plot were spatially referenced by global positioning system (GPS). One corner of each plot was monumented with rebar and referenced to a witness tree, except for plots in Canyon Creek on account of wilderness area regulations.

## Field Methods

All historical structures—live trees, snags, and logs that were believed to have been alive and greater than breast height in 1890—were mapped in the 14 plots. The reference year of 1890 was chosen based on the finding by Heyerdahl et al. (2001) size, season, and severity from fire scars and establishment dates of 1,426 trees sampled on grids in four watersheds (similar to 64 plots, over similar to 1620 ha each that this was the last fire year in the area before fire exclusion began. Bark and crown characteristics were used to determine if live trees were historical (>123 years, breast height age) using guidelines from Van Pelt (2008). Trees whose historical status was questionable were cored at breast height. Cores where age was not easily discernible in the field were analyzed in the lab using techniques described below. Decay class, combined with diameter at breast height (d.b.h.), was used to estimate whether snags and logs were live trees in 1890 using methods from Everett et al. (2007).

Tree locations were recorded in one of two ways: stem maps (11 plots) and "Quickmaps" (3 plots). For the 11 stem map plots, each tree was mapped using a total station survey instrument on a single closed-loop traverse (Nathanson et al. 2006). In total, 10 to 20 survey stations were established on each plot from which the distance and angle to each tree, snag, or log was measured within the total station. On the remaining three plots—one plot in each potential vegetation series—a new method to map spatial pattern was used. This method, termed "Quickmapping," was designed to reduce the time required to obtain sufficiently accurate spatial data needed to quantify stand-level spatial pattern. Mapping is done on the basis of tree clumps rather than discrete trees (Churchill et al. 2013). First, clumps of historical structures are identified in the field using a 6-m limiting distance from tree center to tree center (see section 2.6 for more information on clump delineation). Clumps are sequentially numbered and clump membership is recorded for each historical structure. Structures with no neighbors within 6 m are termed individuals. A GPS point is recorded at the center of each clump, or adjacent to the bole for individuals. For each clump the following characteristics are recorded: shape (circle, oval, or line), size (radius for circles, major and minor axes for ellipses, length for lines), and azimuth for lines and major axes. For large (more than five trees), irregularly shaped clumps, a boundary line is also recorded with a GPS in addition to the clump center.

For this project, a minimum of 50 GPS locations were averaged for each point using a Trimble GEO XT[1] with an external Hurricane antenna and differential correction.

For each live tree, we recorded species, d.b.h., age class, and vigor. Age class and vigor were determined using rating systems from Van Pelt (2008). A subset of live trees (15 percent, 60 to 100 live trees per plot) was sampled more intensively to determine age class distribution and develop growth regressions. One tree from each vigor class per species was randomly chosen at each survey station to ensure a random sample of live measure trees across species, diameters, and tree condition. Cores were taken at breast height and were saved in paper straws for laboratory analysis. For these live measure trees, we recorded three additional measurements in order to calibrate allometric equations and report height information: diameter at stump height (30 cm), height to live crown, and total tree height.

For each snag and log with evidence of having been alive in 1890, we recorded species, diameter, and decay class (Cline et al. 1980). Height was also recorded for snags. Although species was generally evident, some logs with advanced decay could not be identified. Because diameter measurement outside bark at breast height was not always possible, we measured either at stump height or breast height and either inside or outside bark. A few cut stumps were found on several plots and were treated as snags.

## Stem Map Reconstruction

Increment cores from 940 live measure trees were air dried, mounted, and sanded. Blocks of processed cores were scanned using an Epson Expression 11000XL scanner at 3,000 dots per inch. Ring widths and total rings to pith at breast height were measured from the digital images of each core using CooRecorder software (Larsson 2003). Cores were not cross-dated as radial growth was the primary metric of interest. The loss of accuracy in growth measurements from not cross-dating was deemed to be minimal after inspection of a large sample of the cores showed minimal number of missing rings. For cores with a missing pith, curvature of rings was used to estimate distance and number of rings to pith where possible using a tool within the CooRecorder software (Larsson 2003). This was not possible for all cores with missing piths resulting from rot. These cores were eliminated from the sample. Automated ring detection was used, but ring locations were visually checked for each core and corrected when necessary. The sample of "live measure trees" was used to develop growth regressions for diameter reconstruction, and also to generate an age class distribution for each plot in 50-year age classes.

---

[1] The use of trade or firm names in this publication is for reader information and does not imply endorsement by the U.S. Department of Agriculture of any product or service.

We followed methods of North et al. (2007) and Bakker (2005) to reconstruct outside bark d.b.h. in 1890 for all live trees on the plot. A regression model was built using the live measure trees to predict total inside bark basal area increment from 1890 to 2013, which was then used to estimate 1890 d.b.h. for all live trees. For snags and logs that were believed to be alive in 1890, a similar approach was used, but year of death had to be estimated using equations from Everett et al. (1999). A full description of diameter reconstruction methods and model results is provided in appendix 1.

Coordinates in local coordinate geometry were derived for each historical structure from survey data to generate stem maps for each plot. For the Quickmaps, a tool was built in ArcMap 10.1 to generate coordinates for each tree. The tool uses the recorded shape, size, and axies azimuth information for each clump to create a temporary shape (line, circle, oval). Trees within the clump are then randomly placed along the boundary of the shape, with minimum distance of 1.5 m apart. The line feature was used to outline large, irregular clumps. Geographic coordinates of trees were then converted and rotated to the same (0,0) grid as the stem maps.

For all plots, stem density, composition, and size distribution information was calculated from species and reconstructed diameter. Trees within the 10-m buffer were not counted in summary inventory metrics, nor was the buffer included in the final plot size. All trees less than 15 cm d.b.h. in 1890 were removed from the dataset and were not counted in structure and pattern metrics. Accurately reconstructing tree populations less than 15 cm is challenging because of the faster decay of small trees (Barth et al. 2015). Historical canopy cover was also estimated for each plot by projecting the crowns of all trees onto a stem map, calculating the two-dimensional area covered by crowns, and dividing by the total area of the plot. This spatially explicit method thus accounted for crown overlap between neighboring trees. Crown projections were based on d.b.h. to crown radius models developed from U.S. Forest Service Current Vegetation Survey plots from the Blue Mountains and eastern Washington (see app. 2 for more information on these models).

## Current Conditions

To assess the change in density and species composition from 1890 to 2013, five 0.04-ha fixed-area plots were installed in 6 of the 14 stem-mapped plots, all within the Dugout RNA. Two stem-mapped plots from each potential vegetation series were selected. All live trees and snags greater than 15 cm d.b.h. were measured and tallied within each fixed-area plot. The fixed-area plots were located on a systematic grid within each stem-mapped plot.

## Spatial Pattern Analysis

We quantified spatial patterns in terms of widely spaced individual trees, tree clumps, and openings using three metrics: (1) a clump identification algorithm from Plotkin et al. (2002), (2) the empty space distribution (Diggle 2003), and (3) opening sizes using a new delineation approach. The clump algorithm partitions a stem map of tree locations into clumps at a specified intertree distance (*t*), measured from tree center to tree center. Trees are members of the same clump if they are within distance *t* of at least one other tree in the clump. Trees with no neighbors within distance *t* are termed individuals.

The clump algorithm can be used in two ways: a single intertree distance threshold, or crown radius modeled from allometric equations. For the single-distance method, trees are part of the same clump if they are within the threshold distance. This distance is based on the average distance at which mature trees of the dominant species in the study area display interlocking crowns. When using modeled crown radius, trees are members of the same clump if their projected crowns intersect. The crown radius method is a more accurate description of which trees have interlocking canopies (Fry et al. 2014, Lydersen et al. 2013). However, the single distance is faster and less subjective to use in the field and easier to translate into management guidelines (Churchill et al. 2013).

As the primary purpose of this study was to generate reference conditions for management, we chose to use a single intertree distance to delineate clumps. We selected a threshold of 6 m based on the observed distance at which most mature and old ponderosa pine trees (>120 years) in our study have interlocking crowns. This method has been previously used to identify tree clumps in frequent-fire forests using the same or very similar distances (Abella and Denton 2009, Churchill et al. 2013, Sánchez Meador et al. 2011).

The number of clumps of different sizes, measured in numbers of trees, was then tabulated and converted to a clump size distribution. This distribution summarizes the percentage of trees arranged as individuals and in clumps of different sizes. To facilitate translation to management guidelines, clump sizes were also reported in bins: individuals (1 tree), small clumps (2 to 4 trees), medium clumps (5 to 9 trees), large clumps (10 to 14 trees), and super clumps (15 to 30+ trees) based on functional differences (e.g., understory shading, number of interior trees) (Churchill et al. 2013). The proportion of basal area in each clump size bin and the quadratic mean diameter of trees in each clump size were derived. The proportion of trees and basal area in these five bin sizes was also generated for intertree distances of 3, 4, 5, and 7 m should managers want to select a different threshold distance to define clumps. A 10-m distance was also included to provide information on the proportion of widely spaced trees. We also generated clump size distributions at 6 m for all trees >10 cm (app. 3).

Open space in low-canopy-cover forests is difficult to quantify as it typically does not occur in clearly definable canopy gaps. Instead, openings are the matrix or interspace component in which individual trees or clumps are distributed (Reynolds et al. 2013). Methods have been developed to delineate gaps in frequent-fire forests (see Lydersen et al. 2013), but require setting a distance on where gaps "close" or are pinched off. We found that a single distance does not work well for plots with varying tree densities and opening configurations; gap delineation ends up being quite arbitrary. Instead of focusing on gap delineation, we quantified openings based on the distance to the nearest tree. When standing in an open area (or anywhere in a plot), this is simply the distance to the nearest tree or gap edge. Many ecological processes such as regeneration and growth of shade-intolerant species  (York et al. 2004), insect spread (Fettig et al. 2007), and crown fire spread can be related to distance from the nearest tree. A similar concept is used in variable-retention harvesting to quantify the amount of area beyond the "tree influence zone," typically one tree height from a retention patch (Baker and Read 2011).

We quantified distance to the nearest tree using the empty space function, *F(t)*. This function quantifies what percentage of each plot is greater than a specified distance away from a tree (Diggle 2003). The function generates a grid of points across a plot, set to 0.5 m in our case, and then derives the distance from each point to its nearest tree. These distances are pooled to create a cumulative distribution that has no subjective settings and thus can be compared across plots. The function thereby quantifies the total amount of open area in a plot and distinguishes whether the total amount of opening is distributed in many small openings or fewer, larger ones. To facilitate use of *F(t)*, we converted the cumulative distribution into 3-m bins. A graphical plot of this function was created to visually assess the spatial distribution of cells in the 3-m bins across each plot.

We also choose a threshold distance to define what we consider to be open space in dry forests. We chose 9 m for several reasons: this distance is beyond where trees share resources across root and mycorrhizal networks (Simard et al. 2012), adequate for ponderosa pine regeneration and growth (York et al. 2004), and wide enough to impede spread of active crown fire in all but very extreme fire weather (Peterson and Johnson 2007, Powell 2010). The percentage of plot area greater than 9 m away from a tree was then derived, which is the total open space that is at least 18 m across.

We then delineated large openings within each plot based on the 9-m threshold. First, polygons were created for all areas greater than 9 m away from a tree. Each polygon was then buffered by 5 m to expand the polygon to within 4 m of tree piths. The distance of 4 m was chosen as this was determined to be the average distance for which crowns of mature trees in these plots extend into openings. Intersecting and adjoining polygons were then dissolved (merged) to form contiguous polygons. The area for each polygon was derived in order to generate an opening size distribution and percentage of the plot in large openings.

We used a similar edge correction method (Sanchez Meador et al. 2011) for all spatial analyses, but with some important differences. Here, the cluster algorithm was run using the plot and 10-m buffer. We then used a reduced sample edge correction in which all trees in the buffer are dropped from the tree list. However, the clump sizes of the trees within the plots still reflect the trees in the buffer that were dropped. Where clumps extended past the buffer, the total clump size noted in the field was used. For example, for a 12-tree clump with five trees inside the plot, five trees in the buffer, and two trees outside the buffer, the five trees in the plot would be tabulated as being part of a 12-tree clump. We used the same edge correction approach for the empty space function. F*(t)* was first run for the plot and buffer zone. We then removed the grid points in the buffer zone from the F(*t*) distribution. Large openings were cut off at the 10-m plot buffer.

Two additional spatial pattern metrics were calculated. We measured the distribution of basal area and trees per hectare across each stem map using circular 0.04- and 0.08-ha fixed-area plots, plus variable-radius plots with a 4.6-basal area factor (20 BAF). Plots were simulated on a square grid every 20 m on the computer. We derived the pair correlation function, g(*t*), for each plot to determine if they were statistically different from a random pattern, either clumped or uniformly spaced. This information permits inferences as to the nature of the processes that are creating the observed patterns. This analysis also allowed us to compare our results to other studies of reference spatial patterns (Larson and Churchill 2012). The pair correlation function is commonly used in analysis of tree patterns to investigate whether there is a nonrandom process creating patterns and to better understand the processes driving patterns (Fortin and Dale 2005, Larson and Churchill 2012, Perry et al. 2006). The g(*t*) function is a noncumulative form of Ripley's *K(t)* (Ripley 1988). We first tested for overall departure from complete spatial randomness from 0.1 to 30 m using the Cramer–von Mises goodness-of-fit test from Loosmore and Ford (2006) with *g(t)* for each plot. The g(*t*) curves were then compared with 1,000 random patterns (complete spatial randomness) to assess distances at which patterns where clumped, random, or inhibited. We used an isotropic (Ripley 1988) edge correction for all g(*t*) tests.

## Assessing Relationships Among Pattern, Density, and Potential Vegetation Series

We assessed differences in pattern types among potential vegetation series in two ways. First, we sorted the plots by the proportion of trees occurring as individual trees and visually examined the results to see the extent to which the plots sorted by vegetation series. Next, we used PERMANOVA, which is a nonparametric permutation version of ANOVA (Anderson 2001), to test for overall statistical differences in clump size distributions among vegetation series. We ran PERMANOVA using a distance matrix of the proportions of trees in each plot in the five clump bins: individuals (1 tree), small clumps (2 to 4 trees), medium clumps (5 to 9 trees), large clumps (10 to 14 trees), and super clumps (15 to 30+ trees). Contrast Tests and PERMANOVA were then used to test for differences between each pair of potential vegetation series (see Churchill [2013] for a full description of this method).

To facilitate translation of the pattern results into marking guidelines, we grouped patterns into "low," "medium," and "high" levels of clumping using hierarchical cluster analysis with the distance matrix of binned clump size proportions (McCune and Grace 2002). We reported the mean values for proportions of trees in each clump size bin for the three clumping levels. Finally, we examined the relationship between pattern and tree density by calculating the mean clump size for each plot (Plotkin et al. 2002) and the total plot area greater than 9 m away from the nearest tree ($F > 9$). Tree density was quantified as trees per hectare.

# Chapter 3: Summary Results

Historical forest size, density, composition, and pattern information are summarized for all 14 plots in tables 3.1 through 3.4 and figs. 3.1 through 3.6. In addition, more detailed information and a stem map are provided for each plot in chapter 4. Model information and results for diameter reconstruction methods are provided in appendix 1.

## Structure, Density, Composition, and Age

Basic forest structure information was compiled for all 14 plots based on reconstructed diameters. A wide range of tree densities was found, ranging from 53 to 197 trees per hectare (tph) (table 3.1). Basal area ranged from 11.1 to 24.2 $m^2 \cdot ha^{-1}$. Mean diameters ranged from 35.2 to 57.8 cm, and Stand Density Index ranged from 183 to 415 (metric). In all plots except for G2, well over 50 percent of the basal area was composed of trees greater than 50 cm diameter at breast height (d.b.h.) (fig. 3.1). Most plots had somewhat normal or log-normal shaped diameter distributions with the majority of trees in the 30- to 50-cm range (fig. 4.1 panel A). Density of trees 50 to 70 cm ranged from 20 to 40 tph. All plots had trees greater than 90 cm, but generally at a density level of less than five tph.

Species composition was entirely or heavily dominated by ponderosa pine (*Pinus ponderosa* Lawson and C. Lawson) on plots within the ponderosa pine and Douglas-fir series (fig. 3.1). Douglas-fir (*Pseudotsuga menziesii* (Mirb.) Franco) made up less than 10 percent of the basal area on plots within the Douglas-fir and grand fir series. Grand fir (*Abies grandis* (Douglas ex D. Don) Lindley), on the other hand, was abundant on three of the four plots within the grand fir series comprising 44 to 48 percent of the basal area on these three plots. Western larch (*Larix occidentalis* Nutt.) only was present on one of the plots within the Douglas-fir series and made up less than 10 percent of the basal area on plots within the grand fir series. Rocky mountain juniper (*Juniperus scopulorum* Sarg.), lodgepole pine (*Pinus contorta* Douglas ex Loudon), and mountain mahogany (*Cercocarpus* Kunth) were present in very small amounts, primarily in the Douglas-fir and ponderosa pine series (fig. 3.1). All plots had a wide range in ages of trees that were alive in 1890 (fig. 4.1 panel B). In 12 of the 14 plots, the sample of live measure trees included 400- to 500-year-old trees. The other two plots had 300-year-old trees. Tree establishment occurred relatively continuously in most plots, although some pulses are apparent in the Canyon Creek plots.

Current density (2013) was higher than historical density for all six plots that were sampled (fig. 3.2). Trees-per-hectare values increased by 41 to 460 percent, while basal area increased by 16 to 186 percent. This greater increase in tree density vs. basal area indicates that current mean diameters have decreased relative to historical conditions. The proportion of basal area in ponderosa pine decreased on the plots in the Douglas-fir and grand fir potential vegetation series (fig. 3.2).

**Table 3.1—Summary information for 14 historical reference plots on the Malheur National Forest (forest structure was reconstructed to 1890)**

| Plot | Plant series | Basal area | Trees | Average d.b.h. | QMD[a] | Max height | Canopy cover | Openings[a] | Basal area | Trees | Avg. d.b.h. | QMD[b] | SDIc[c] | Max height |
|---|---|---|---|---|---|---|---|---|---|---|---|---|---|---|
| | | $m^2/ha^{-1}$ | $Ha^{-1}$ | *cm* | | *m* | *Percent* | | $Ft^2/ac^{-1}$ | $ac^{-1}$ | - - - - *inch* | - - - - | | *ft* |
| P1 | PIPO | 13 | 65 | 46.9 | 50.2 | 37 | 15 | 62 | 56 | 26 | 18.5 | 19.8 | 86 | 120 |
| P2 | PIPO | 21 | 101 | 47.1 | 51 | 40 | 22 | 52 | 90 | 41 | 18.6 | 20.1 | 137 | 130 |
| P3 | PIPO | 19 | 103 | 46.1 | 48.8 | 41 | 20 | 54 | 84 | 42 | 18.1 | 19.2 | 131 | 133 |
| P4 | PIPO | 19 | 98 | 47 | 49.7 | 45 | 21 | 53 | 83 | 40 | 18.5 | 19.6 | 127 | 146 |
| P5 | PIPO | 19 | 94 | 47.4 | 50.1 | 41 | 21 | 51 | 81 | 38 | 18.7 | 19.7 | 124 | 134 |
| D1 | PSME | 14 | 59 | 51.1 | 54.6 | 41 | 16 | 72 | 61 | 24 | 20.1 | 21.5 | 91 | 134 |
| D2 | PSME | 14 | 79 | 43.4 | 48 | 40 | 18 | 53 | 63 | 32 | 17.1 | 18.9 | 98 | 130 |
| D3 | PSME | 14 | 87 | 41.7 | 44.6 | 44 | 18 | 49 | 59 | 35 | 16.4 | 17.5 | 94 | 144 |
| D4 | PSME | 13 | 64 | 47.2 | 50.6 | 37 | 15 | 67 | 56 | 26 | 18.6 | 19.9 | 86 | 120 |
| D5 | PSME | 22 | 74 | 57.8 | 61.3 | 37 | 23 | 62 | 95 | 30 | 22.8 | 24.1 | 137 | 119 |
| G1 | ABGR | 24 | 161 | 40.3 | 43.6 | 40 | 31 | 24 | 105 | 65 | 15.9 | 17.2 | 168 | 130 |
| G2 | ABGR | 23 | 197 | 35.2 | 38.3 | 41 | 33 | 15 | 99 | 80 | 13.9 | 15.1 | 165 | 135 |
| G3 | ABGR | 11 | 53 | 44.1 | 51.5 | 43 | 13 | 66 | 48 | 22 | 17.3 | 20.3 | 74 | 141 |
| G4 | ABGR | 20 | 122 | 41.8 | 45.3 | 43 | 25 | 40 | 85 | 49 | 16.5 | 17.8 | 135 | 142 |

Note: Data are for all trees >14.9 cm diameter at breast height (d.b.h.). Canopy cover is based on modeled crown widths.
[a] QMD = quadratic mean diameter.
[b] Stand density index (SDI) in English units. An exponent of 1.7 was used to calculate SDI.
[c] Percentage of plot in large openings. See section 2.6 for an explanation of how large openings were delineated.
PIPO = *Pinus ponderosa.*
PSME = *Pseudotsuga menziesii.*
ABGR = *Abies grandis.*

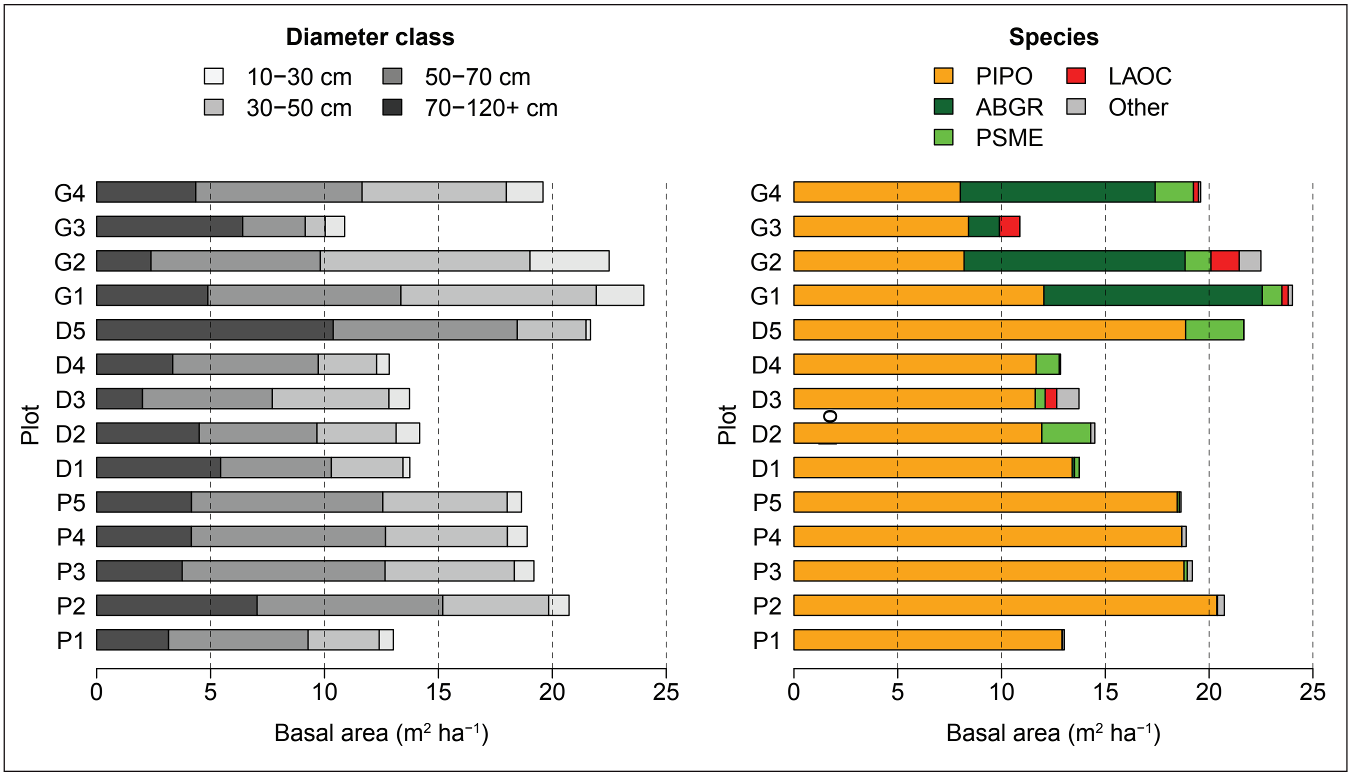


Figure 3.1—Left panel displays historical (1890) basal area in different size classes for 14 reference plots. Right panel displays breakdown of plot basal area by species. Other species include lodgepole pine, Rocky Mountain juniper, and mountain mahogany. PIPO = *Pinus ponderosa*, ABGR = *Abies grandis*, PSME = *Pseudotsuga menziesii*, LACO = *Larix occidentalis.*

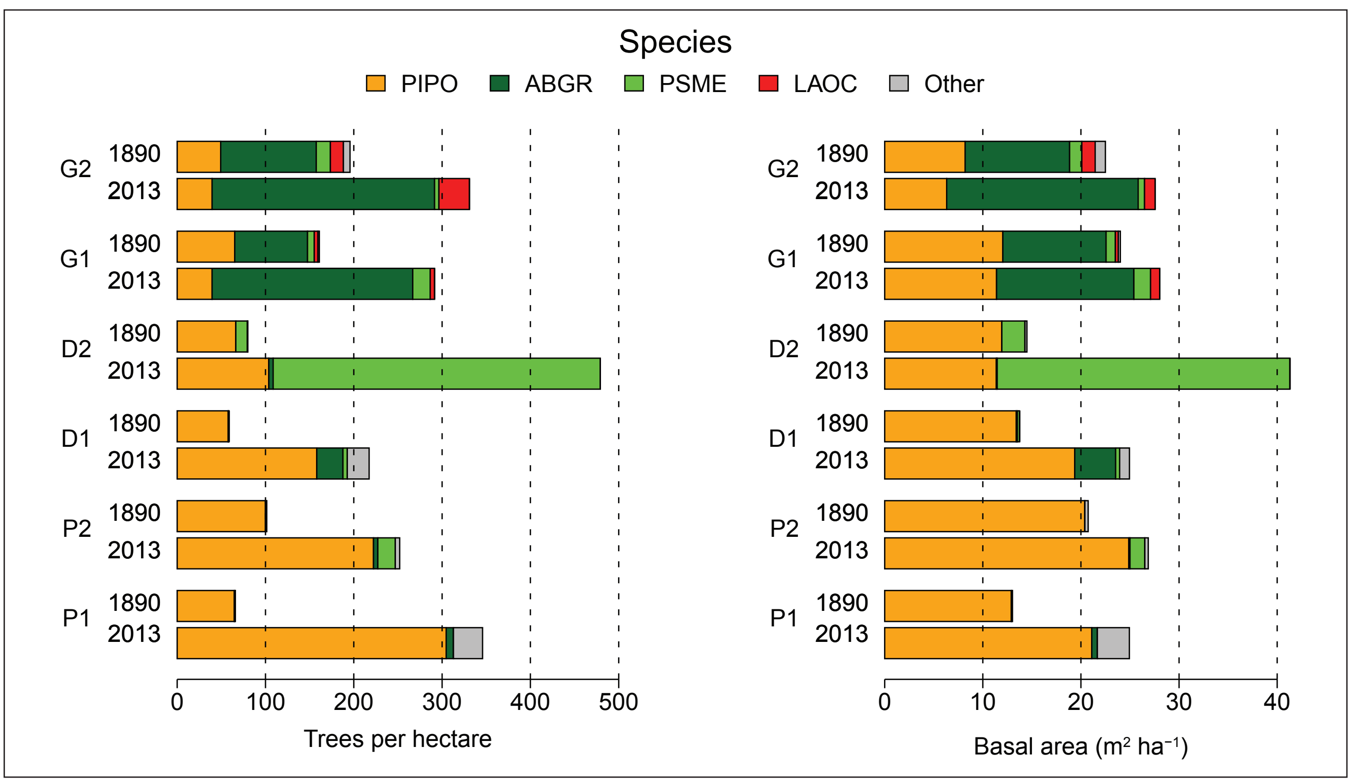


Figure 3.2—Current (2013) vs. historical (1890) density (left panel) and basal area (right panel) for 14 reference plots. Current information is from five 0.04-ha fixed-area plots installed in each historical stem map. PIPO = *Pinus ponderosa*, ABGR = *Abies grandis*, PSME = *Pseudotsuga menziesii*, LACO = *Larix occidentalis.* Other species include lodgepole pine, Rocky Mountain juniper, and mountain mahogany.

## Spatial Pattern

Clump size distributions were generated using an intertree distance of 6 m with the Plotkin et al. (2002) clump detection algorithm. The cumulative form of these distributions are shown in figure 3.3, while the values grouped into five clump-size bins are displayed in table 3.2. The proportion of individual trees ranged from 0.53 to 0.10. Ten of the plots had large clumps (10 to 15 trees), with the proportion of trees in large clumps ranging from 0.03 to 0.16. Five plots had super clumps (16 to 30+ trees) with proportions ranging from 0.05 to 0.27. The largest clump identified was 32 trees in plot G2. The proportion of basal area in different clump sizes was consistently higher for individual trees and lower for large and super clumps (table 3.2), indicating that individual trees and small clumps had larger diameter trees. Individual trees had mean QMD values of 45 to 70 cm (fig. 4.1 panel D), while the QMD of trees in large and super clumps was generally around 30 to 50 cm. However, large trees (>50 cm) did occur in large and super clumps.

**Table 3.2—Clump size distributions for Malheur National Forest reference plots ordered by the proportion of trees that are individuals (clump size = 1)**

| | | | Proportion of trees | | | | | Proportion of basal area | | | | |
|---|---|---|---|---|---|---|---|---|---|---|---|---|
| | | | Clump size (number of trees) | | | | | | | | | |
| Plot | Series | Clumping level | 1 | 2-4 | 5-9 | 10-15 | 16-30+ | 1 | 2-4 | 5-9 | 10-15 | 16-30+ |
| G3 | ABGR | Low | 0.53 | 0.34 | 0.04 | 0.08 | 0.00 | 0.68 | 0.26 | 0.02 | 0.03 | 0.00 |
| P1 | PIPO | Low | 0.38 | 0.49 | 0.13 | 0.00 | 0.00 | 0.46 | 0.47 | 0.07 | 0.00 | 0.00 |
| D2 | PSME | Low | 0.38 | 0.41 | 0.16 | 0.06 | 0.00 | 0.52 | 0.36 | 0.09 | 0.03 | 0.00 |
| D1 | PSME | Low | 0.36 | 0.42 | 0.11 | 0.11 | 0.00 | 0.50 | 0.39 | 0.06 | 0.06 | 0.00 |
| D4 | PSME | Low | 0.34 | 0.44 | 0.22 | 0.00 | 0.00 | 0.43 | 0.39 | 0.17 | 0.00 | 0.00 |
| D3 | PSME | Low | 0.34 | 0.42 | 0.24 | 0.00 | 0.00 | 0.36 | 0.45 | 0.19 | 0.00 | 0.00 |
| D5 | PSME | Low | 0.33 | 0.57 | 0.10 | 0.00 | 0.00 | 0.45 | 0.48 | 0.07 | 0.00 | 0.00 |
| P5 | PIPO | Moderate | 0.23 | 0.34 | 0.38 | 0.05 | 0.00 | 0.28 | 0.37 | 0.31 | 0.05 | 0.00 |
| P4 | PIPO | Moderate | 0.21 | 0.39 | 0.29 | 0.11 | 0.00 | 0.26 | 0.38 | 0.28 | 0.08 | 0.00 |
| P2 | PIPO | Moderate | 0.21 | 0.29 | 0.25 | 0.15 | 0.11 | 0.31 | 0.30 | 0.20 | 0.09 | 0.09 |
| P3 | PIPO | Moderate | 0.18 | 0.40 | 0.35 | 0.03 | 0.05 | 0.22 | 0.41 | 0.32 | 0.02 | 0.03 |
| G4 | ABGR | High | 0.17 | 0.33 | 0.22 | 0.11 | 0.18 | 0.25 | 0.33 | 0.19 | 0.10 | 0.14 |
| G1 | ABGR | High | 0.13 | 0.27 | 0.35 | 0.11 | 0.14 | 0.19 | 0.31 | 0.29 | 0.08 | 0.13 |
| G2 | ABGR | High | 0.10 | 0.20 | 0.27 | 0.16 | 0.27 | 0.14 | 0.23 | 0.27 | 0.15 | 0.22 |

[a] The clump size distribution is the proportion of trees or basal area by clump size. Clump size is the number of trees in a clump. Clumps are defined as trees within at least 6.1 m of another tree in the clump. Plots are grouped by plant series and clumping level. Clumping levels were derived using hierarchical cluster analysis. PIPO = *Pinus ponderosa,* PSME = *Pseudotsuga menziesii*, ABGR = *Abies grandis*

**Table 3.3—Clump size distributions from table 3.2 summarized by clumping level and plant association group[a]**

| | Proportion of trees | | | | | Proportion of basal area | | | | |
|---|---|---|---|---|---|---|---|---|---|---|
| | Clump size (No. of trees) | | | | | Clump size (No. of trees) | | | | |
| | 1 | 2-4 | 5-9 | 10-15 | 16-30+ | 1 | 2-4 | 5-9 | 10-15 | 16-30+ |
| Clumping level | | | | | | | | | | |
| Low | 0.38 | 0.44 | 0.14 | 0.04 | 0.00 | 0.49 | 0.40 | 0.10 | 0.02 | 0.00 |
| Moderate | 0.21 | 0.35 | 0.32 | 0.09 | 0.04 | 0.27 | 0.37 | 0.28 | 0.06 | 0.03 |
| High | 0.13 | 0.27 | 0.28 | 0.13 | 0.19 | 0.19 | 0.29 | 0.25 | 0.11 | 0.17 |
| Series: | | | | | | | | | | |
| PIPO | 0.24 | 0.38 | 0.28 | 0.07 | 0.03 | 0.30 | 0.39 | 0.24 | 0.05 | 0.02 |
| PSME | 0.35 | 0.45 | 0.17 | 0.03 | 0.00 | 0.45 | 0.41 | 0.12 | 0.02 | 0.00 |
| ABGR | 0.23 | 0.29 | 0.22 | 0.12 | 0.15 | 0.31 | 0.28 | 0.19 | 0.09 | 0.12 |

[a] Values are averages for that group.
PIPO = *Pinus ponderosa*, PSME = *Pseudotsuga menziesii,* ABGR = *Abies grandis.*

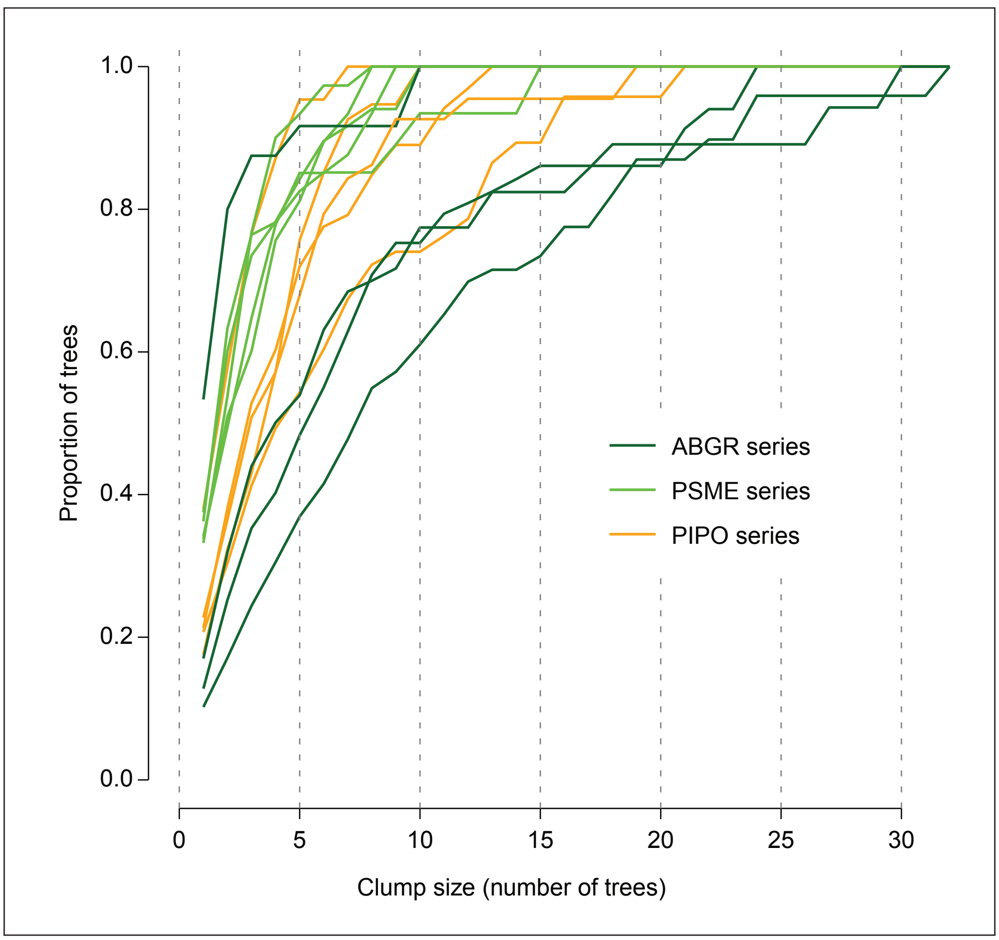


Figure 3.3—Proportional clump size distributions of 14 references plots from the Malheur National Forest. Each line represents one plot. ABGR = *Abies grandis,* PSME = *Pseudotsuga menziesii,* PIPO = *Pinus ponderosa.*

Plots were grouped into three clumping levels (high, moderate, and low) using hierarchical cluster analysis (table 3.3). The high clumping group had a relatively even proportion of trees in all clump sizes with 13 percent of trees as individuals and 19 percent in super clumps (table 3.3). The moderate clumping group was dominated by small and moderate clumps, with 21 percent as individuals, and 13 percent in large and super clumps combined. The low clumping group was dominated by small clumps and individuals, with 38 percent in individuals, 44 percent in small clumps, 14 percent in moderate clumps, 4 percent in large clumps, and no super clumps. We also generated binned clump-size distributions at 6 m for all trees >10 cm (app. 3).

The cumulative distributions of the empty space function varied widely across the plots and were closely related to density (fig. 3.4). The proportion of the plot area greater than 9 m away from a tree ranged from 5 percent in G2 to 32 percent in D1 and G3 (fig. 3.4). Total area in large openings varied from 15 to 72 percent (table 3.1). Most large openings were less than 0.04 ha, however, and only 13 openings greater than 0.4 ha were found across all 14 plots (fig. 3.5). Opening size distributions had a sharp negative exponential or "reverse J" shape (figs. 3.5). Openings were generally sinuous and irregular in shape, ranging from 18 to 45 m across, and were often interconnected across a plot. Relatively few compact, circular gaps were found.

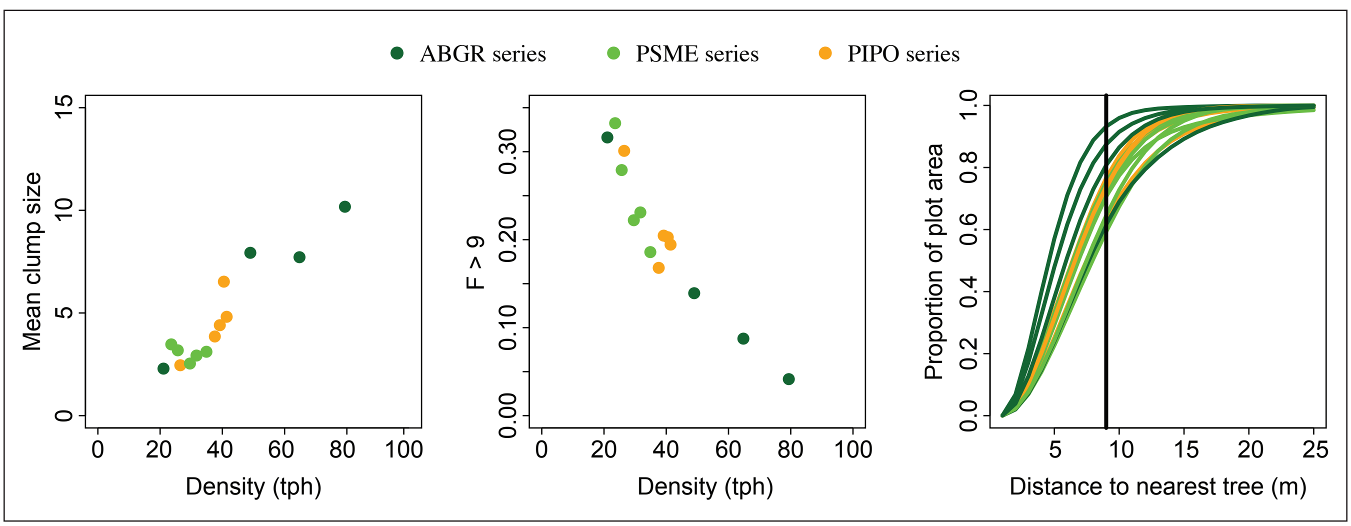


Figure 3.4—Left and center panels show scatterplots of density (trees per hectare [tph]), mean clump size, and F > 9 m (plot area greater than 9 m from the nearest tree or gap edge) for 14 reference plots. Right panel displays cumulative open space distribution, F(*t*), of 14 plots. Vertical bar shows F > 9. ABGR = *Abies grandis*, PSME = *Pseudotsuga menziesii*, PIPO = *Pinus ponderosa*.

The distribution of basal area (BA) from the fixed-area plots that were simulated across each stem map plot showed wide variations in all plots (figs. 3.6 and 4.1 panel G). All stem map plots had low density areas with few or no trees as well as areas of high basal area (60 to 80 $m^2$ $ha^{-1}$). Even the lowest density plot, G3, had areas with 40 to 50 $m^2$ $ha^{-1}$ of basal area. Basal area distributions from the Douglas-fir and grand fir series were not normally distributed (fig. 3.6). Distributions were relatively flat up to the mean and then tapered off into a long right tail. Basal area distributions from the grand fir series were closer to a normal or bell-shaped distribution, but still had long right tails. For all plots, the mean BA value was not the majority condition on the plot (fig. 3.6). These results were the same for 0.08 ha fixed-area plots and 4.6 basal area factor variable radius plots (app. 4).

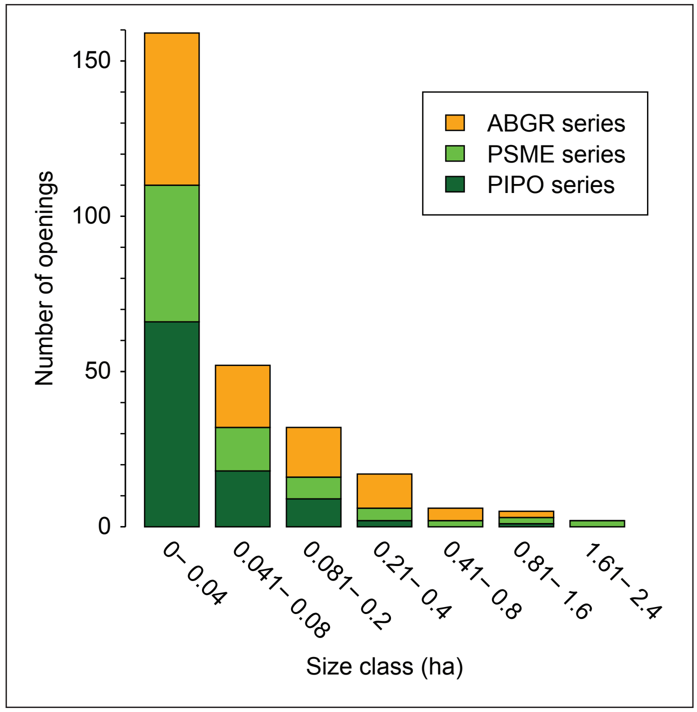


Figure 3.5—Number of large openings by size class and potential vegetation series for 14 reference plots. Openings are pooled together across all 14 plots. See "Spatial Pattern Analysis" on p.14 for an explanation of how large openings were delineated. PIPO = *Pinus ponderosa*, PSME = *Pseudotsuga menziesii*, ABGR = *Abies grandis*.

The Cramer–von Mises goodness-of-fit test from Loosmore and Ford (2006) found that all plots were statistically different from a random pattern ($p < 0.002$) and clustered. The pair correlation function curves, g($t$), showed that all plots were clustered at intertree distances from 1 to 6 m, with 8 out of 14 plots clustered up to 10 to 12 m (app. 5). Four of the plots were clustered at even longer distances. This indicates nonstationary or inhomogeneous patterns where areas of higher density and higher clumping were not randomly or evenly spread out across these plots, but grouped into sections of the plot.

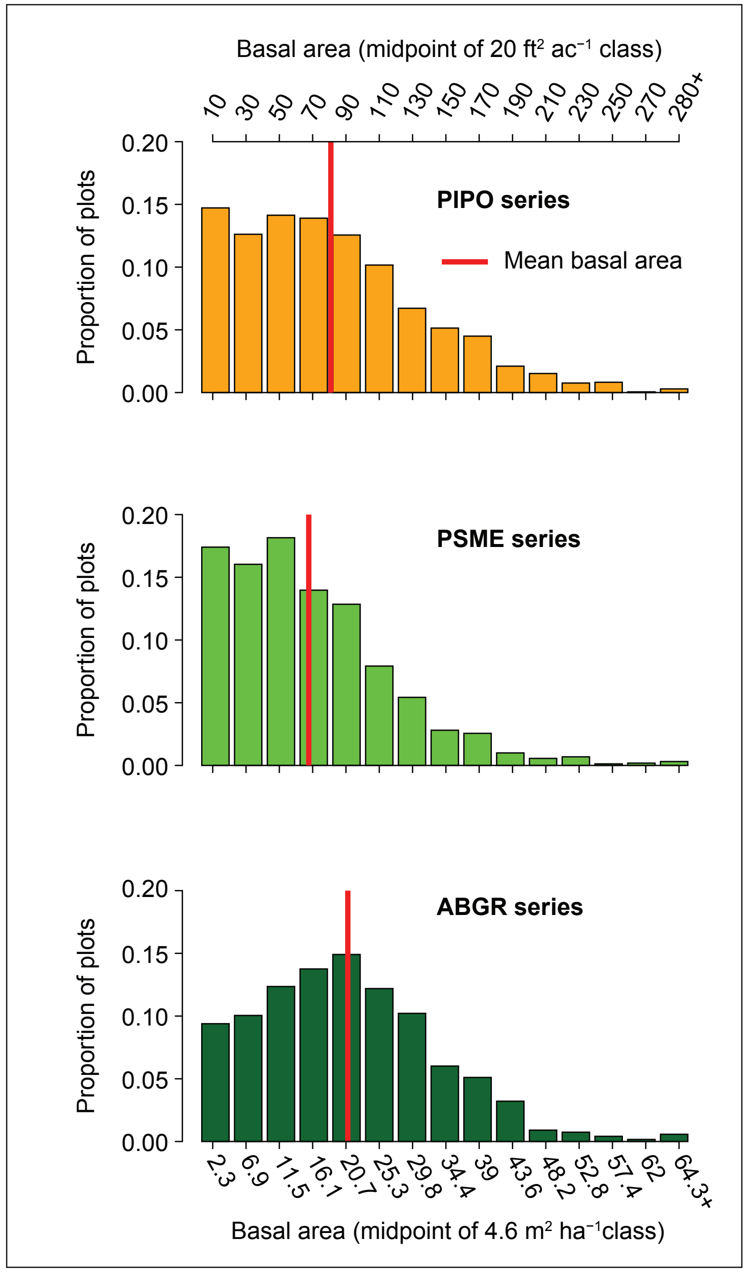


Figure 3.6—Frequency distribution of historical basal area pooled by potential vegetation series. Basal area was calculated for 0.04-ha fixed-area plots on a 20-m grid across each of the 14 reference plots. Fixed-area plots were simulated. The top panel shows the pooled results for the five ponderosa pine plots, the middle panel shows results for the five Douglas-fir plots, and the bottom panel shows results for the four grand-fir plots. Red lines are means for the respective series.

## Relationships Among Pattern, Density, and Plant Series

Some trends were evident in the relationships between clump size distributions, density, openings, and potential vegetation series (tables 3.1 and 3.2, figs. 3.3 through 3.5). The Douglas-fir series plots had the lowest densities (mean tph: 73, sd: 11.3), lowest levels of clumping, and more area in open space. The ponderosa pine series plots supported intermediate stem densities (mean tph: 92, sd: 15.6) and had moderate levels of clumping and openings. The grand fir series plots had the highest stem densities (mean tph: 133, sd: 61.6) and the highest levels of clumping and lowest levels of open space. Sorting the plots by the proportion of trees that occurred as individuals matches quite closely with potential vegetation series (table 3.2).

There were two notable exceptions to these trends, however. Plots G3 and P1 had lower densities and levels of clumping than most Douglas-fir series plots and were both in the Low clumping group. The PERMANOVA test for a significant relationship between potential vegetation series and clumping levels was thus rejected ($p = 0.065$), but was very close to being statistically significant. Contrast tests showed that the Douglas-fir series plots had statistically different clumping levels from the ponderosa pine and grand fir series plots ($p = 0.038$ and $p = 0.047$, respectively), but the ponderosa pine and grand fir series plots were not different ($p = 0.33$).

Overall, there is a clear increase in clumping and decrease in open space with increasing density (fig. 3.4). The relationship between density and mean clump size is roughly linear, while the density and open space ($F > 9$ m) have a reverse exponential distribution.

# Chapter 4: Individual Plot Results

This section provides the range of conditions found in this study, including size, density, composition, and pattern results for each of the 14 plots. The same tables and figures are presented across two pages for each plot. All results are for live trees reconstructed to 1890, except for age class, which is age in 2013. Trees down to a lower diameter at breast height (d.b.h.) cutoff of 15 cm in 1890 are included in all figures. Species abbreviations are as follows: PIPO: ponderosa pine; ABGR: grand fir; PSME: Douglas-fir; LAOC: western larch; JUOC: rocky mountain juniper; PICO: lodgepole pine; and CELE3: mountain mahogany. CAGE = *Carex geyeri* Boott. CARU = *Calamagroustis rubescens* Buckley. VASC = *Vaccinia scoporium* Leiburg ex Colville. Below is a caption for the panels that are presented for each of the 14 plots.

## Panels

**Panel A:** Diameter distribution by species in 10-cm classes. Values on x-axis are diameter-class midpoints. The lower diameter cutoff is 15 cm; 20 equates to a 15- to 24.9-cm class. Diameters are reconstructed to 1890.

**Panel B:** Age-class distribution for live measure trees where age could be determined. Age is from 2013, not 1890.

**Panel C:** Stem map of reconstructed 1890 trees on plot. Tree boles are colored by species and proportional to size. A 3-m radius was used to project tree crowns on all trees to illustrate clump identification using a fixed distance of 6 m. Clump size is the number of trees in the clump. Large openings are shown with a dashed line (see chapter 2, "Spatial Pattern Analysis section," for an explanation of how large openings were identified). Background yellow to red coloration is the graphical display of the empty space function; colors indicate distance to the nearest tree in meters.

**Panel D:** Table showing clump size proportions for trees and basal area for various intertree distances. Quadratic mean diameter of different clump sizes is also shown.

**Panel E:** Bar plot of empty space distribution. Each bar shows the proportion of the plot area that is within that range of distance from the nearest trees. Colors match background coloration from stem map on panel C.

**Panel F:** Bar plot of opening size distribution for plot. Data are for large openings shown on stem map in panel C. See section 2.6 for an explanation of how large openings were identified. Note that size bins are not equal, but get proportionally larger.

**Panel G:** Frequency distribution of historical basal area across plot. Basal area was calculated on 0.04-ha fixed-area plots laid out on a 20-m grid across the stem map plot. Fixed-area plots were run on the computer, not measured in the field. Values shown on x-axis are midpoints for each class or bin: 5 equates to the 0 to 9-$m^2$ $ha^{-1}$ bin. To convert values to $ft^2$ $ac^{-1}$ multiply values by 4.36.

## Ponderosa Pine 1

**Location:** Dugout Research Natural Area

**Plant association:** PIPO/CAGE

**Topography: Slope:** 15 to 40 percent, mean 25 percent; aspect: SW; elevation: 5,480 to 5,695 ft, mean 5,575 ft.

**Description:** Historically low-density site with a preponderance of young pole-sized pine. Located at the upper reach of a south-facing slope above Stink Creek. The northern edge of the plot abuts the exposed rocks of the ridge top, among which grow juniper and mountain mahogany.

### Summary metrics

| Hectares | Basal area | Trees | Avg. d.b.h. | QMD | Max height | Canopy cover | Acres | Basal area | Trees | Avg. d.b.h. | QMD | Max height | SDI |
|---|---|---|---|---|---|---|---|---|---|---|---|---|---|
| | $m^2 \cdot ha^{-1}$ | $ha^{-1}$ | | | *m* | *Percent* | | $ft^2 \cdot ac^{-1}$ | $ac^{-1}$ | | | *ft* | |
| 4.7 | 13 | 65 | 46.9 | 50.2 | 37 | 15 | 11.6 | 56 | 26 | 18.5 | 19.8 | 120 | 86 |

Avg. = average, d.b.h. = diameter at breast height, OMD = quadratic mean diameter, SDI = standard density index.

### Proportion of basal area

| PIPO | ABGR | PSME | LAOC | JUOC | PICO | CELE3 | Unknown |
|---|---|---|---|---|---|---|---|
| 0.992 | 0.002 | 0 | 0 | 0.002 | 0 | 0 | 0.005 |

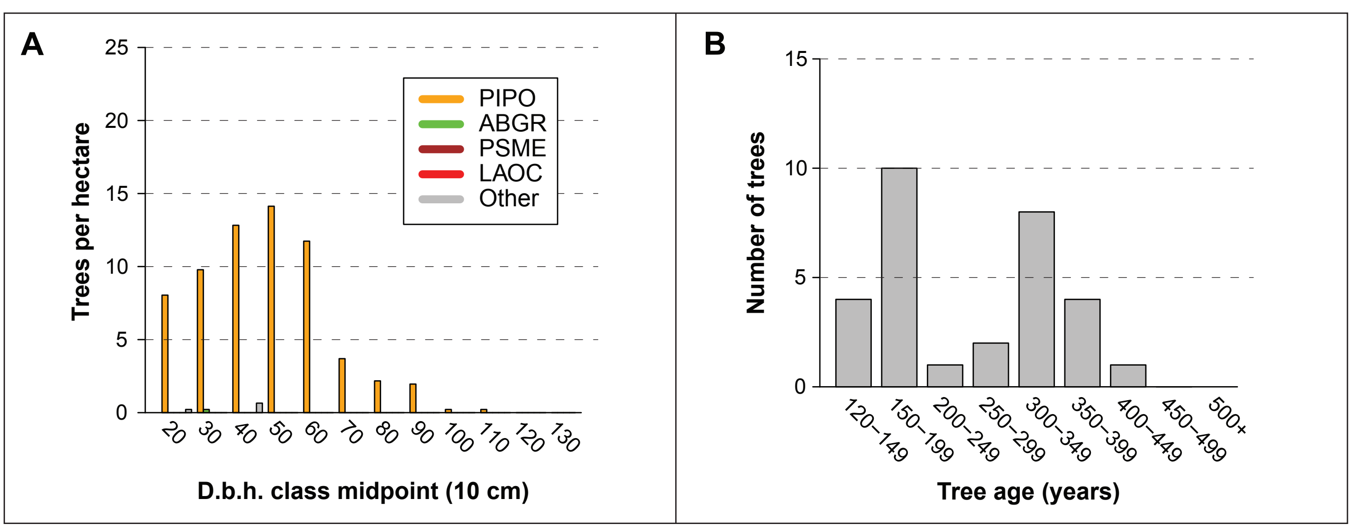

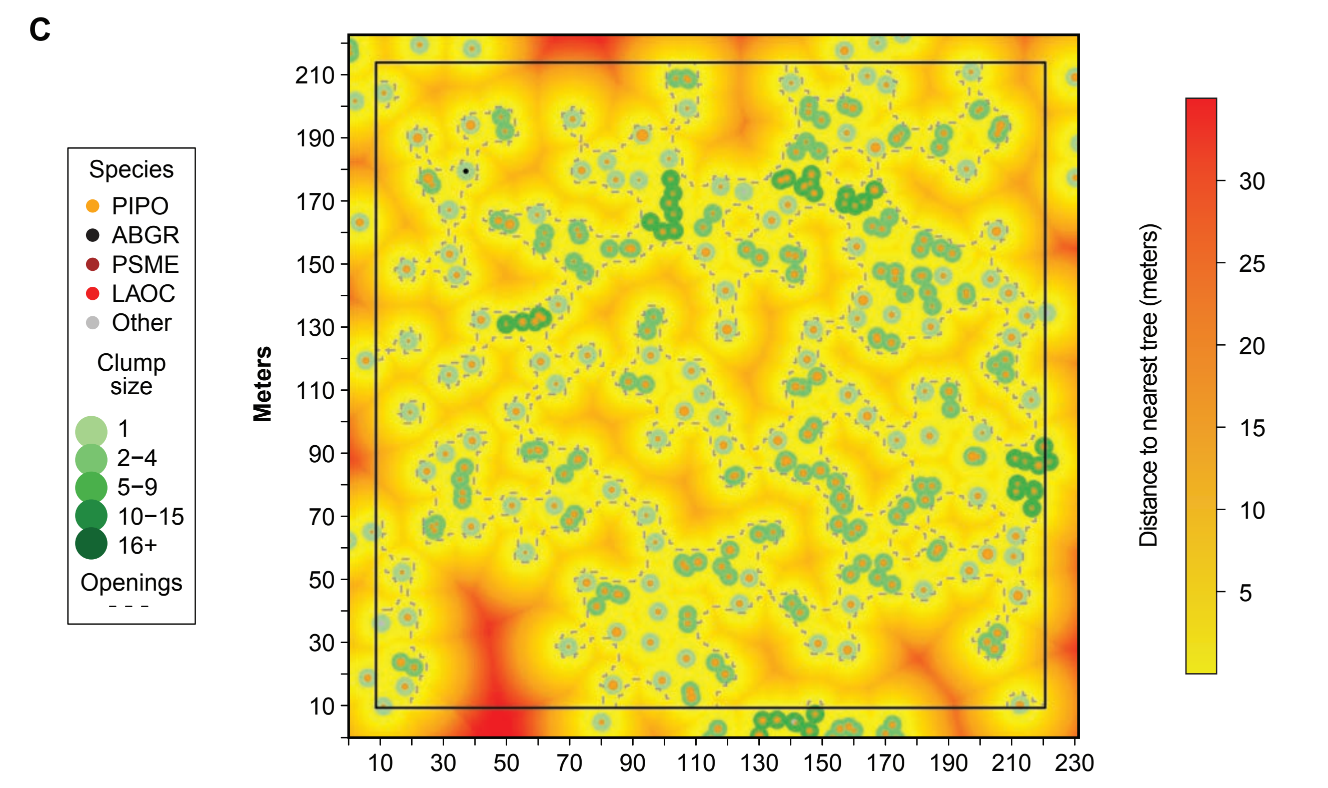


| D Intertree dist. (m) | Clump proportions (trees) | | | | | Clump proportions (basal area) | | | | | Clump quadratic mean diameter (cm) | | | | |
|---|---|---|---|---|---|---|---|---|---|---|---|---|---|---|---|
| | Clump size (No. of trees) | | | | | Clump size (No. of trees) | | | | | Clump size (No. of trees) | | | | |
| | 1 | 2-4 | 5-9 | 10-15 | 16+ | 1 | 2-4 | 5-9 | 10-15 | 16+ | 1 | 2-4 | 5-9 | 10-15 | 16+ |
| 2 | 0.83 | 0.17 | 0 | 0 | 0 | 0.86 | 0.14 | 0 | 0 | 0 | 51 | 45.7 | 0 | 0 | 0 |
| 3 | 0.7 | 0.3 | 0 | 0 | 0 | 0.74 | 0.26 | 0 | 0 | 0 | 51.4 | 47.2 | 0 | 0 | 0 |
| 4 | 0.6 | 0.39 | 0.02 | 0 | 0 | 0.66 | 0.33 | 0.01 | 0 | 0 | 52.6 | 46.7 | 39.5 | 0 | 0 |
| 5 | 0.46 | 0.51 | 0.03 | 0 | 0 | 0.53 | 0.45 | 0.02 | 0 | 0 | 54.3 | 46.9 | 39.3 | 0 | 0 |
| 6 | 0.38 | 0.49 | 0.13 | 0 | 0 | 0.46 | 0.47 | 0.07 | 0 | 0 | 55 | 49.2 | 37.7 | 0 | 0 |
| 7 | 0.31 | 0.44 | 0.2 | 0.04 | 0 | 0.38 | 0.42 | 0.14 | 0.05 | 0 | 55.7 | 49.1 | 41.7 | 56.2 | 0 |
| 10 | 0.12 | 0.3 | 0.29 | 0.13 | 0.16 | 0.16 | 0.31 | 0.29 | 0.1 | 0.14 | 57.8 | 51 | 50.4 | 44.1 | 46.5 |

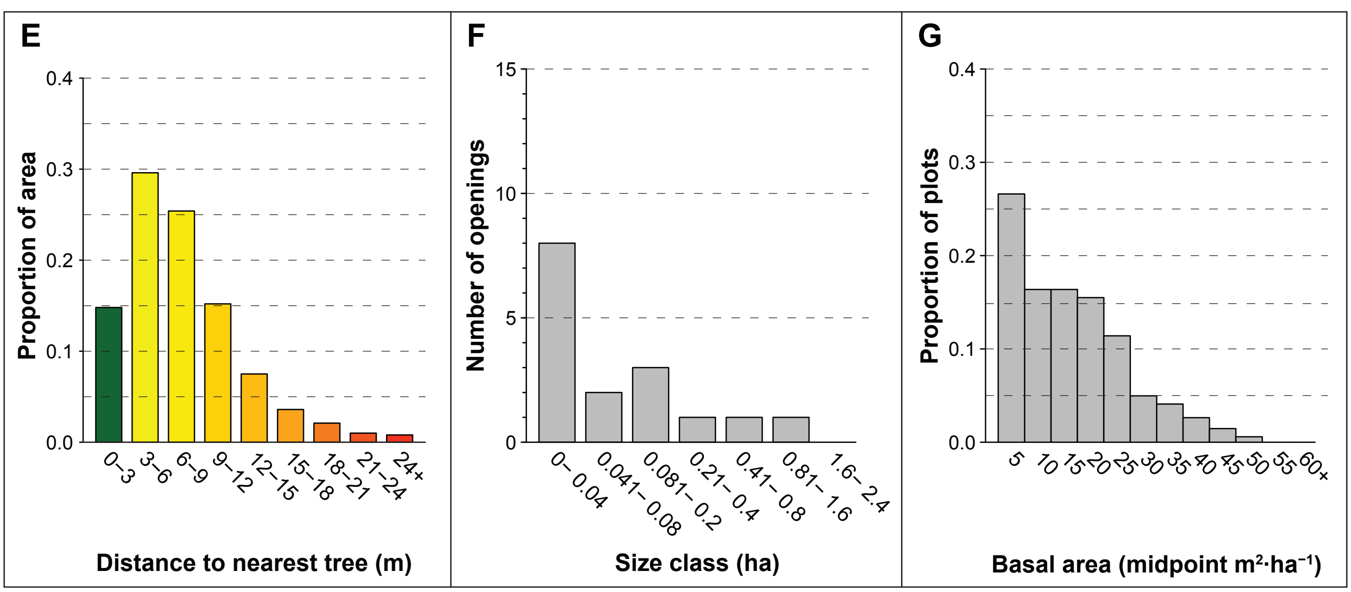

## Ponderosa Pine 2

**Location:** Dugout Research Natural Area

**Plant association:** PIPO/CARU

**Topography:** Slope: 1 to 10 percent, mean 3 percent; aspect: SW; elevation: 5,760 to 5,800 ft, mean 5,775 ft.

**Description:** Large flat table sitting above Dugout Creek. To the south, the stand grades into younger forest, which was apparently not forested until about 90 years ago. To the north, there is a sharp transition into scablands. The plot boasts at least one ponderosa pine older than 500 years and multiple others greater than 400 years. This plot encompasses one sample site from Emily Heyerdahl's fire history reconstruction.

### Summary metrics

| Hectares | Basal area | Trees | Avg. d.b.h. | QMD | Max height | Canopy cover | Acres | Basal area | Trees | Avg. d.b.h. | QMD | Max height | SDI |
|---|---|---|---|---|---|---|---|---|---|---|---|---|---|
| | *m²·ha⁻¹* | *ha⁻¹* | | | *m* | *Percent* | | *ft²·ac⁻¹* | *ac⁻¹* | | | *ft* | |
| 4.4 | 21 | 101 | 47.1 | 51 | 40 | 22 | 10.9 | 90 | 41 | 18.6 | 20.1 | 130 | 137 |

Avg. = average, d.b.h. = diameter at breast height, OMD = quadratic mean diameter, SDI = standard density index.

### Proportion of basal area

| PIPO | ABGR | PSME | LAOC | JUOC | PICO | CELE3 | Unknown |
|---|---|---|---|---|---|---|---|
| 0.983 | 0 | 0.001 | 0 | 0.002 | 0 | 0 | 0.016 |

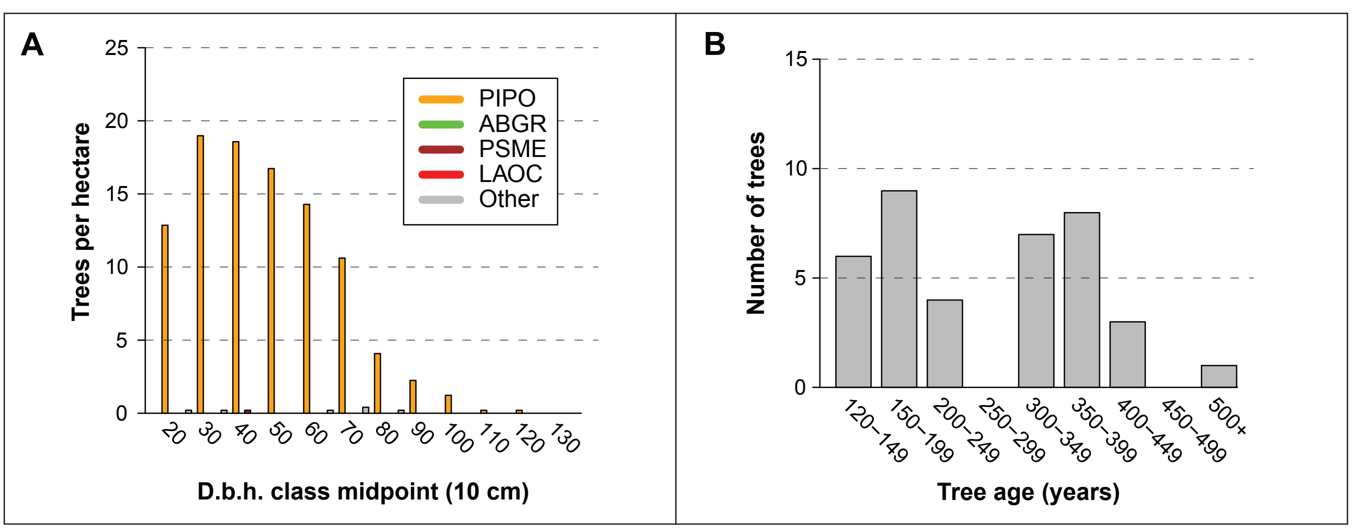

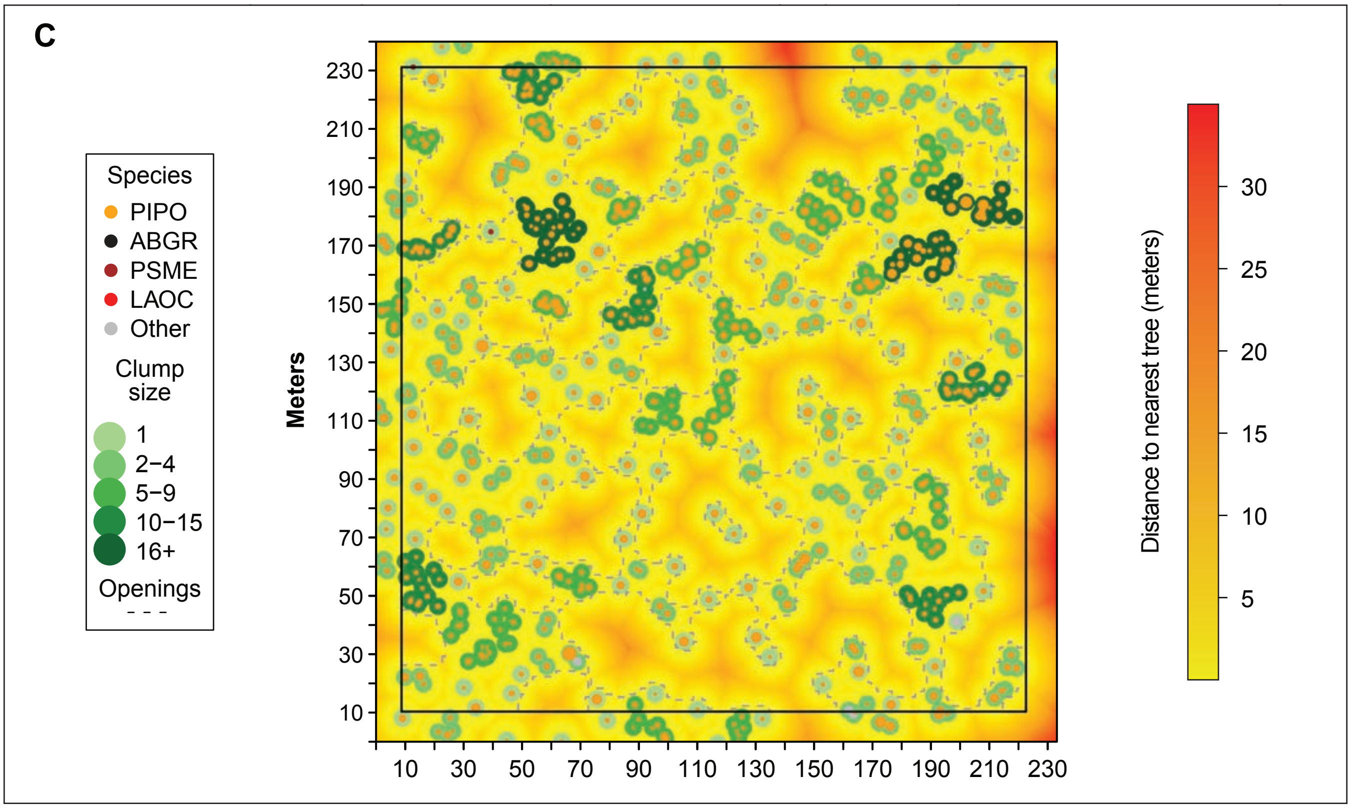


| D Intertree dist. (m) | Clump proportions (trees) | | | | | Clump proportions (basal area) | | | | | Clump quadratic mean diameter (cm) | | | | |
|---|---|---|---|---|---|---|---|---|---|---|---|---|---|---|---|
| | Clump size (No. of trees) | | | | | Clump size (No. of trees) | | | | | Clump size (No. of trees) | | | | |
| | 1 | 2-4 | 5-9 | 10-15 | 16+ | 1 | 2-4 | 5-9 | 10-15 | 16+ | 1 | 2-4 | 5-9 | 10-15 | 16+ |
| 2 | 0.73 | 0.24 | 0.03 | 0 | 0 | 0.81 | 0.18 | 0.02 | 0 | 0 | 53.6 | 44.5 | 34 | 0 | 0 |
| 3 | 0.54 | 0.33 | 0.13 | 0 | 0 | 0.65 | 0.25 | 0.1 | 0 | 0 | 55.7 | 44.7 | 45.2 | 0 | 0 |
| 4 | 0.36 | 0.4 | 0.19 | 0.05 | 0 | 0.47 | 0.36 | 0.15 | 0.03 | 0 | 58.2 | 48.1 | 45.2 | 37.8 | 0 |
| 5 | 0.28 | 0.34 | 0.29 | 0.05 | 0.03 | 0.39 | 0.33 | 0.22 | 0.04 | 0.01 | 59.9 | 50.3 | 44.4 | 47.3 | 33.4 |
| 6 | 0.21 | 0.29 | 0.25 | 0.15 | 0.11 | 0.31 | 0.3 | 0.2 | 0.09 | 0.09 | 62.8 | 52.6 | 46.2 | 38.6 | 47.2 |
| 7 | 0.16 | 0.26 | 0.25 | 0.15 | 0.18 | 0.25 | 0.29 | 0.22 | 0.1 | 0.14 | 63.8 | 53.8 | 48 | 40.3 | 45.9 |
| 10 | 0.05 | 0.1 | 0.19 | 0.17 | 0.49 | 0.08 | 0.13 | 0.22 | 0.13 | 0.43 | 64.8 | 58 | 55.1 | 45.3 | 48 |

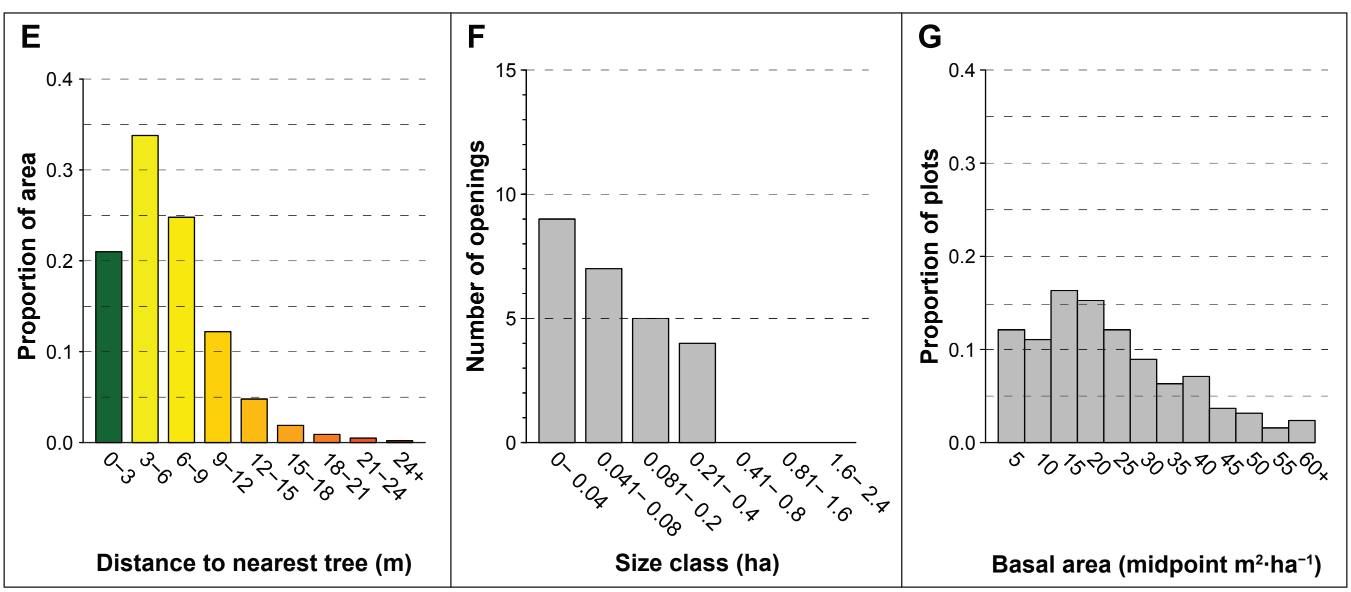

## Ponderosa Pine 3

**Location:** Canyon Creek Research Natural Area

**Plant association:** PIPO/CARU

**Topography:** Slope: 1 to 45 percent, mean 30 percent; aspect: SW; elevation: 4,975 to 5,210 ft, mean 5,120 ft.

**Description:** This plot extends down the south-facing slope from the ridgetop northwest of Yokum Corrals Camp. The eastern edge of the plot includes some rocky outcrops featuring juniper and mountain mahogany. The site is noticeably dominated by old trees, many of which have large fire scars.

### Summary metrics

| Hectares | Basal area | Trees | Avg. d.b.h. | QMD | Max height | Canopy cover | Acres | Basal area | Trees | Avg. d.b.h. | QMD | Max height | SDI |
|---|---|---|---|---|---|---|---|---|---|---|---|---|---|
| | *$m^2 \cdot ha^{-1}$* | *$ha^{-1}$* | | | *m* | *Percent* | | *$ft^2 \cdot ac^{-1}$* | *$ac^{-1}$* | | | *ft* | |
| 4.1 | 19 | 103 | 46.1 | 48.8 | 41 | 20 | 10.1 | 84 | 42 | 18.1 | 19.2 | 133 | 131 |

Avg. = average, d.b.h. = diameter at breast height, OMD = quadratic mean diameter, SDI = standard density index.

### Proportion of basal area

| PIPO | ABGR | PSME | LAOC | JUOC | PICO | CELE3 | Unknown |
|---|---|---|---|---|---|---|---|
| 0.979 | 0 | 0.008 | 0 | 0 | 0 | 0 | 0.013 |

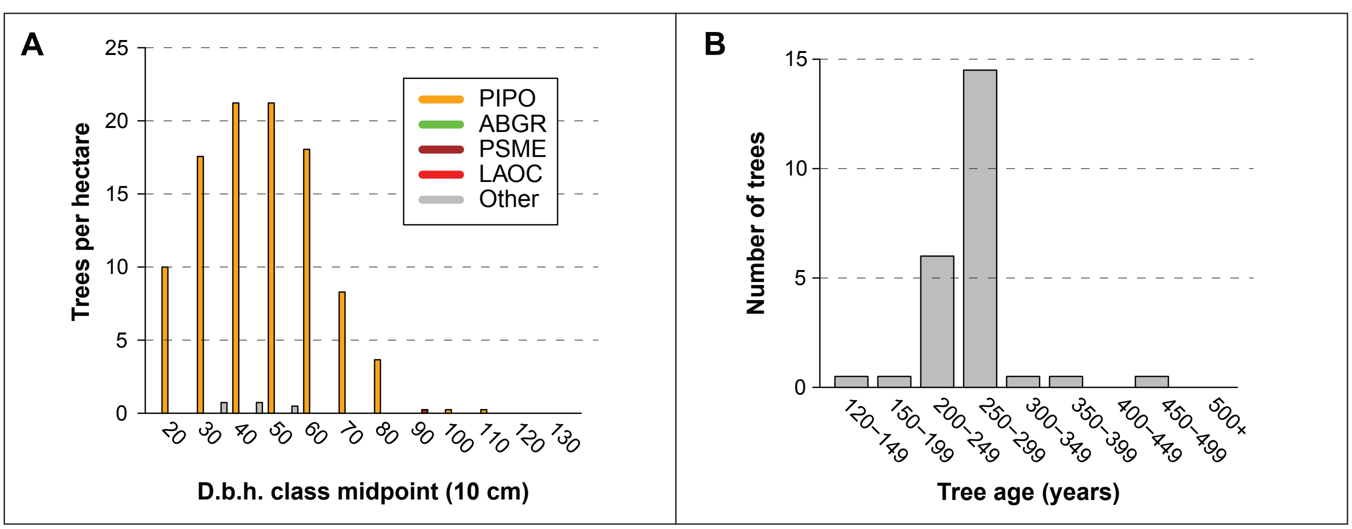

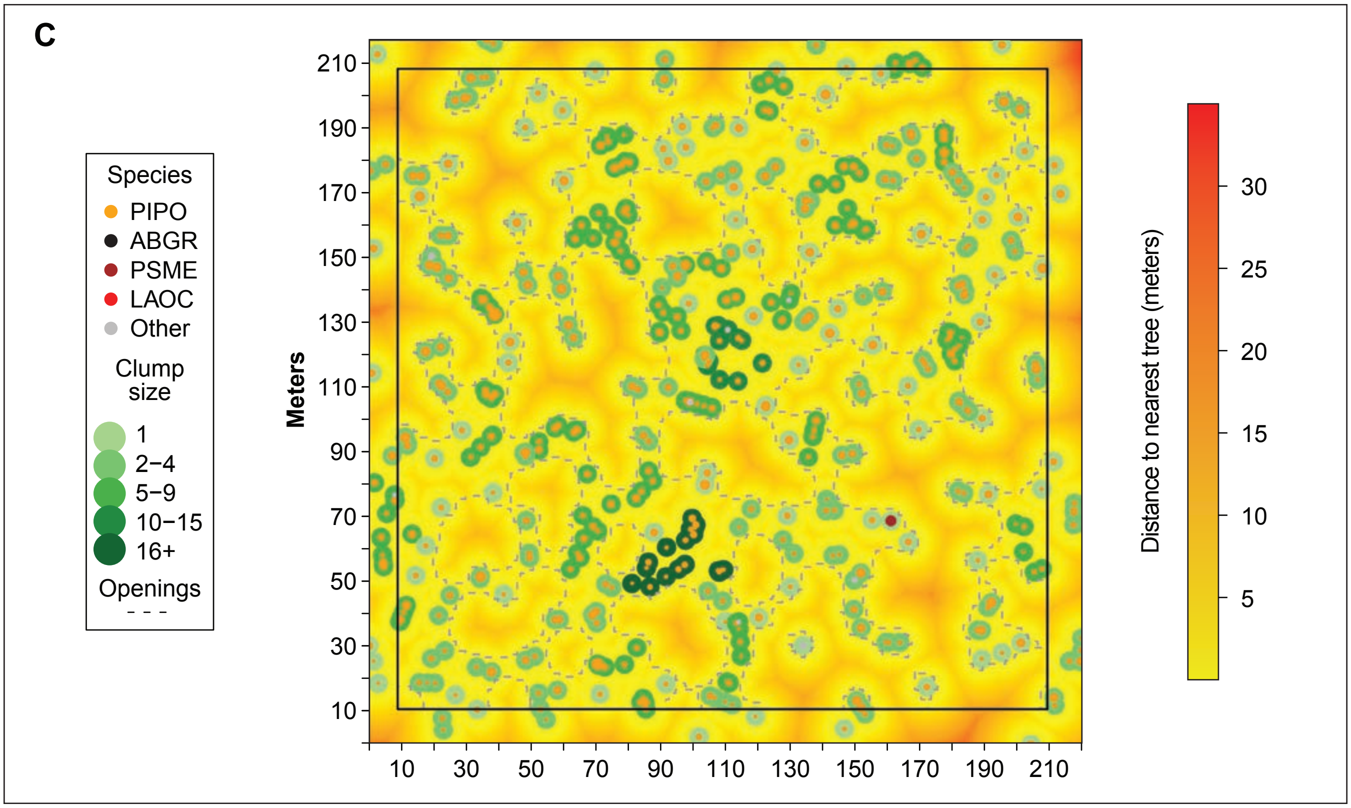


| D Intertree dist. (m) | Clump proportions (trees) | | | | | Clump proportions (basal area) | | | | | Clump quadratic mean diameter (cm) | | | | |
|---|---|---|---|---|---|---|---|---|---|---|---|---|---|---|---|
| | Clump size (No. of trees) | | | | | Clump size (No. of trees) | | | | | Clump size (No. of trees) | | | | |
| | 1 | 2-4 | 5-9 | 10-15 | 16+ | 1 | 2-4 | 5-9 | 10-15 | 16+ | 1 | 2-4 | 5-9 | 10-15 | 16+ |
| 6 | 0.18 | 0.40 | 0.35 | 0.03 | 0.05 | 0.22 | 0.41 | 0.32 | 0.02 | 0.03 | 54.4 | 49.7 | 46.6 | 40.6 | 37.8 |

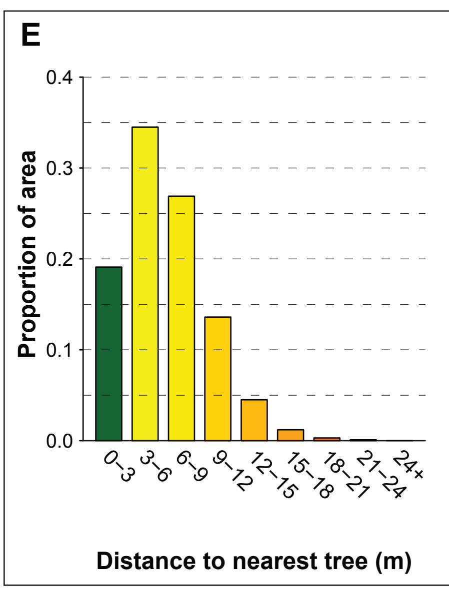


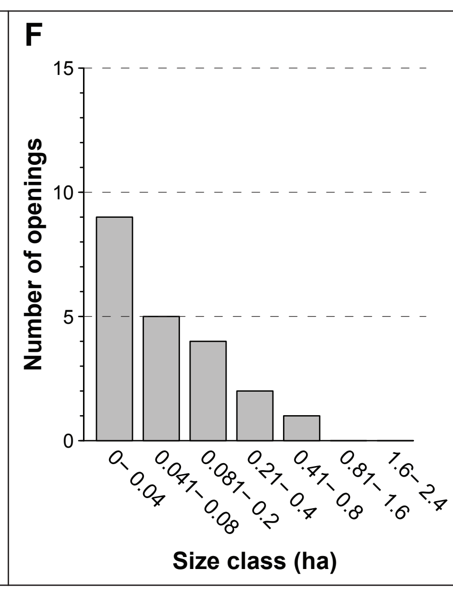


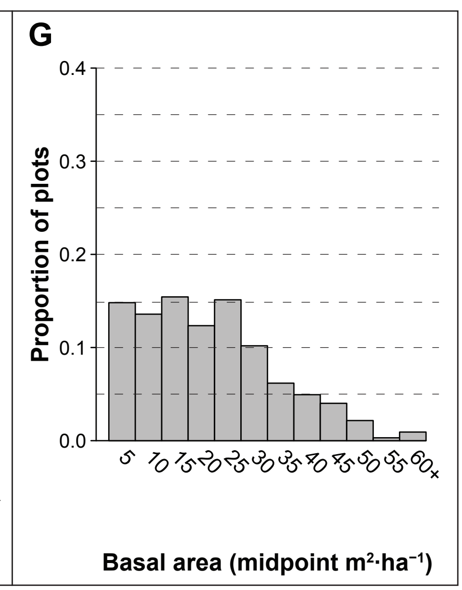

## Ponderosa Pine 4

**Location:** Malheur Ford

**Plant association:** PIPO/CARU

**Topography:** Slope: 2 to 24 percent, mean 4 percent; aspect: SW; elevation: 5,060 to 5,130 ft, mean 5,070 ft.

**Description:** This plot is located on a flat table directly east of the Malheur Ford and north of Black Canyon. The northeastern portion of the plot sits on a small step above the rest. Many of the older pines are declining in vigor, possibly towing to defoliating insects.

### Summary metrics

| Hectares | Basal area | Trees | Avg. d.b.h. | QMD | Max height | Canopy cover | Acres | Basal area | Trees | Avg. d.b.h. | QMD | Max height | SDI |
|---|---|---|---|---|---|---|---|---|---|---|---|---|---|
| | *$m^2 \cdot ha^{-1}$* | *$ha^{-1}$* | | | *m* | *Percent* | | *$ft^2 \cdot ac^{-1}$* | *$ac^{-1}$* | | | *ft* | |
| 4.4 | 19 | 98 | 47 | 49.7 | 45 | 21 | 10.8 | 83 | 40 | 18.5 | 19.6 | 146 | 127 |

Avg. = average, d.b.h. = diameter at breast height, OMD = quadratic mean diameter, SDI = standard density index.

### Proportion of basal area

| PIPO | ABGR | PSME | LAOC | JUOC | PICO | CELE3 | Unknown |
|---|---|---|---|---|---|---|---|
| 0.989 | 0 | 0 | 0 | 0 | 0 | 0 | 0.011 |

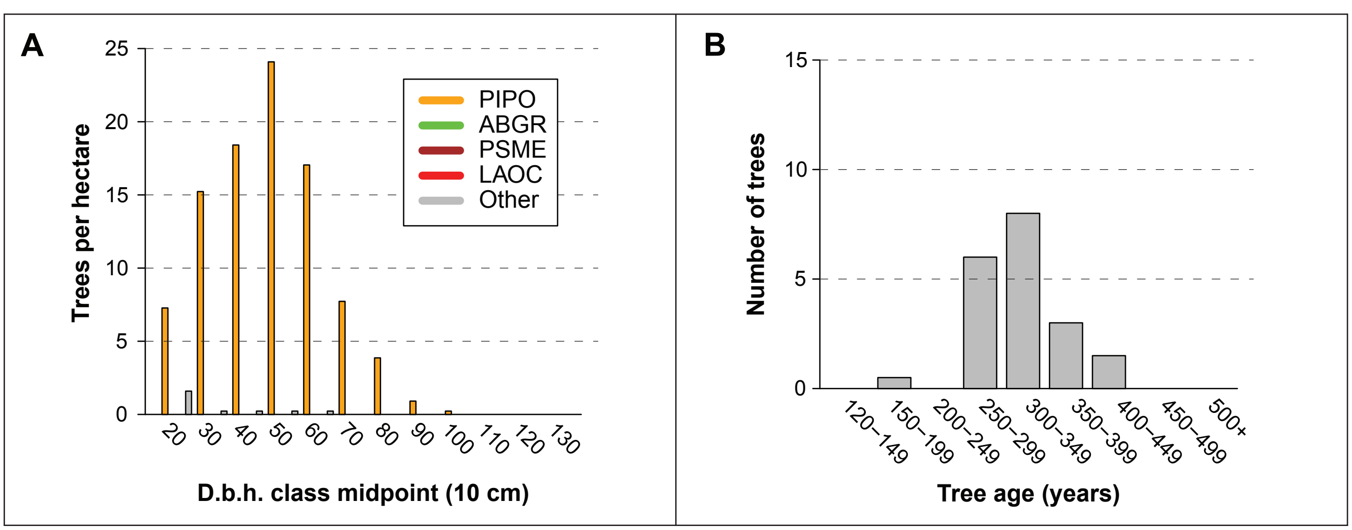

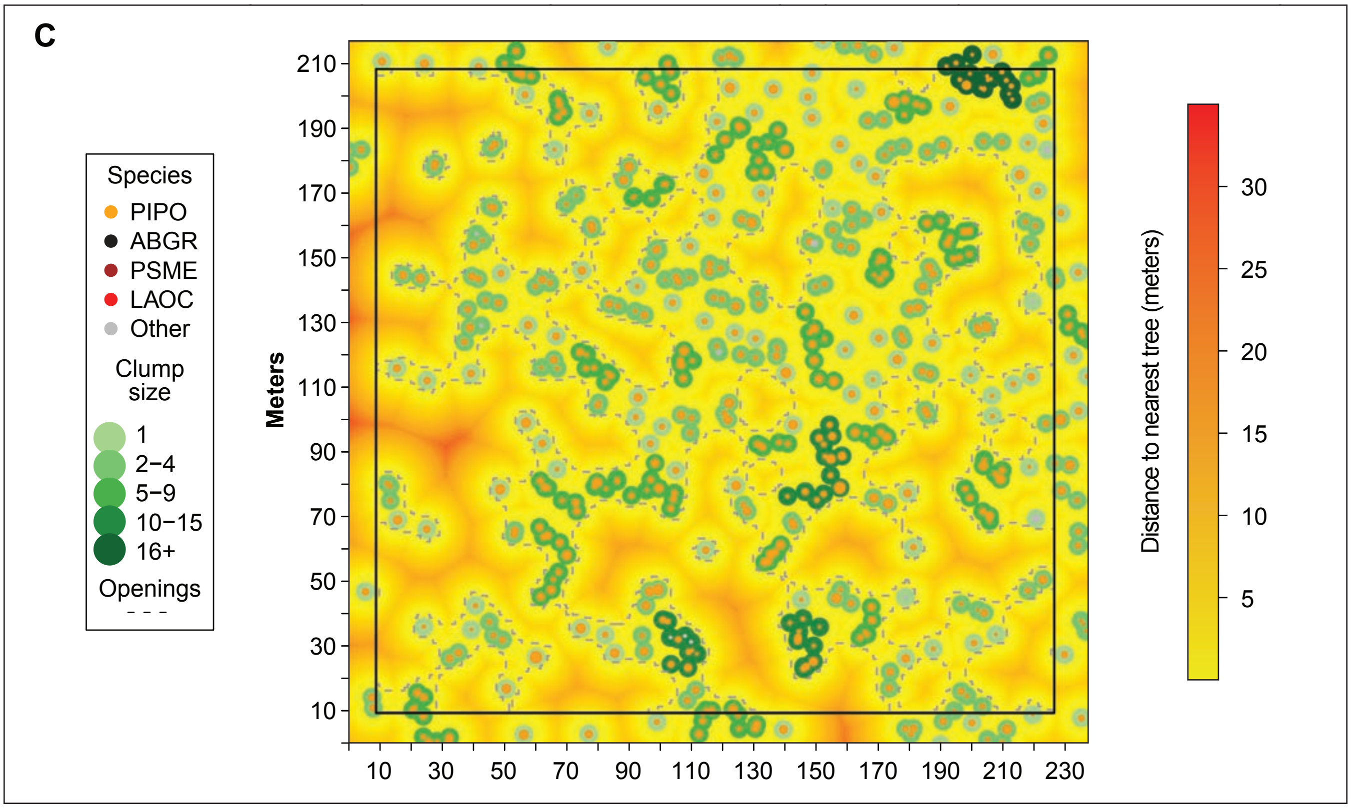


| D<br>Intertree dist. (m) | Clump proportions (trees) | | | | | Clump proportions (basal area) | | | | | Clump quadratic mean diameter (cm) | | | | |
|---|---|---|---|---|---|---|---|---|---|---|---|---|---|---|---|
| | Clump size (No. of trees) | | | | | Clump size (No. of trees) | | | | | Clump size (No. of trees) | | | | |
| | 1 | 2-4 | 5-9 | 10-15 | 16+ | 1 | 2-4 | 5-9 | 10-15 | 16+ | 1 | 2-4 | 5-9 | 10-15 | 16+ |
| 2 | 0.73 | 0.27 | 0 | 0 | 0 | 0.78 | 0.22 | 0 | 0 | 0 | 51.5 | 44.7 | 0 | 0 | 0 |
| 3 | 0.52 | 0.43 | 0.04 | 0 | 0 | 0.58 | 0.38 | 0.03 | 0 | 0 | 52.6 | 46.6 | 45 | 0 | 0 |
| 4 | 0.4 | 0.52 | 0.08 | 0 | 0 | 0.46 | 0.47 | 0.07 | 0 | 0 | 53.4 | 47.3 | 45.9 | 0 | 0 |
| 5 | 0.28 | 0.48 | 0.21 | 0.03 | 0 | 0.33 | 0.46 | 0.2 | 0.01 | 0 | 53.7 | 48.8 | 48.4 | 31.6 | 0 |
| 6 | 0.21 | 0.39 | 0.29 | 0.11 | 0 | 0.26 | 0.38 | 0.28 | 0.08 | 0 | 55 | 49 | 49.1 | 42.6 | 0 |
| 7 | 0.12 | 0.29 | 0.38 | 0.13 | 0.08 | 0.15 | 0.31 | 0.37 | 0.11 | 0.05 | 56.4 | 51.2 | 49.6 | 45.2 | 41.1 |
| 10 | 0.04 | 0.14 | 0.11 | 0.15 | 0.56 | 0.06 | 0.16 | 0.1 | 0.13 | 0.55 | 60.8 | 53.6 | 46.7 | 47.4 | 49.1 |

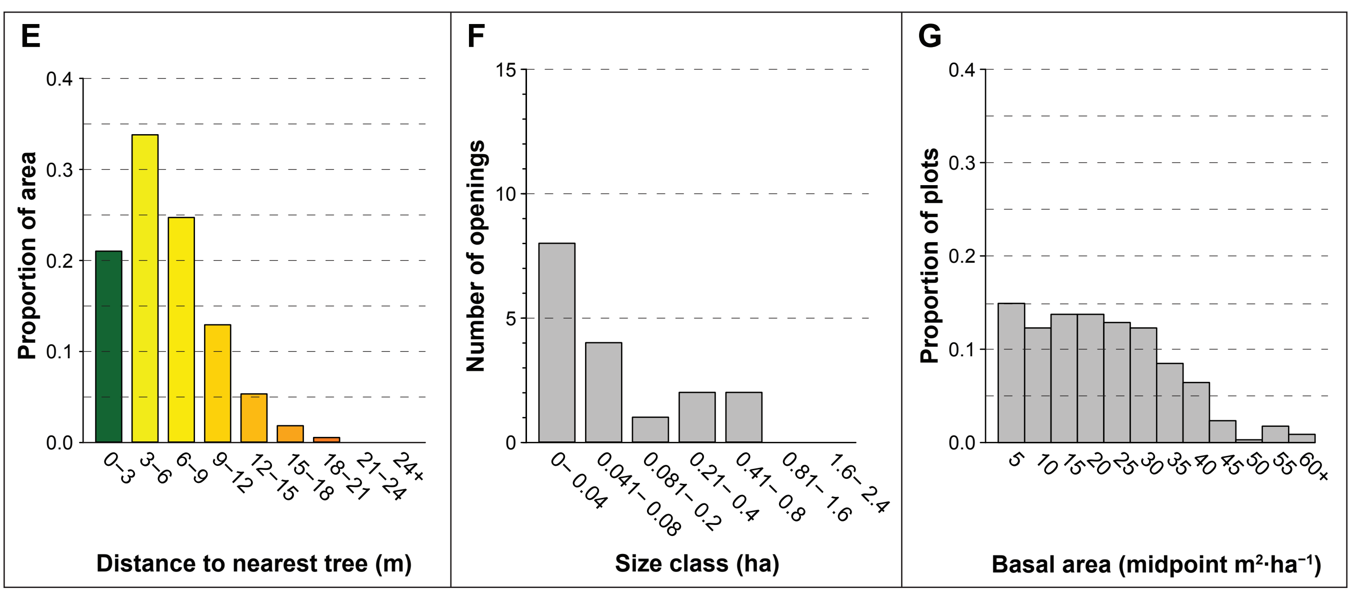

## Ponderosa Pine 5

**Location:** Malheur Ford

**Plant association:** PIPO/CARU

**Topography:** Slope: 10 to 30 percent, mean 15 percent; aspect: SW; elevation: 5,020 to 5,150 ft, mean 5,120 ft.

**Description:** This plot is located ¾ of a mi southeast of ponderosa pine 4, also on a table east of the Malheur River. This plot appears to have burned at a very low severity sometime in the 1980s; many small trees have recent bole char.

### Summary metrics

| Hectares | Basal area | Trees | Avg. d.b.h. | QMD | Max height | Canopy cover | Acres | Basal area | Trees | Avg. d.b.h. | QMD | Max height | SDI |
|---|---|---|---|---|---|---|---|---|---|---|---|---|---|
| | *$m^2 \cdot ha^{-1}$* | *$ha^{-1}$* | | | *m* | *Percent* | | *$ft^2 \cdot ac^{-1}$* | *$ac^{-1}$* | | | *ft* | |
| 4 | 19 | 94 | 47.4 | 50.1 | 41 | 21 | 10 | 81 | 38 | 18.7 | 19.7 | 134 | 124 |

Avg. = average, d.b.h. = diameter at breast height, OMD = quadratic mean diameter, SDI = standard density index.

### Proportion of basal area

| PIPO | ABGR | PSME | LAOC | JUOC | PICO | CELE3 | Unknown |
|---|---|---|---|---|---|---|---|
| 0.99 | 0 | 0.006 | 0 | 0 | 0 | 0 | 0.004 |

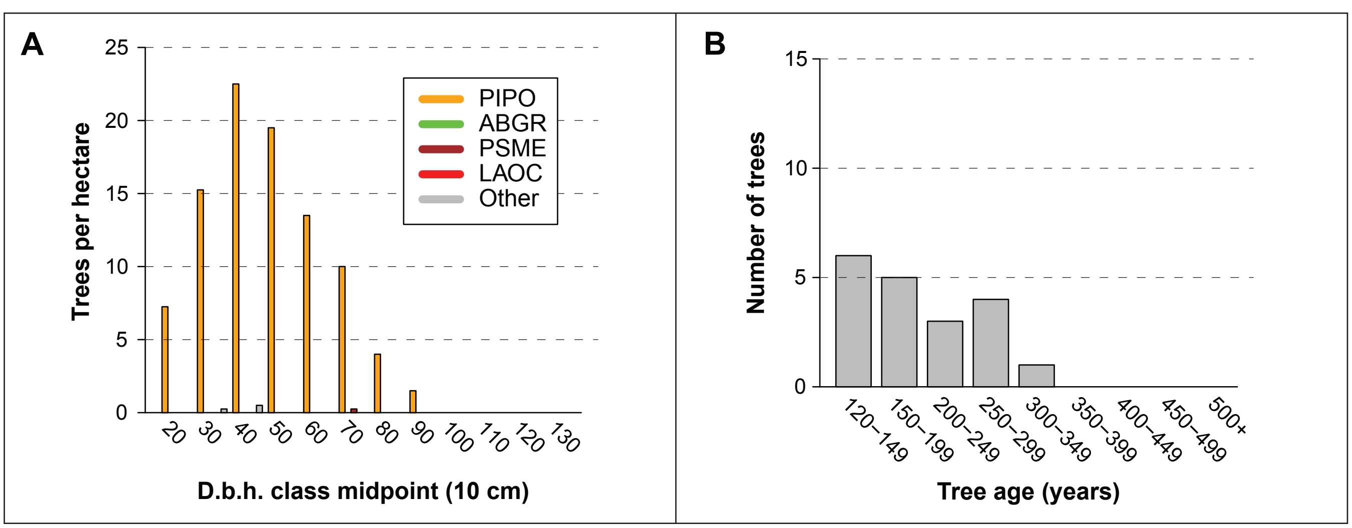

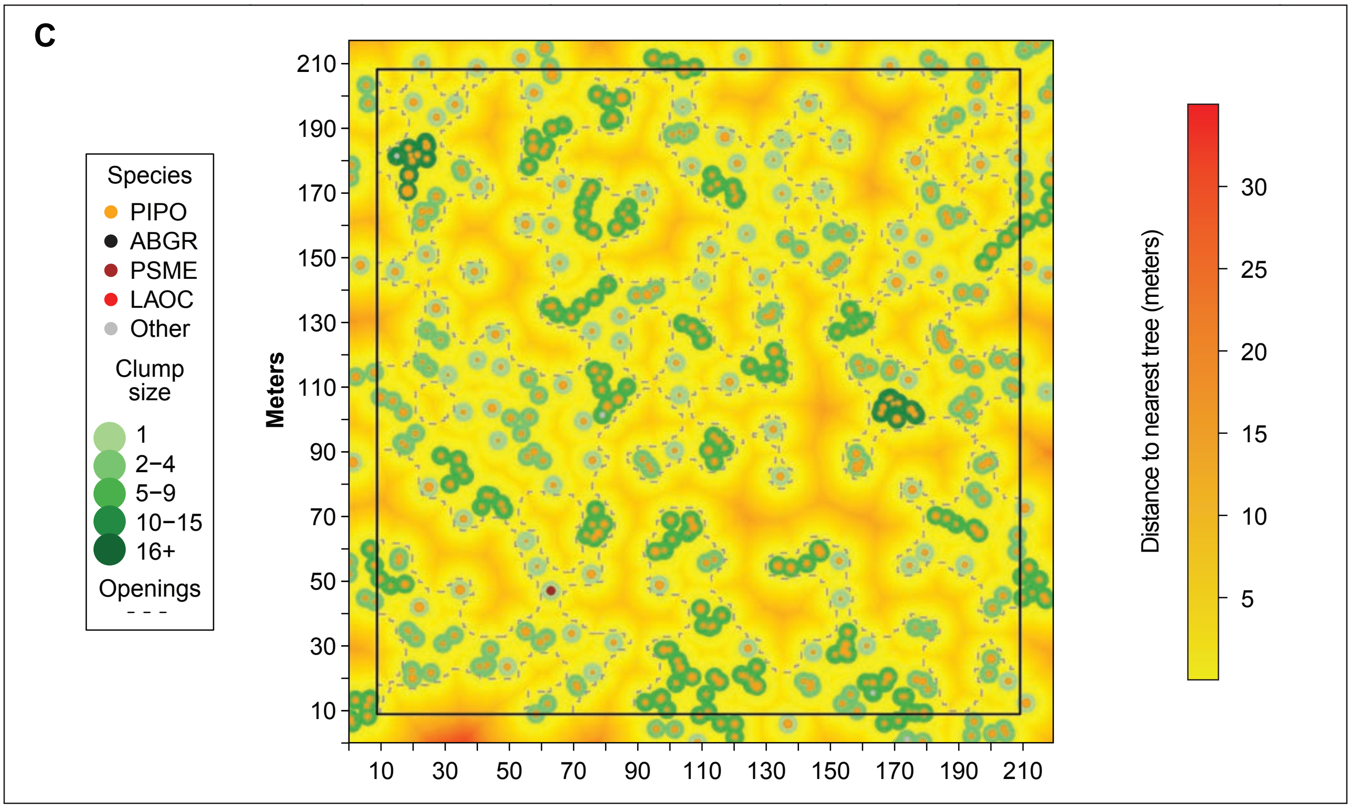


| D Intertree dist. (m) | Clump proportions (trees) | | | | | Clump proportions (basal area) | | | | | Clump quadratic mean diameter (cm) | | | | |
|---|---|---|---|---|---|---|---|---|---|---|---|---|---|---|---|
| | Clump size (No. of trees) | | | | | Clump size (No. of trees) | | | | | Clump size (No. of trees) | | | | |
| | 1 | 2-4 | 5-9 | 10-15 | 16+ | 1 | 2-4 | 5-9 | 10-15 | 16+ | 1 | 2-4 | 5-9 | 10-15 | 16+ |
| 2 | 0.76 | 0.23 | 0.01 | 0 | 0 | 0.81 | 0.18 | 0.01 | 0 | 0 | 51.8 | 44.3 | 49 | 0 | 0 |
| 3 | 0.56 | 0.4 | 0.04 | 0 | 0 | 0.64 | 0.33 | 0.03 | 0 | 0 | 53.5 | 45.5 | 45.4 | 0 | 0 |
| 4 | 0.45 | 0.45 | 0.1 | 0 | 0 | 0.53 | 0.39 | 0.08 | 0 | 0 | 54.6 | 46.4 | 45.3 | 0 | 0 |
| 5 | 0.33 | 0.42 | 0.25 | 0 | 0 | 0.39 | 0.42 | 0.19 | 0 | 0 | 54.9 | 50 | 43.4 | 0 | 0 |
| 6 | 0.23 | 0.34 | 0.38 | 0.05 | 0 | 0.28 | 0.37 | 0.31 | 0.05 | 0 | 55.3 | 51.7 | 45.3 | 49 | 0 |
| 7 | 0.16 | 0.3 | 0.41 | 0.05 | 0.08 | 0.21 | 0.32 | 0.35 | 0.05 | 0.07 | 57.5 | 51.8 | 46.5 | 49 | 46.9 |
| 10 | 0.07 | 0.11 | 0.29 | 0.25 | 0.28 | 0.09 | 0.12 | 0.27 | 0.22 | 0.3 | 56.9 | 51.8 | 48.2 | 47.8 | 51.6 |

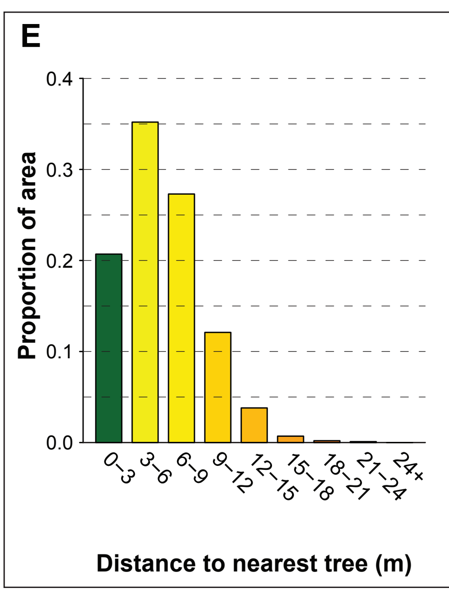


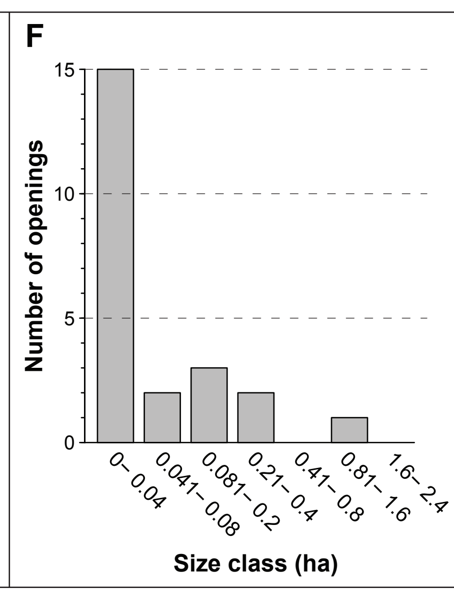


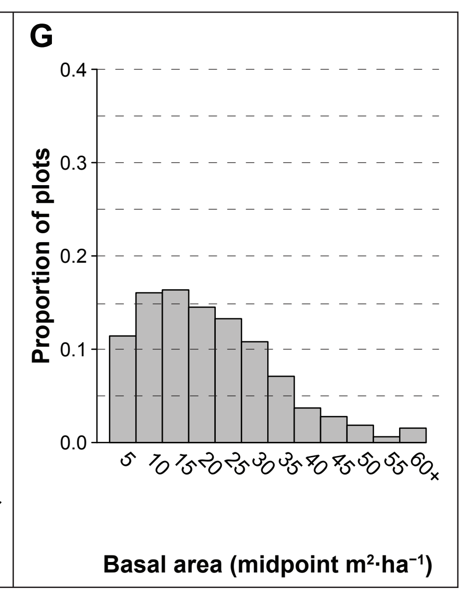

## Douglas-fir 1

**Location:** Dugout Creek Research Natural Area

**Plant association:** PSME/CARU

**Topography:** Slope: 25 to 40 percent, mean 30 percent; aspect: W; elevation: 5,300 to 5,545 ft, mean 5,410 ft.

**Description:** This plot sits on a side slope at the head of a dry gulch between Stink Creek and Dugout Creek. The plot is quite open in places, but scattered patches of denser Douglas-fir and grand fir regeneration do exist. Vegetation uphill from the plot grades into an orchard-like stand of mountain mahogany.

### Summary metrics

| Hectares | Basal area | Trees | Avg. d.b.h. | QMD | Max height | Canopy cover | Acres | Basal area | Trees | Avg. d.b.h. | QMD | Max height | SDI |
|---|---|---|---|---|---|---|---|---|---|---|---|---|---|
| | *$m^2 \cdot ha^{-1}$* | *$ha^{-1}$* | | | *m* | *Percent* | | *$ft^2 \cdot ac^{-1}$* | *$ac^{-1}$* | | | *ft* | |
| 3.9 | 14 | 59 | 51.1 | 54.6 | 41 | 16 | 9.5 | 61 | 24 | 20.1 | 21.5 | 134 | 91 |

Avg. = average, d.b.h. = diameter at breast height, OMD = quadratic mean diameter, SDI = standard density index.

### Proportion of basal area

| PIPO | ABGR | PSME | LAOC | JUOC | PICO | CELE3 | Unknown |
|---|---|---|---|---|---|---|---|
| 0.975 | 0.008 | 0.017 | 0 | 0 | 0 | 0 | 0 |

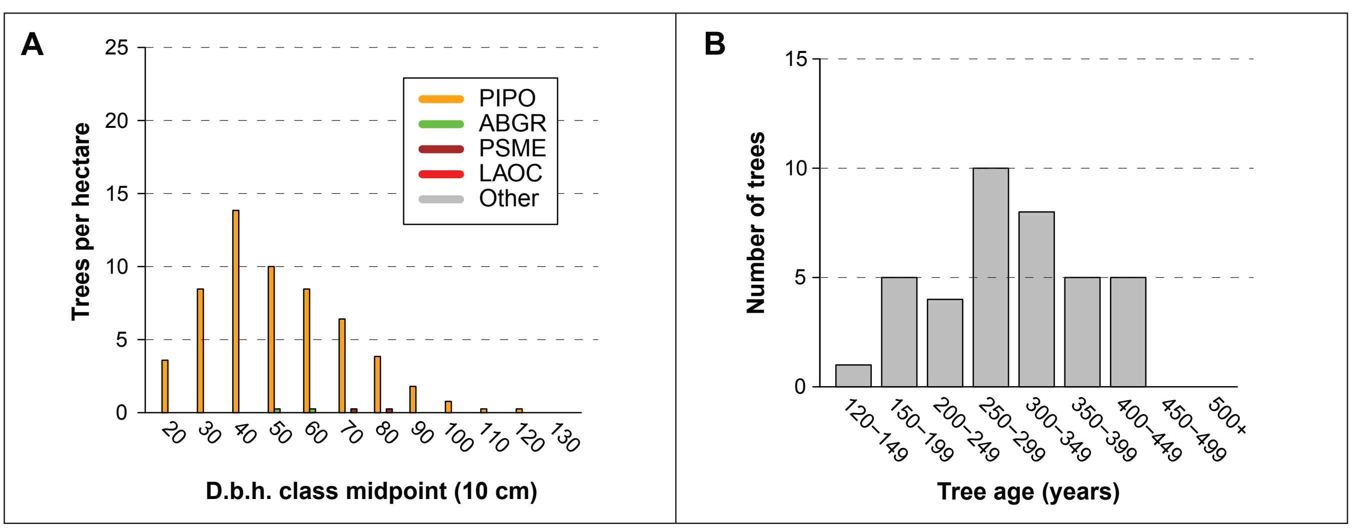

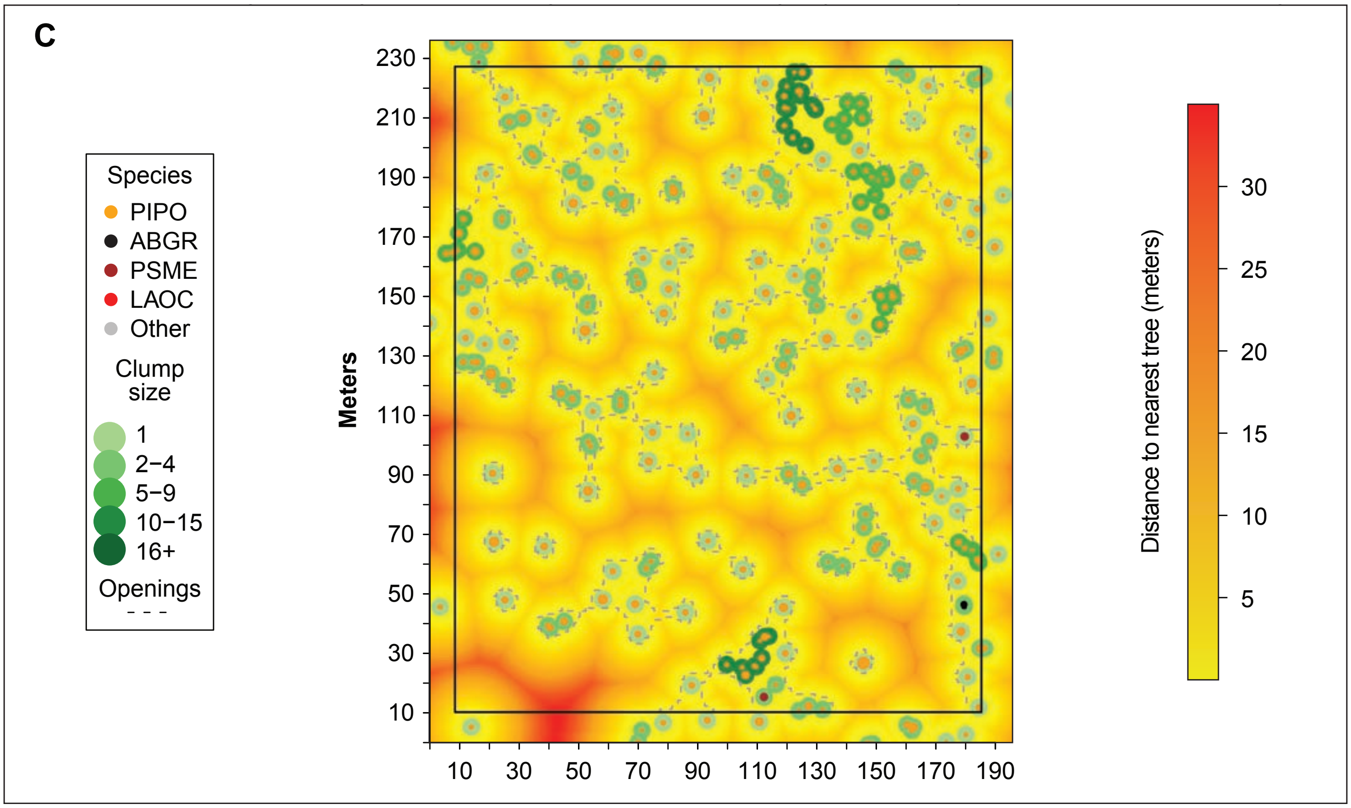


| D Intertree dist. (m) | Clump proportions (trees) | | | | | Clump proportions (basal area) | | | | | Clump quadratic mean diameter (cm) | | | | |
|---|---|---|---|---|---|---|---|---|---|---|---|---|---|---|---|
| | Clump size (No. of trees) | | | | | Clump size (No. of trees) | | | | | Clump size (No. of trees) | | | | |
| | 1 | 2-4 | 5-9 | 10-15 | 16+ | 1 | 2-4 | 5-9 | 10-15 | 16+ | 1 | 2-4 | 5-9 | 10-15 | 16+ |
| 2 | 0.76 | 0.23 | 0.01 | 0 | 0 | 0.81 | 0.18 | 0.01 | 0 | 0 | 51.8 | 44.3 | 49 | 0 | 0 |
| 3 | 0.56 | 0.4 | 0.04 | 0 | 0 | 0.64 | 0.33 | 0.03 | 0 | 0 | 53.5 | 45.5 | 45.4 | 0 | 0 |
| 4 | 0.45 | 0.45 | 0.1 | 0 | 0 | 0.53 | 0.39 | 0.08 | 0 | 0 | 54.6 | 46.4 | 45.3 | 0 | 0 |
| 5 | 0.33 | 0.42 | 0.25 | 0 | 0 | 0.39 | 0.42 | 0.19 | 0 | 0 | 54.9 | 50 | 43.4 | 0 | 0 |
| 6 | 0.23 | 0.34 | 0.38 | 0.05 | 0 | 0.28 | 0.37 | 0.31 | 0.05 | 0 | 55.3 | 51.7 | 45.3 | 49 | 0 |
| 7 | 0.16 | 0.3 | 0.41 | 0.05 | 0.08 | 0.21 | 0.32 | 0.35 | 0.05 | 0.07 | 57.5 | 51.8 | 46.5 | 49 | 46.9 |
| 10 | 0.07 | 0.11 | 0.29 | 0.25 | 0.28 | 0.09 | 0.12 | 0.27 | 0.22 | 0.3 | 56.9 | 51.8 | 48.2 | 47.8 | 51.6 |

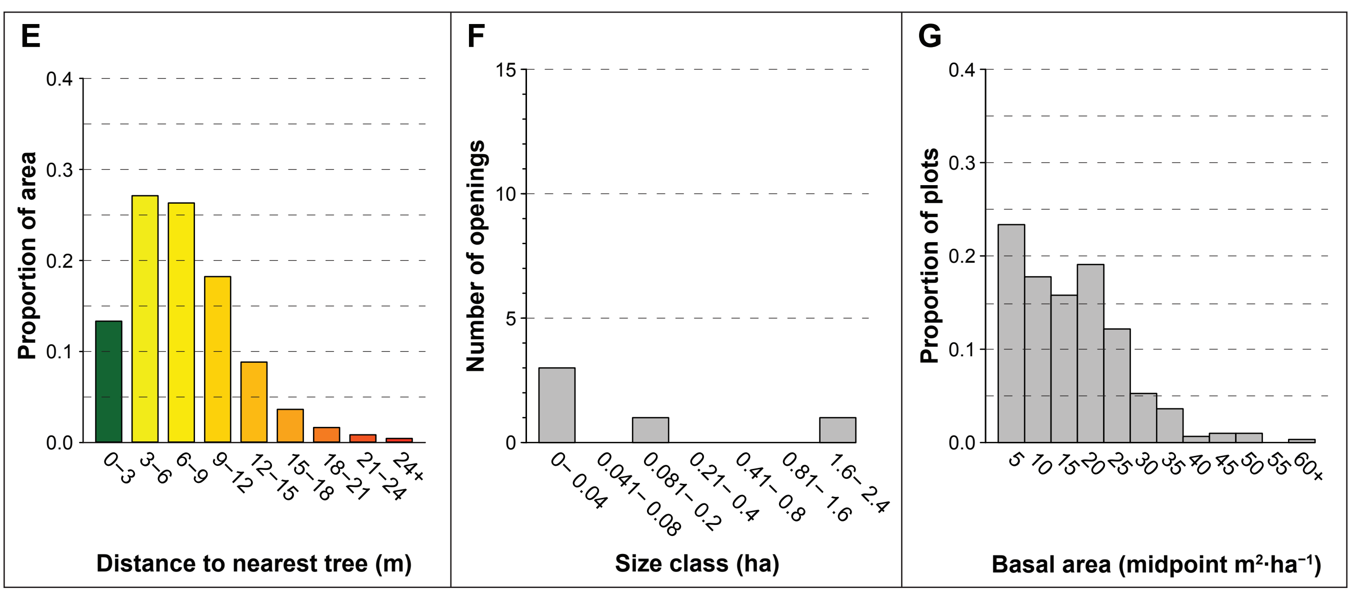

## Douglas-fir 2

**Location:** Dugout Creek Research Natural Area

**Plant association:** PSME/CAGE

**Topography:** Slope: 20 to 40 percent, mean 30 percent; aspect: NW; elevation: 5,040 to 5,310 ft, mean 5,180 ft.

**Description:** This plot spans the slope south of Dugout Creek from the creek bottom to the ridge top. The lower areas of the plot are relatively dense with young Douglas-fir and ponderosa pine. Close to the ridge top, composition shifts more toward pine and becomes sparser.

### Summary metrics

| Hectares | Basal area | Trees | Avg. d.b.h. | QMD | Max height | Canopy cover | Acres | Basal area | Trees | Avg. d.b.h. | QMD | Max height | SDI |
|---|---|---|---|---|---|---|---|---|---|---|---|---|---|
| | *$m^2 \cdot ha^{-1}$* | *$ha^{-1}$* | | | *m* | *Percent* | | *$ft^2 \cdot ac^{-1}$* | *$ac^{-1}$* | | | *ft* | |
| 4.2 | 14 | 79 | 43.4 | 48 | 40 | 18 | 10.4 | 63 | 32 | 17.1 | 18.9 | 130 | 98 |

Avg. = average, d.b.h. = diameter at breast height, OMD = quadratic mean diameter, SDI = standard density index.

### Proportion of basal area

| PIPO | ABGR | PSME | LAOC | JUOC | PICO | CELE3 | Unknown |
|---|---|---|---|---|---|---|---|
| 0.824 | 0 | 0.162 | 0 | 0 | 0 | 0 | 0.014 |

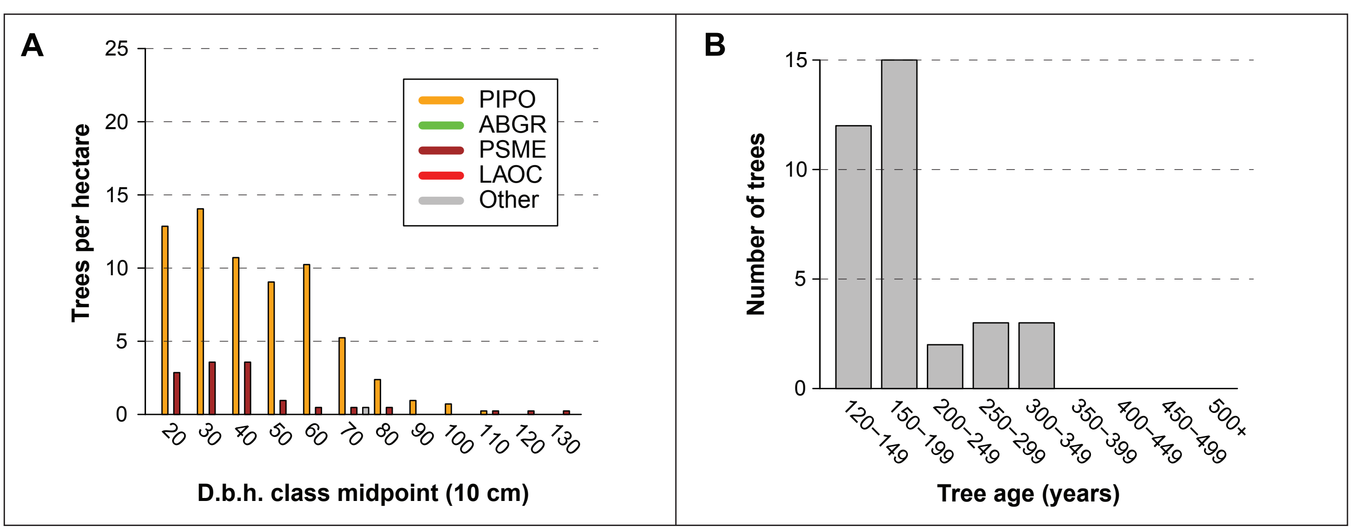

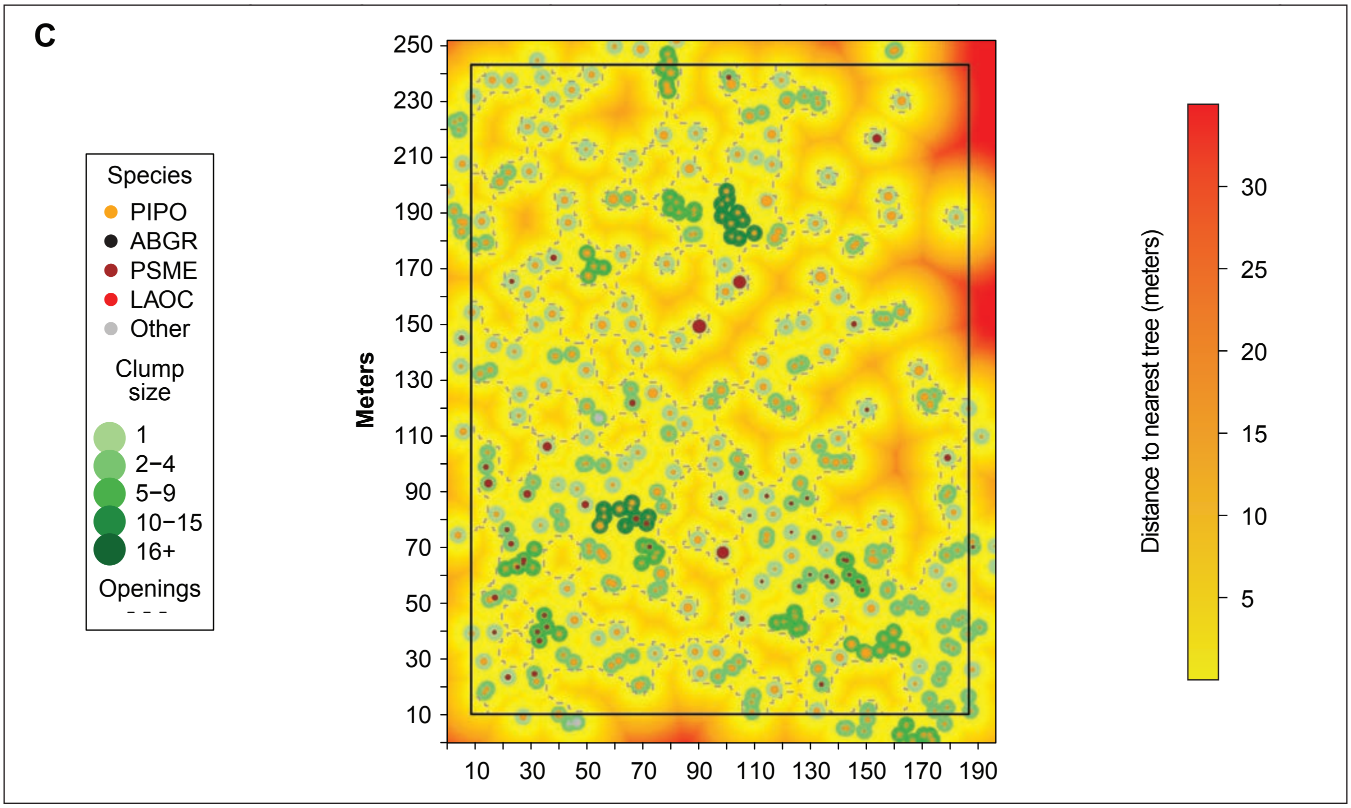


| D Intertree dist. (m) | Clump proportions (trees) | | | | | Clump proportions (basal area) | | | | | Clump quadratic mean diameter (cm) | | | | |
|---|---|---|---|---|---|---|---|---|---|---|---|---|---|---|---|
| | Clump size (No. of trees) | | | | | Clump size (No. of trees) | | | | | Clump size (No. of trees) | | | | |
| | 1 | 2-4 | 5-9 | 10-15 | 16+ | 1 | 2-4 | 5-9 | 10-15 | 16+ | 1 | 2-4 | 5-9 | 10-15 | 16+ |
| 2 | 0.83 | 0.17 | 0 | 0 | 0 | 0.9 | 0.1 | 0 | 0 | 0 | 49.9 | 37.5 | 0 | 0 | 0 |
| 3 | 0.71 | 0.29 | 0 | 0 | 0 | 0.81 | 0.19 | 0 | 0 | 0 | 51.5 | 38.6 | 0 | 0 | 0 |
| 4 | 0.61 | 0.37 | 0.02 | 0 | 0 | 0.74 | 0.26 | 0.01 | 0 | 0 | 52.8 | 39.8 | 33.1 | 0 | 0 |
| 5 | 0.5 | 0.37 | 0.13 | 0 | 0 | 0.66 | 0.28 | 0.06 | 0 | 0 | 55 | 41.8 | 33.2 | 0 | 0 |
| 6 | 0.38 | 0.41 | 0.16 | 0.06 | 0 | 0.52 | 0.36 | 0.09 | 0.03 | 0 | 56.6 | 45.2 | 36.6 | 32.6 | 0 |
| 7 | 0.26 | 0.43 | 0.2 | 0.11 | 0 | 0.41 | 0.4 | 0.14 | 0.05 | 0 | 59.9 | 46.3 | 40.2 | 33.8 | 0 |
| 0 | 0.08 | 0.28 | 0.2 | 0.04 | 0.41 | 0.14 | 0.39 | 0.18 | 0.02 | 0.27 | 64.9 | 56.9 | 45.7 | 38.2 | 38.7 |

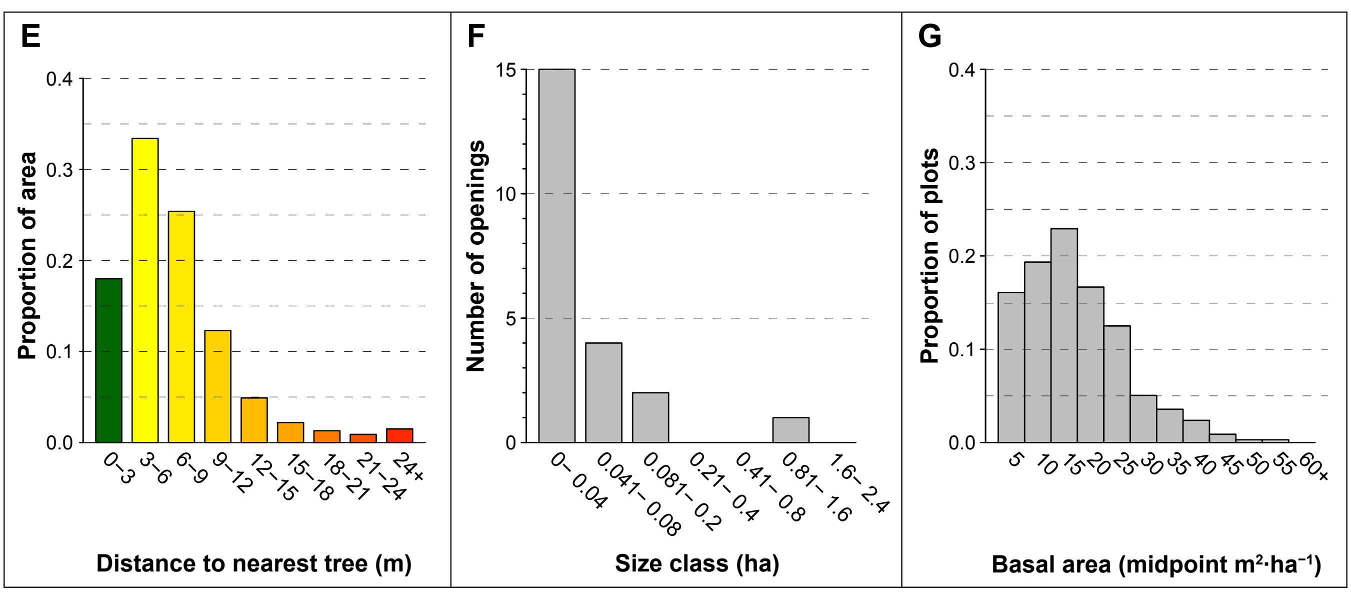

## Douglas-fir 3

**Location:** Canyon Creek Research Natural Area

**Plant association:** PSME/CARU-VASC

**Topography:** Slope: 10 to 25 percent, mean 15 percent; aspect: SE; elevation: 4,825 to 4,960 ft, mean 4,890 ft.

**Description:** This plot is on a southeast-facing slope above the East Fork of Canyon Creek. The northern portion of the plot is fairly dry and rocky, mostly composed of ponderosa pine. In contrast, the southern portion of the plot is more mesic, with an understory of grouseberry and a greater proportion of Douglas-fir.

### Summary metrics

| Hectares | Basal area | Trees | Avg. d.b.h. | QMD | Max height | Canopy cover | Acres | Basal area | Trees | Avg. d.b.h. | QMD | Max height | SDI |
|---|---|---|---|---|---|---|---|---|---|---|---|---|---|
| | *m²·ha⁻¹* | *ha⁻¹* | | | *m* | *Percent* | | *ft²·ac⁻¹* | *ac⁻¹* | | | *ft* | |
| 4.1 | 14 | 87 | 41.7 | 44.6 | 44 | 18 | 10.2 | 59 | 35 | 16.4 | 17.5 | 144 | 94 |

Avg. = average, d.b.h. = diameter at breast height, OMD = quadratic mean diameter, SDI = standard density index.

### Proportion of basal area

| PIPO | ABGR | PSME | LAOC | JUOC | PICO | CELE3 | Unknown |
|---|---|---|---|---|---|---|---|
| 0.847 | 0 | 0.035 | 0.041 | 0 | 0 | 0 | 0.078 |

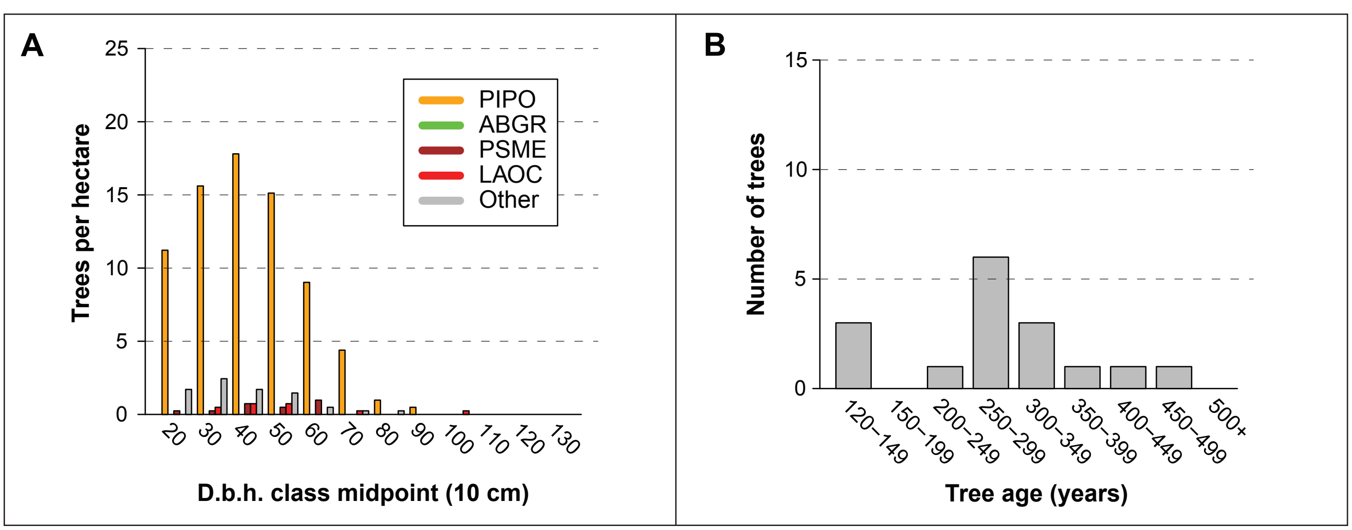

C

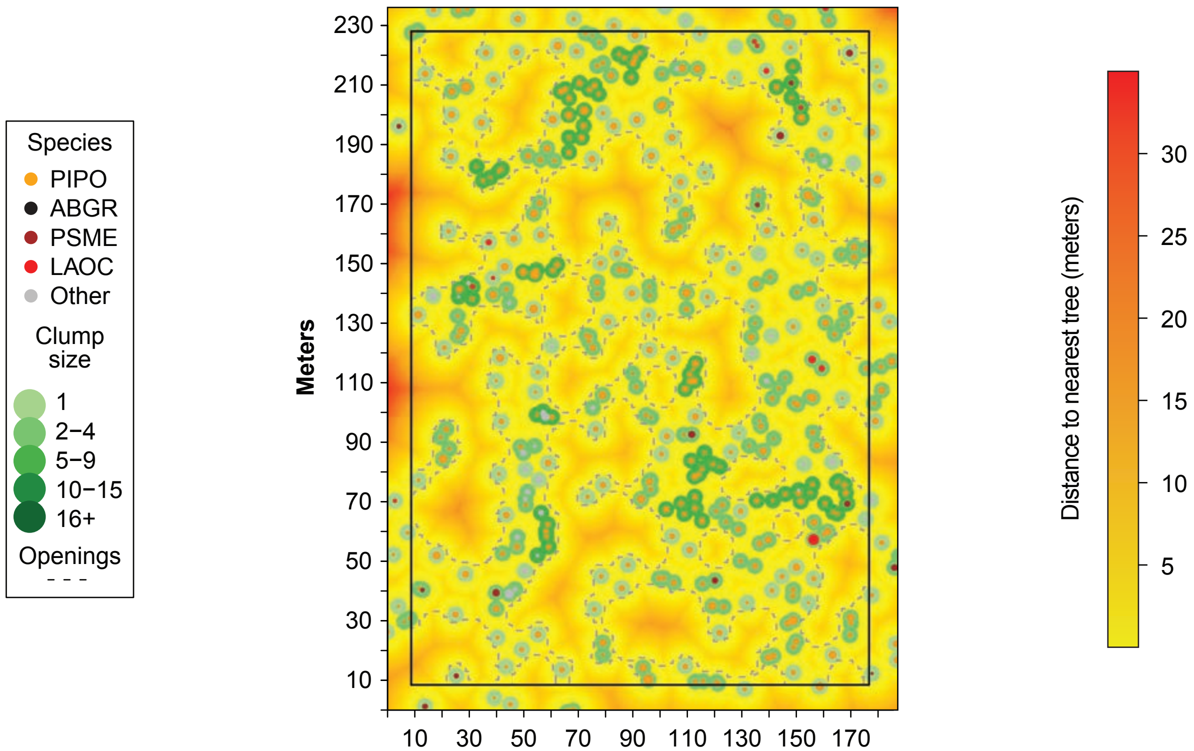


| D<br>Intertree dist. (m) | Clump proportions (trees)<br>Clump size (No. of trees) | | | | | Clump proportions (basal area)<br>Clump size (No. of trees) | | | | | Clump quadratic mean diameter (cm)<br>Clump size (No. of trees) | | | | |
|---|---|---|---|---|---|---|---|---|---|---|---|---|---|---|---|
| | 1 | 2-4 | 5-9 | 10-15 | 16+ | 1 | 2-4 | 5-9 | 10-15 | 16+ | 1 | 2-4 | 5-9 | 10-15 | 16+ |
| 2 | 0.86 | 0.14 | 0 | 0 | 0 | 0.87 | 0.13 | 0 | 0 | 0 | 44.9 | 42.2 | 0 | 0 | 0 |
| 3 | 0.68 | 0.29 | 0.03 | 0 | 0 | 0.72 | 0.25 | 0.03 | 0 | 0 | 45.8 | 41.5 | 43.8 | 0 | 0 |
| 4 | 0.61 | 0.34 | 0.06 | 0 | 0 | 0.66 | 0.29 | 0.05 | 0 | 0 | 46.5 | 41.5 | 41 | 0 | 0 |
| 5 | 0.47 | 0.39 | 0.13 | 0 | 0 | 0.5 | 0.4 | 0.1 | 0 | 0 | 45.9 | 44.9 | 38.3 | 0 | 0 |
| 6 | 0.34 | 0.42 | 0.24 | 0 | 0 | 0.36 | 0.45 | 0.19 | 0 | 0 | 46.2 | 46 | 39.4 | 0 | 0 |
| 7 | 0.25 | 0.32 | 0.24 | 0.1 | 0.1 | 0.28 | 0.36 | 0.2 | 0.08 | 0.08 | 47.4 | 47.5 | 40.6 | 39.7 | 41 |
| 10 | 0.09 | 0.18 | 0.16 | 0.13 | 0.45 | 0.1 | 0.22 | 0.13 | 0.11 | 0.44 | 47.8 | 49.8 | 39.8 | 41.9 | 44.1 |

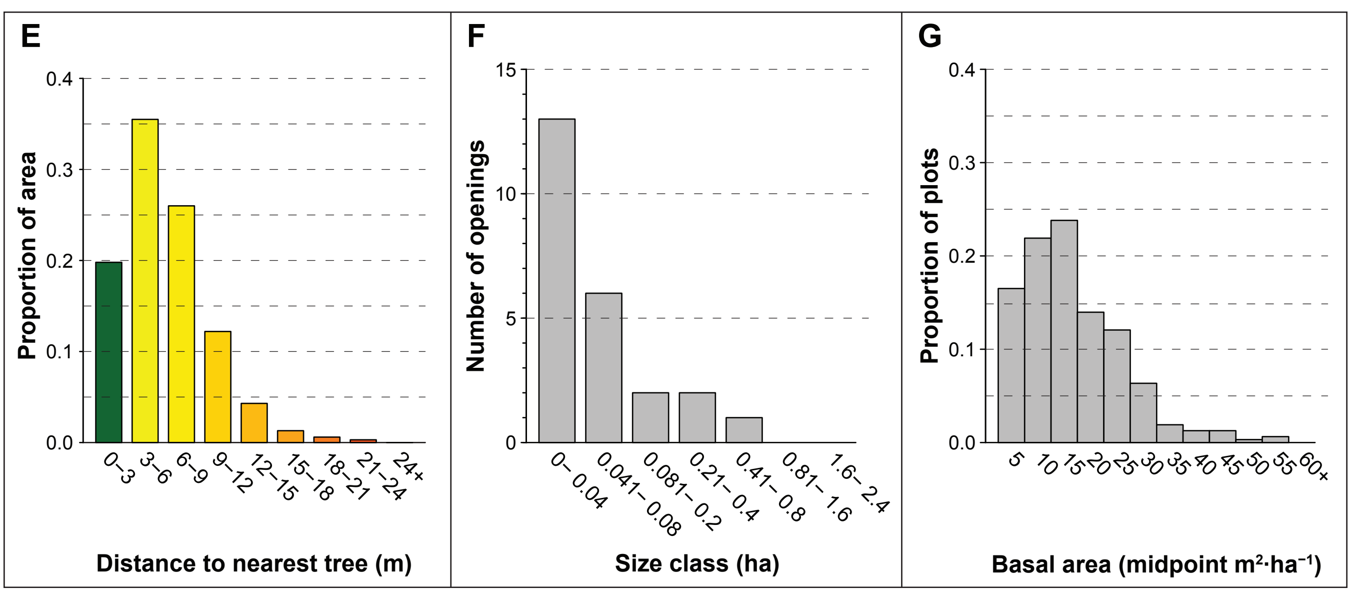

## Douglas-fir 4

**Location:** North of Dugout Creek Research Natural Area

**Plant association:** PSME/CARU

**Topography:** Slope: 20 to 40 percent, mean 25 percent; aspect: W; elevation: 5,200 to 5,380 ft, mean 5,300 ft.

**Description:** The plot is divided roughly in half by a large gulch. The southern portion, which faces to the northwest, is composed of smaller, denser Douglas-fir. The northern portion has a more prominent population of older pines. The south-facing downslope areas are occupied by small open patches of mountain mahogany.

### Summary metrics

| Hectares | Basal area | Trees | Avg. d.b.h. | QMD | Max height | Canopy cover | Acres | Basal area | Trees | Avg. d.b.h. | QMD | Max height | SDI |
|---|---|---|---|---|---|---|---|---|---|---|---|---|---|
| | *$m^2 \cdot ha^{-1}$* | *$ha^{-1}$* | | | *m* | *Percent* | | *$ft^2 \cdot ac^{-1}$* | *$ac^{-1}$* | | | *ft* | |
| 4.3 | 13 | 64 | 47.2 | 50.6 | 37 | 15 | 10.7 | 56 | 26 | 18.6 | 19.9 | 120 | 86 |

Avg. = average, d.b.h. = diameter at breast height, OMD = quadratic mean diameter, SDI = standard density index.

### Proportion of basal area

| PIPO | ABGR | PSME | LAOC | JUOC | PICO | CELE3 | Unknown |
|---|---|---|---|---|---|---|---|
| 0.908 | 0 | 0.087 | 0.041 | 0 | 0 | 0 | 0.005 |

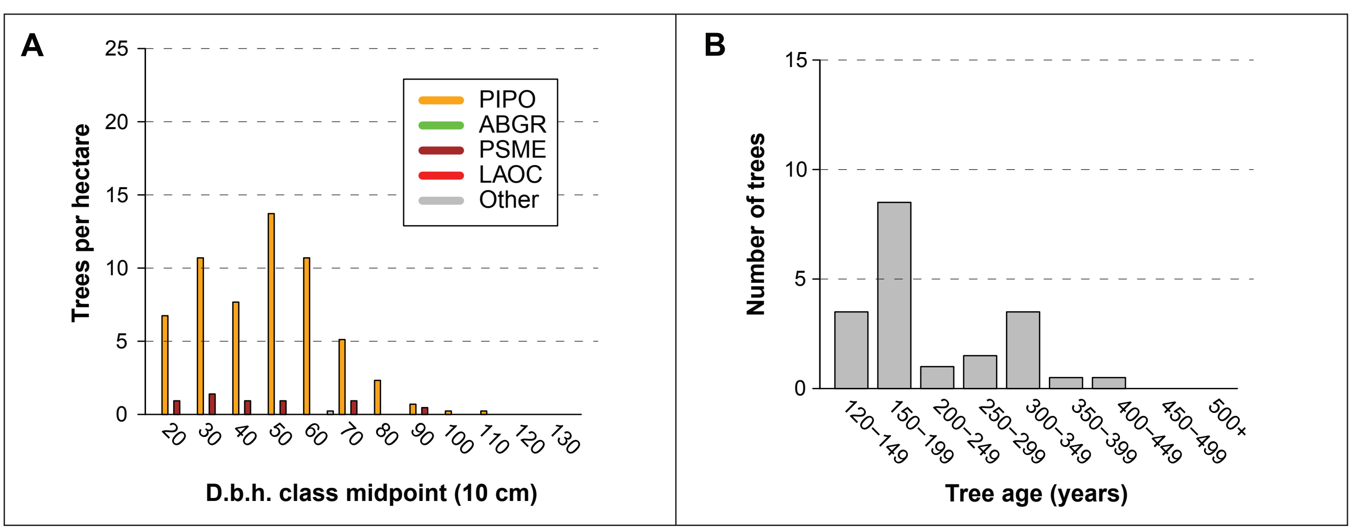

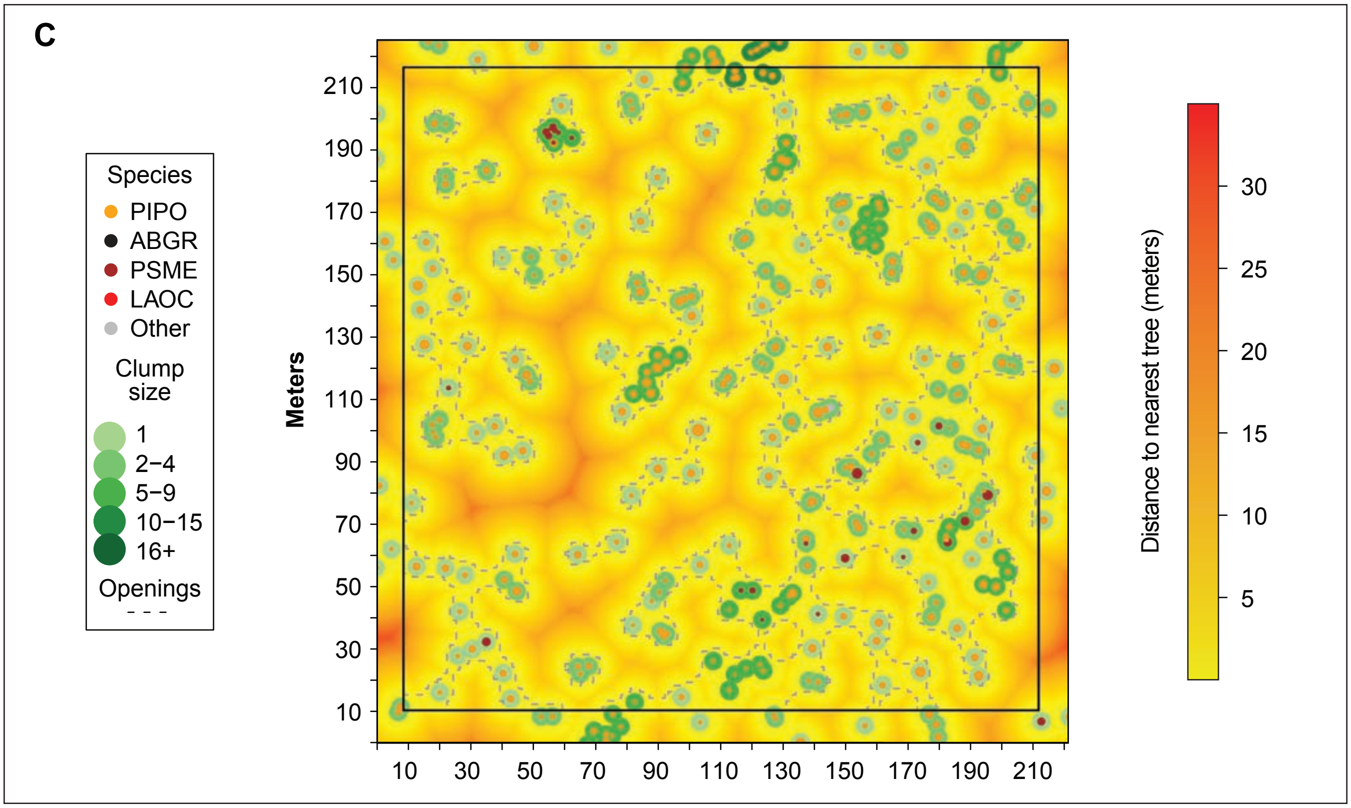


| D<br>Intertree dist. (m) | Clump proportions (trees) | | | | | Clump proportions (basal area) | | | | | Clump quadratic mean diameter (cm) | | | | |
|---|---|---|---|---|---|---|---|---|---|---|---|---|---|---|---|
| | Clump size (No. of trees) | | | | | Clump size (No. of trees) | | | | | Clump size (No. of trees) | | | | |
| | 1 | 2-4 | 5-9 | 10-15 | 16+ | 1 | 2-4 | 5-9 | 10-15 | 16+ | 1 | 2-4 | 5-9 | 10-15 | 16+ |
| 6 | 0.34 | 0.44 | 0.22 | 0 | 0 | 0.43 | 0.39 | 0.17 | 0 | 0 | 57.0 | 48.1 | 44.5 | 0 | 0 |

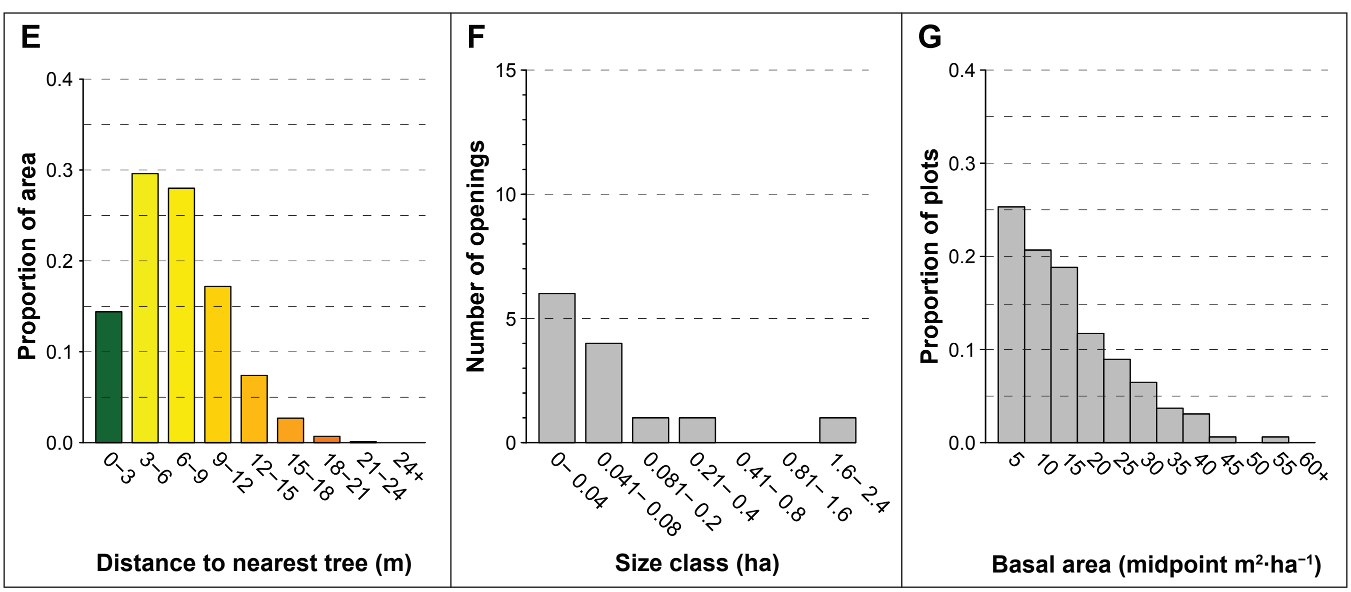

## Douglas-fir 5

**Location:** North of Dugout Creek Research Natural Area

**Plant association:** PSME/CAGE

**Topography:** Slope: 15 to 30 percent, mean 25 percent; aspect: W; elevation: 5,440 to 5,640 ft, mean 5,540 ft.

**Description:** This plot sits between Telephone Creek to the north and an unnamed perennial stream to the south. The plot's northeastern and southeastern corners feature large rocky outcrops. The remainder of the plot is an interspersed mixture of widely spaced old ponderosa pine and denser pole-sized Douglas-fir patches. The southwestern portion of the plot, which is lower on the slope, contains most of the old pines.

### Summary metrics

| Hectares | Basal area | Trees | Avg. d.b.h. | QMD | Max height | Canopy cover | Acres | Basal area | Trees | Avg. d.b.h. | QMD | Max height | SDI |
|---|---|---|---|---|---|---|---|---|---|---|---|---|---|
| | *$m^2 \cdot ha^{-1}$* | *$ha^{-1}$* | | | *m* | *Percent* | | *$ft^2 \cdot ac^{-1}$* | *$ac^{-1}$* | | | *ft* | |
| 4.1 | 22 | 74 | 57.8 | 61.3 | 37 | 23 | 10.1 | 95 | 30 | 22.8 | 24.1 | 119 | 137 |

Avg. = average, d.b.h. = diameter at breast height, OMD = quadratic mean diameter, SDI = standard density index.

### Proportion of basal area

| PIPO | ABGR | PSME | LAOC | JUOC | PICO | CELE3 | Unknown |
|---|---|---|---|---|---|---|---|
| 0.87 | 0 | 0.13 | 0 | 0 | 0 | 0 | 0 |

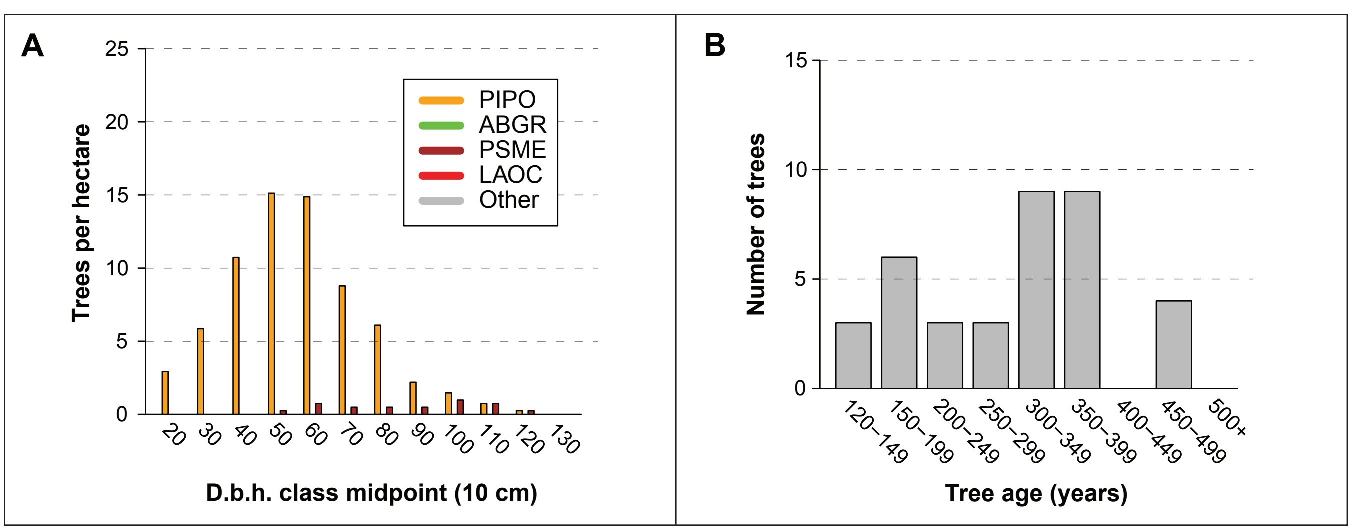

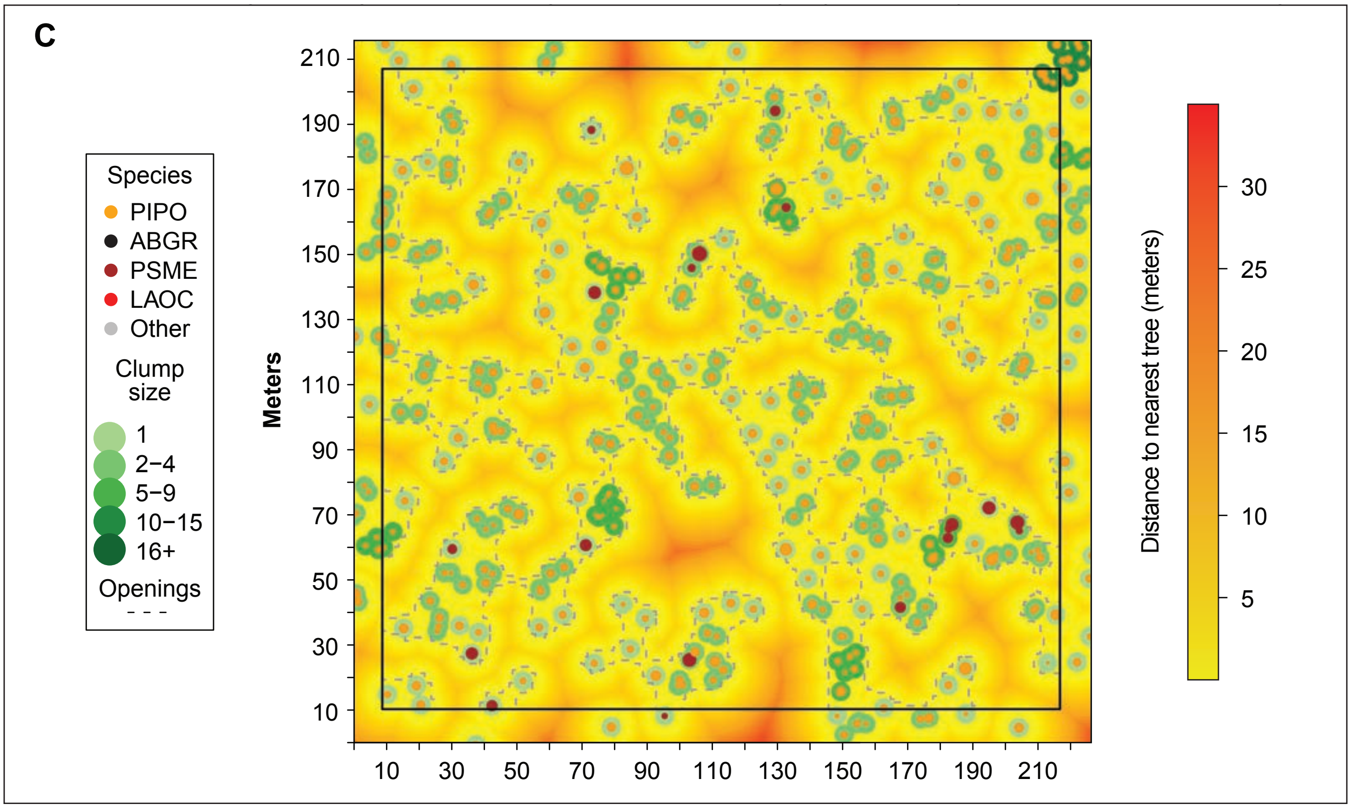


| D<br>Intertree dist. (m) | Clump proportions (trees) | | | | | Clump proportions (basal area) | | | | | Clump quadratic mean diameter (cm) | | | | |
|---|---|---|---|---|---|---|---|---|---|---|---|---|---|---|---|
| | Clump size (No. of trees) | | | | | Clump size (No. of trees) | | | | | Clump size (No. of trees) | | | | |
| | 1 | 2-4 | 5-9 | 10-15 | 16+ | 1 | 2-4 | 5-9 | 10-15 | 16+ | 1 | 2-4 | 5-9 | 10-15 | 16+ |
| 2 | 0.86 | 0.14 | 0 | 0 | 0 | 0.87 | 0.13 | 0 | 0 | 0 | 44.9 | 42.2 | 0 | 0 | 0 |
| 3 | 0.68 | 0.29 | 0.03 | 0 | 0 | 0.72 | 0.25 | 0.03 | 0 | 0 | 45.8 | 41.5 | 43.8 | 0 | 0 |
| 4 | 0.61 | 0.34 | 0.06 | 0 | 0 | 0.66 | 0.29 | 0.05 | 0 | 0 | 46.5 | 41.5 | 41 | 0 | 0 |
| 5 | 0.47 | 0.39 | 0.13 | 0 | 0 | 0.5 | 0.4 | 0.1 | 0 | 0 | 45.9 | 44.9 | 38.3 | 0 | 0 |
| 6 | 0.34 | 0.42 | 0.24 | 0 | 0 | 0.36 | 0.45 | 0.19 | 0 | 0 | 46.2 | 46 | 39.4 | 0 | 0 |
| 7 | 0.25 | 0.32 | 0.24 | 0.1 | 0.1 | 0.28 | 0.36 | 0.2 | 0.08 | 0.08 | 47.4 | 47.5 | 40.6 | 39.7 | 41 |
| 10 | 0.09 | 0.18 | 0.16 | 0.13 | 0.45 | 0.1 | 0.22 | 0.13 | 0.11 | 0.44 | 47.8 | 49.8 | 39.8 | 41.9 | 44.1 |

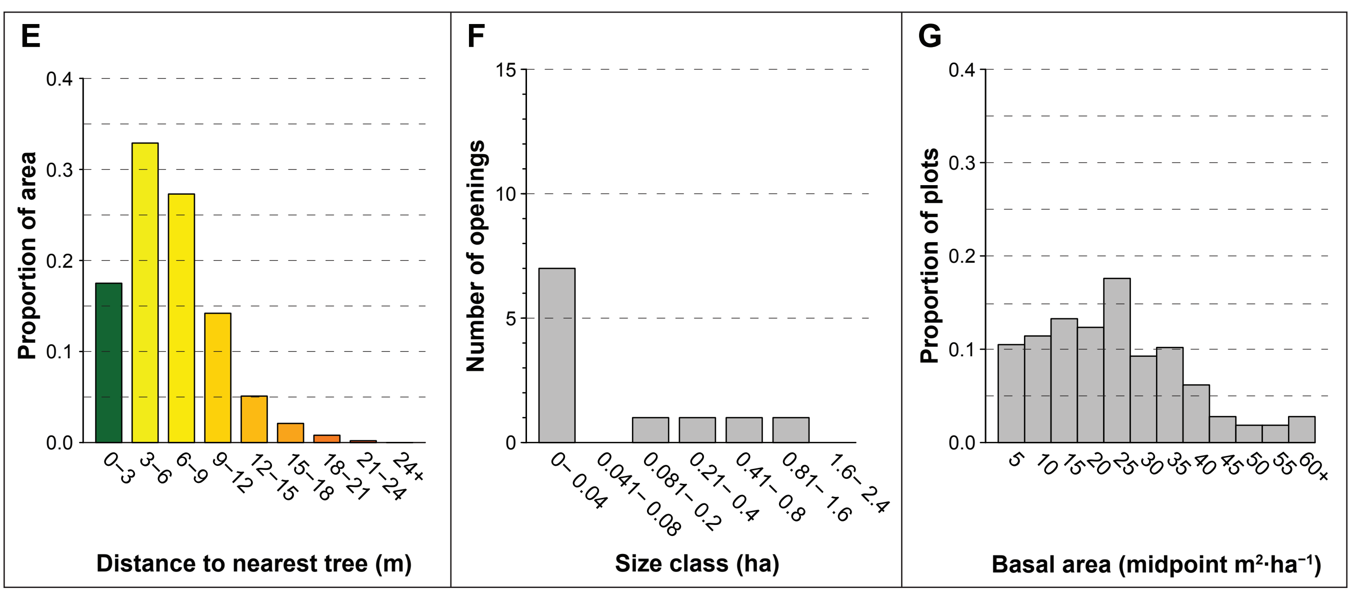

## Grand Fir 1

**Location:** Dugout Creek Research Natural Area

**Plant association:** ABGR/CARU

**Topography:** Slope: 15 to 25 percent, mean 20 percent; aspect: N; elevation: 5,650 to 5,790 ft, mean 5,710 ft.

**Description:** This plot is in the middle of a long slope running down to Stink Creek. The plot is contemporarily quite dense, and large openings are scarce. Almost all under- and mid-story trees are grand fir, with occasional western larch.

### Summary metrics

| Hectares | Basal area | Trees | Avg. d.b.h. | QMD | Max height | Canopy cover | Acres | Basal area | Trees | Avg. d.b.h. | QMD | Max height | SDI |
|---|---|---|---|---|---|---|---|---|---|---|---|---|---|
| | *$m^2 \cdot ha^{-1}$* | *$ha^{-1}$* | | | *m* | *Percent* | | *$ft^2 \cdot ac^{-1}$* | *$ac^{-1}$* | | | *ft* | |
| 5 | 24 | 161 | 40.3 | 43.6 | 40 | 31 | 12.3 | 105 | 65 | 15.9 | 17.2 | 130 | 168 |

Avg. = average, d.b.h. = diameter at breast height, OMD = quadratic mean diameter, SDI = standard density index.

### Proportion of basal area

| PIPO | ABGR | PSME | LAOC | JUOC | PICO | CELE3 | Unknown |
|---|---|---|---|---|---|---|---|
| 0.501 | 0.438 | 0.039 | 0.013 | 0 | 0 | 0 | 0.008 |

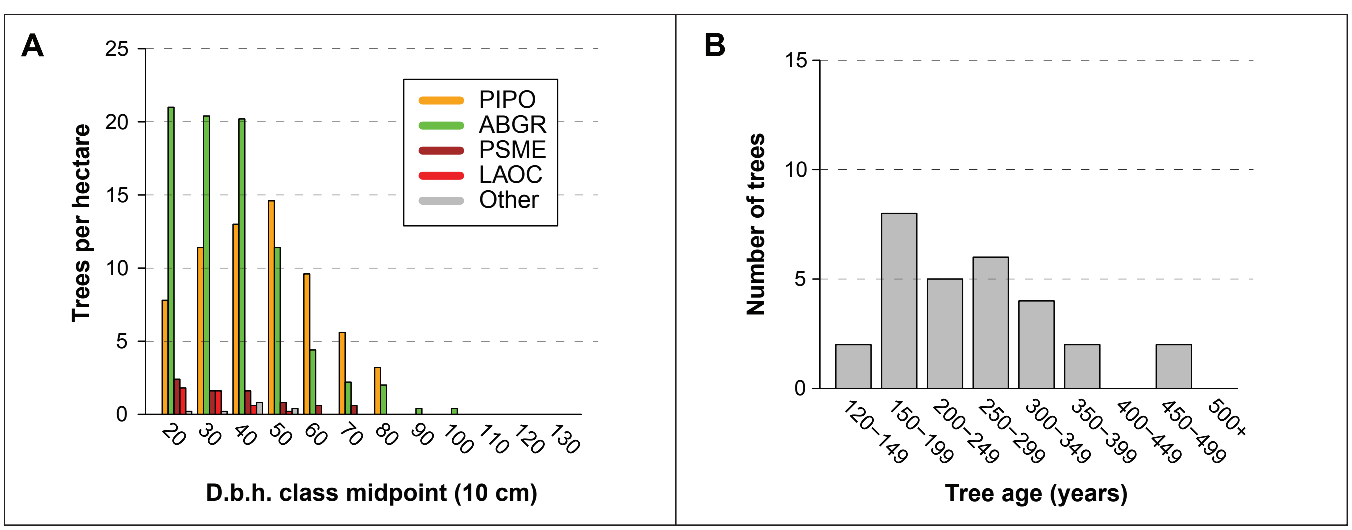

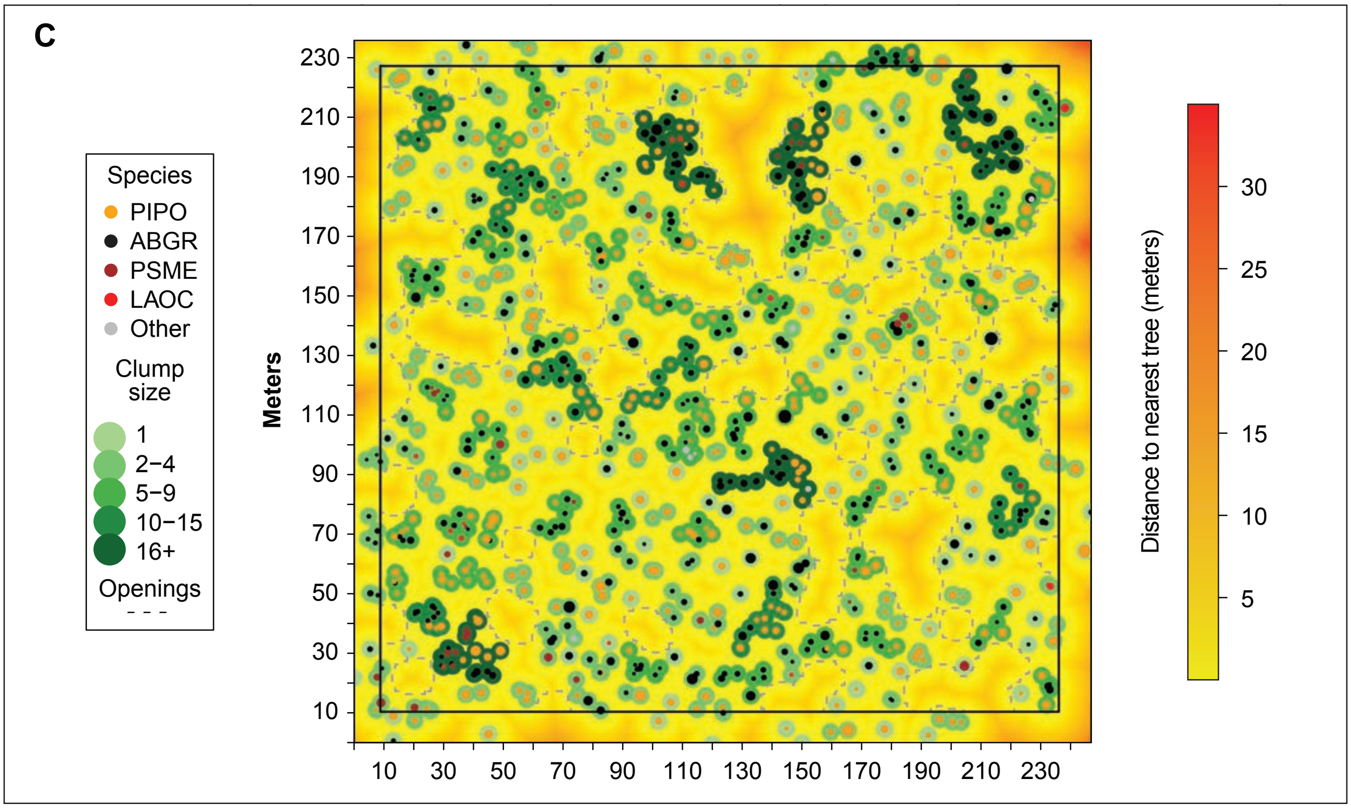


**D**

| Intertree dist. (m) | Clump proportions (trees) | | | | | Clump proportions (basal area) | | | | | Clump quadratic mean diameter (cm) | | | | |
|---|---|---|---|---|---|---|---|---|---|---|---|---|---|---|---|
| | Clump size (No. of trees) | | | | | Clump size (No. of trees) | | | | | Clump size (No. of trees) | | | | |
| | 1 | 2-4 | 5-9 | 10-15 | 16+ | 1 | 2-4 | 5-9 | 10-15 | 16+ | 1 | 2-4 | 5-9 | 10-15 | 16+ |
| 2 | 0.71 | 0.27 | 0.02 | 0 | 0 | 0.77 | 0.22 | 0.01 | 0 | 0 | 45.5 | 39 | 29.7 | 0 | 0 |
| 3 | 0.49 | 0.46 | 0.05 | 0 | 0 | 0.58 | 0.39 | 0.03 | 0 | 0 | 47.5 | 40.2 | 31.8 | 0 | 0 |
| 4 | 0.35 | 0.47 | 0.15 | 0.03 | 0 | 0.43 | 0.44 | 0.1 | 0.03 | 0 | 48.6 | 42 | 35.6 | 42.3 | 0 |
| 5 | 0.22 | 0.36 | 0.31 | 0.09 | 0.02 | 0.28 | 0.38 | 0.24 | 0.09 | 0.01 | 49.5 | 44.3 | 38.5 | 43.3 | 36.1 |
| 6 | 0.13 | 0.27 | 0.35 | 0.11 | 0.14 | 0.19 | 0.31 | 0.29 | 0.08 | 0.13 | 52.7 | 46 | 39.9 | 37.2 | 42.9 |
| 7 | 0.08 | 0.19 | 0.24 | 0.15 | 0.34 | 0.11 | 0.22 | 0.2 | 0.13 | 0.33 | 52.3 | 46.2 | 40.2 | 41.3 | 43.1 |
| 10 | 0.01 | 0.02 | 0.04 | 0.08 | 0.84 | 0.03 | 0.03 | 0.04 | 0.08 | 0.82 | 61.6 | 47.9 | 42.9 | 43.1 | 43.2 |

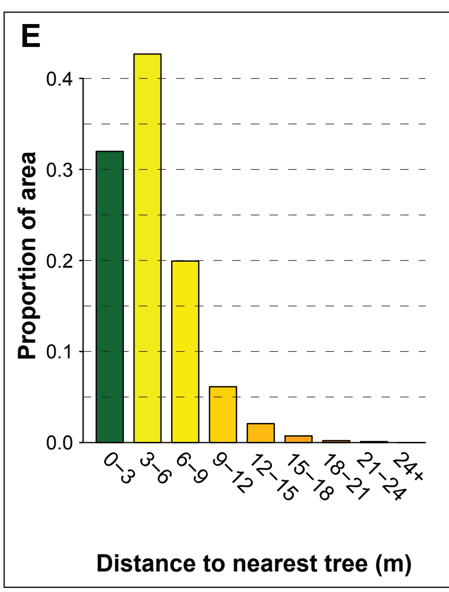


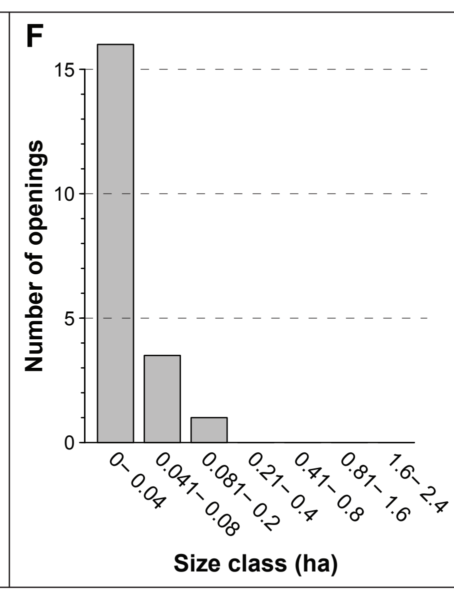


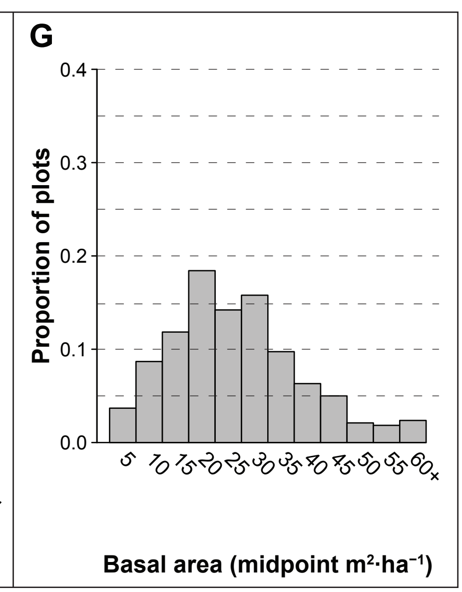

## Grand Fir 2

**Location:** Dugout Creek Research Natural Area

**Plant association:** ABGR/CARU

**Topography:** Slope: 20 to 40 percent, mean 30 percent; aspect: N; elevation: 5,400 to 5,600 ft, mean 5,495 ft.

**Description:** This plot sits below Grand fir 1 and immediately south of Stink Creek. It is somewhat steep, and vegetation is quite dense. Most of the plot is a combination of small patches of dense grand fir regeneration and larger patches of mid- and overstory trees. Some large, very old grand fir are present.

### Summary metrics

| Hectares | Basal area | Trees | Avg. d.b.h. | QMD | Max height | Canopy cover | Acres | Basal area | Trees | Avg. d.b.h. | QMD | Max height | SDI |
|---|---|---|---|---|---|---|---|---|---|---|---|---|---|
| | *$m^2 \cdot ha^{-1}$* | *$ha^{-1}$* | | | *m* | *Percent* | | *$ft^2 \cdot ac^{-1}$* | *$ac^{-1}$* | | | *ft* | |
| 4 | 23 | 197 | 35.2 | 38.3 | 41 | 33 | 9.8 | 99 | 80 | 13.9 | 15.1 | 135 | 165 |

Avg. = average, d.b.h. = diameter at breast height, OMD = quadratic mean diameter, SDI = standard density index.

### Proportion of basal area

| PIPO | ABGR | PSME | LAOC | JUOC | PICO | CELE3 | Unknown |
|---|---|---|---|---|---|---|---|
| 0.364 | 0.473 | 0.055 | 0.06 | 0 | 0.001 | 0 | 0.046 |

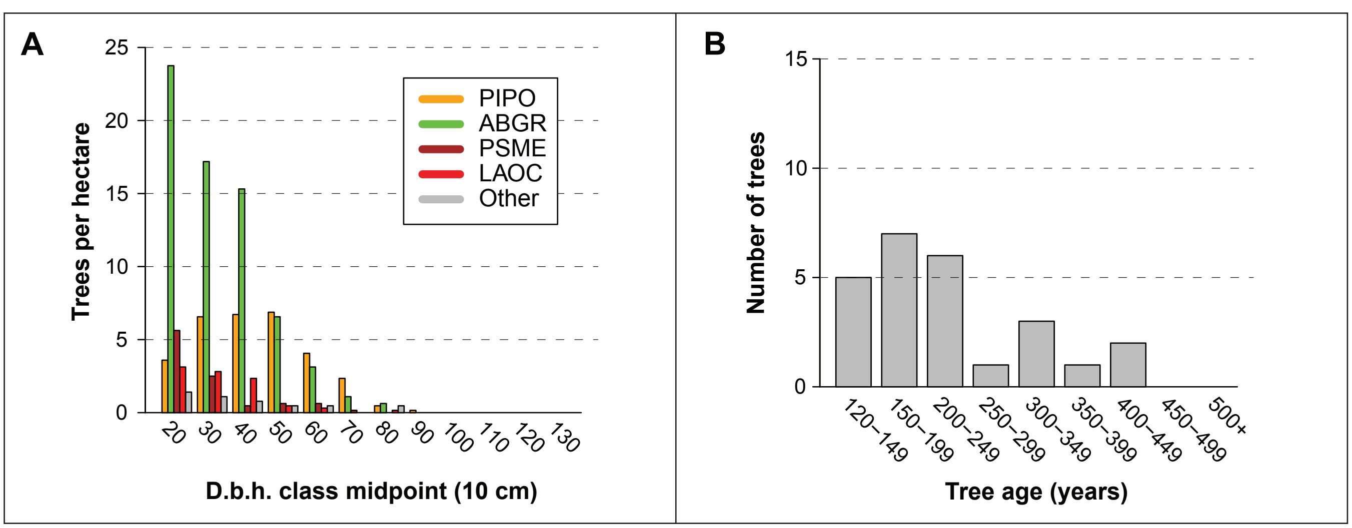

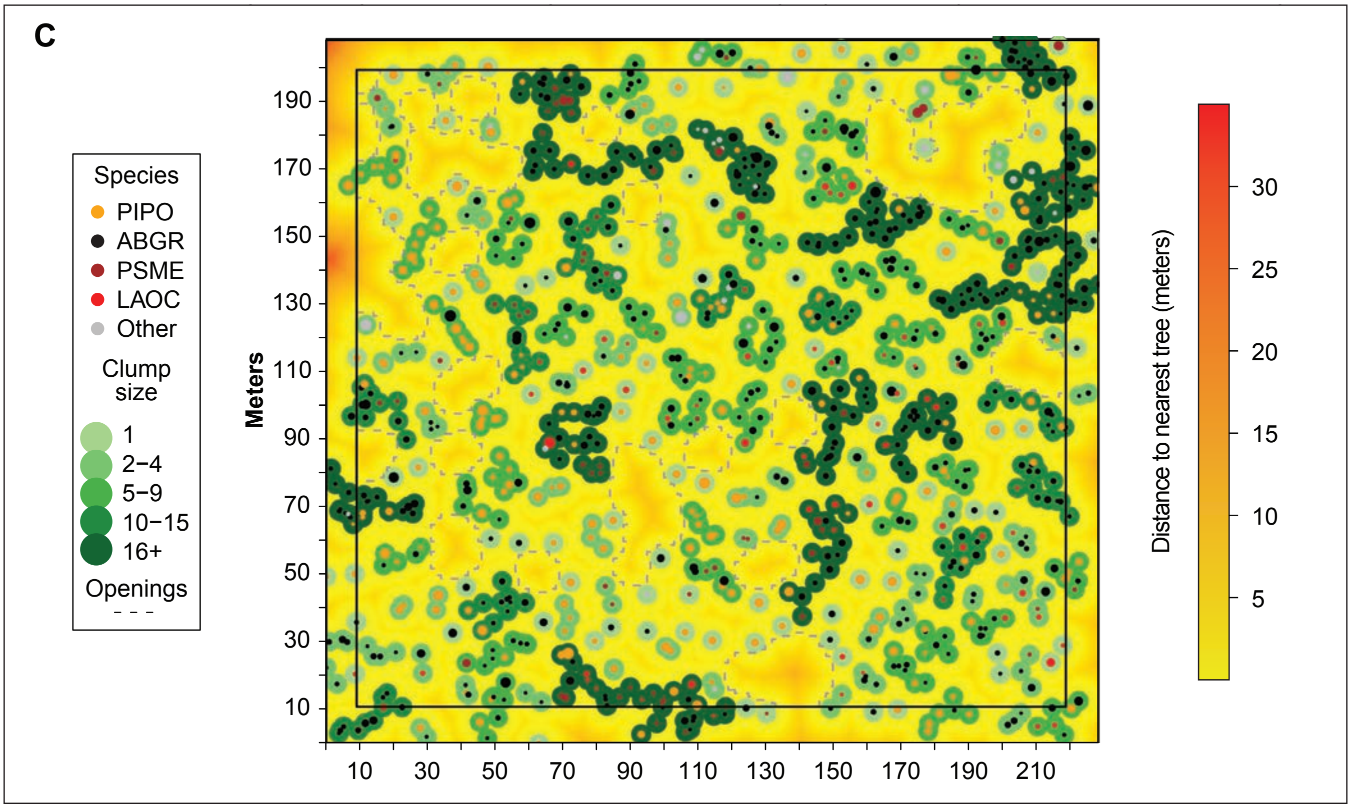


| D Intertree dist. (m) | Clump proportions (trees) | | | | | Clump proportions (basal area) | | | | | Clump quadratic mean diameter (cm) | | | | |
|---|---|---|---|---|---|---|---|---|---|---|---|---|---|---|---|
| | Clump size (No. of trees) | | | | | Clump size (No. of trees) | | | | | Clump size (No. of trees) | | | | |
| | 1 | 2-4 | 5-9 | 10-15 | 16+ | 1 | 2-4 | 5-9 | 10-15 | 16+ | 1 | 2-4 | 5-9 | 10-15 | 16+ |
| 2 | 0.71 | 0.29 | 0 | 0 | 0 | 0.74 | 0.26 | 0 | 0 | 0 | 39 | 36.4 | 0 | 0 | 0 |
| 3 | 0.49 | 0.46 | 0.06 | 0 | 0 | 0.53 | 0.43 | 0.04 | 0 | 0 | 40.1 | 36.9 | 32.2 | 0 | 0 |
| 4 | 0.33 | 0.44 | 0.16 | 0.05 | 0.02 | 0.39 | 0.42 | 0.13 | 0.04 | 0.02 | 41.4 | 37.6 | 34.7 | 35.1 | 33.8 |
| 5 | 0.2 | 0.34 | 0.27 | 0.08 | 0.11 | 0.24 | 0.34 | 0.26 | 0.06 | 0.09 | 42.3 | 38 | 37.8 | 35.3 | 34.4 |
| 6 | 0.1 | 0.2 | 0.27 | 0.16 | 0.27 | 0.14 | 0.23 | 0.27 | 0.15 | 0.22 | 44.4 | 40.4 | 38.5 | 36.2 | 34.9 |
| 7 | 0.05 | 0.11 | 0.18 | 0.12 | 0.53 | 0.09 | 0.14 | 0.21 | 0.12 | 0.45 | 49.7 | 42.1 | 41.5 | 37.7 | 34.9 |
| 10 | 0.01 | 0.03 | 0.03 | 0.03 | 0.91 | 0.01 | 0.04 | 0.04 | 0.03 | 0.89 | 41.2 | 45.2 | 42.8 | 40.3 | 37.8 |

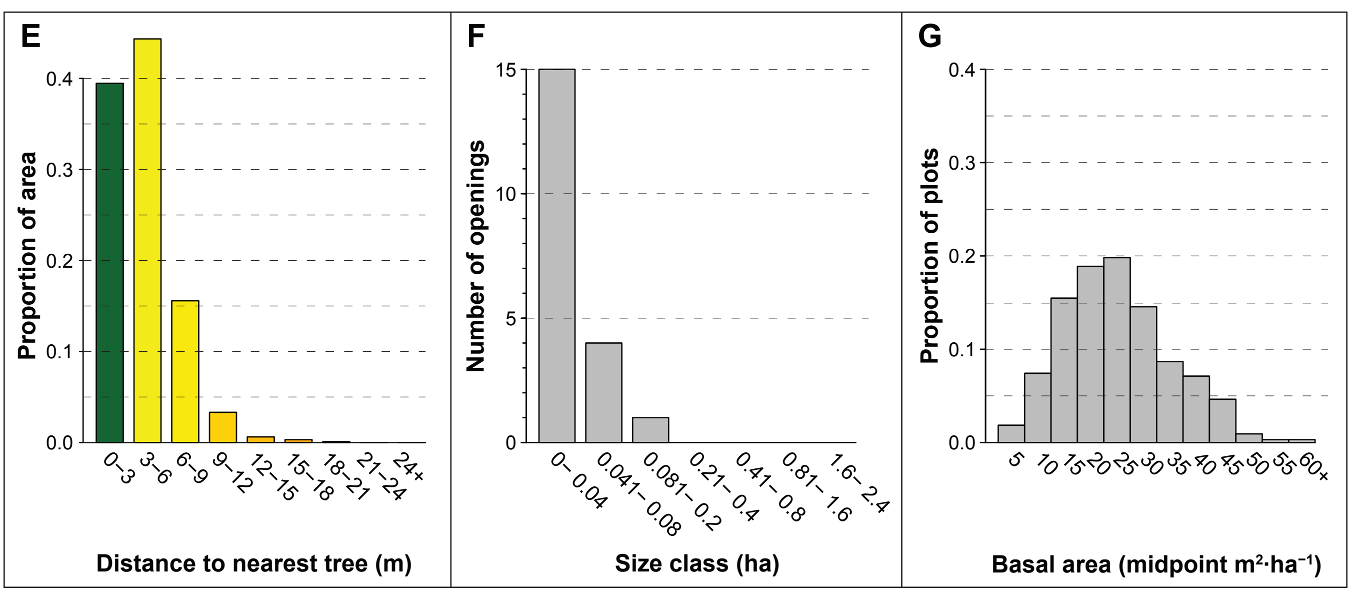

## Grand Fir 3

**Location:** Canyon Creek Research Natural Area

**Plant association:** ABGR/CARU

**Topography:** Slope: 15 to 30 percent, mean 20 percent; aspect: E; elevation: 5,390 to 5,520 ft, mean 5,450 ft.

**Description:** This plot lies on a narrow flat above an unnamed tributary of East Fork Canyon Creek. The flatter portions of the plot consist of young grand fir and old ponderosa pine. The upslope portions are mainly composed of 150-year-old western larch, many of which have died or are declining in vigor. A high-severity fire appears to have occurred in portions of this plot around 150 years ago, which initiated the larch cohort.

### Summary metrics

| Hectares | Basal area | Trees | Avg. d.b.h. | QMD | Max height | Canopy cover | Acres | Basal area | Trees | Avg. d.b.h. | QMD | Max height | SDI |
|---|---|---|---|---|---|---|---|---|---|---|---|---|---|
| | *$m^2 \cdot ha^{-1}$* | *$ha^{-1}$* | | | *m* | *Percent* | | *$ft^2 \cdot ac^{-1}$* | *$ac^{-1}$* | | | *ft* | |
| 2.3 | 11 | 53 | 44.1 | 51.5 | 43 | 13 | 5.6 | 48 | 22 | 17.3 | 20.3 | 141 | 74 |

Avg. = average, d.b.h. = diameter at breast height, OMD = quadratic mean diameter, SDI = standard density index.

### Proportion of basal area

| PIPO | ABGR | PSME | LAOC | JUOC | PICO | CELE3 | Unknown |
|---|---|---|---|---|---|---|---|
| 0.773 | 0.137 | 0 | 0.09 | 0 | 0 | 0 | 0 |

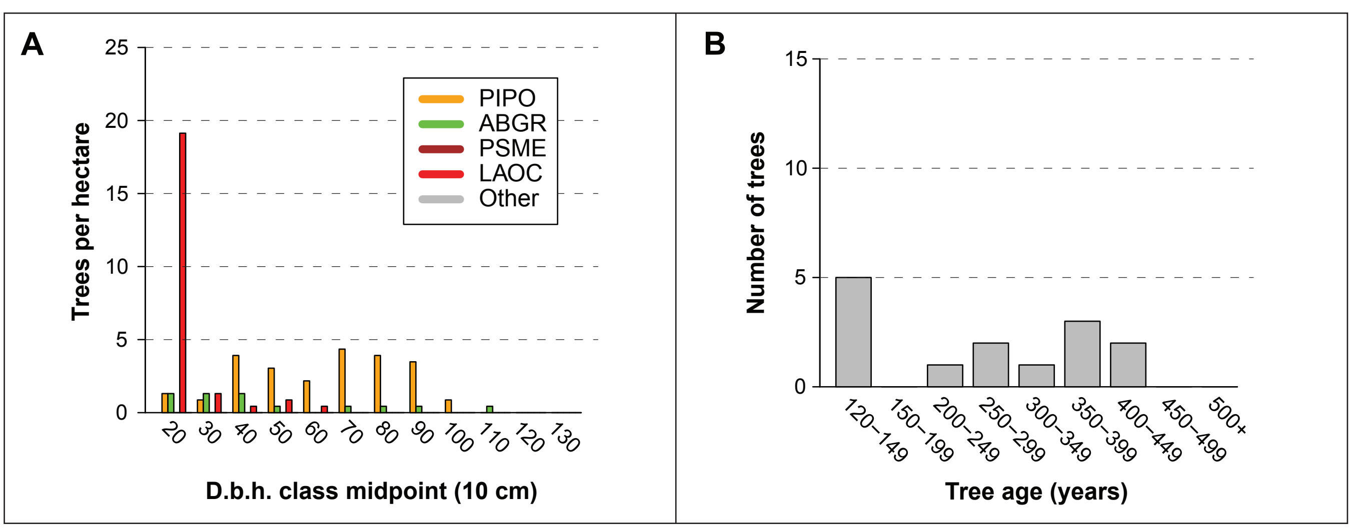

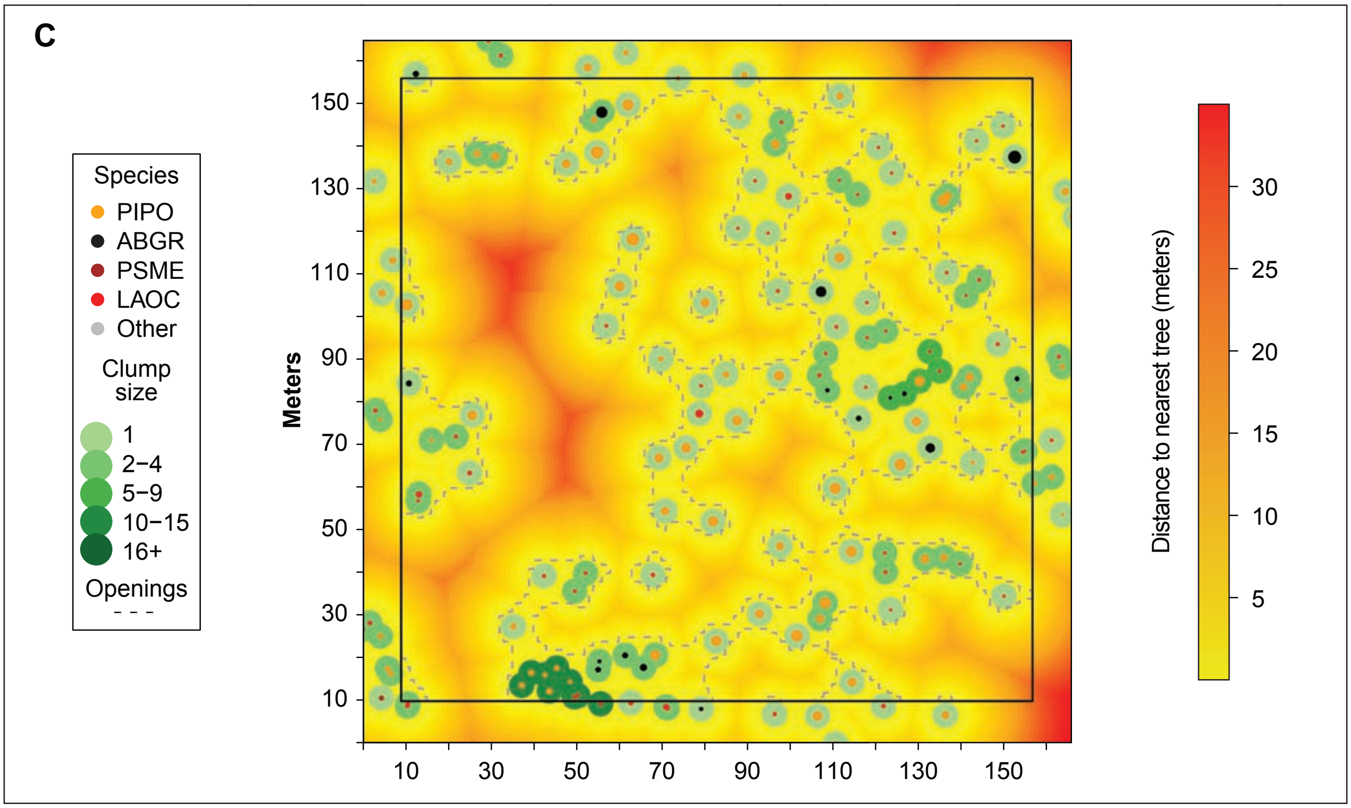


| D<br>Intertree dist. (m) | Clump proportions (trees) | | | | | Clump proportions (basal area) | | | | | Clump quadratic mean diameter (cm) | | | | |
|---|---|---|---|---|---|---|---|---|---|---|---|---|---|---|---|
| | Clump size (No. of trees) | | | | | Clump size (No. of trees) | | | | | Clump size (No. of trees) | | | | |
| | 1 | 2-4 | 5-9 | 10-15 | 16+ | 1 | 2-4 | 5-9 | 10-15 | 16+ | 1 | 2-4 | 5-9 | 10-15 | 16+ |
| 2 | 0.9 | 0.1 | 0 | 0 | 0 | 0.94 | 0.06 | 0 | 0 | 0 | 52.7 | 39.5 | 0 | 0 | 0 |
| 3 | 0.85 | 0.15 | 0 | 0 | 0 | 0.88 | 0.12 | 0 | 0 | 0 | 52.6 | 45.2 | 0 | 0 | 0 |
| 4 | 0.77 | 0.15 | 0.08 | 0 | 0 | 0.82 | 0.15 | 0.03 | 0 | 0 | 53.3 | 51.8 | 30.7 | 0 | 0 |
| 5 | 0.62 | 0.3 | 0 | 0.08 | 0 | 0.71 | 0.26 | 0 | 0.03 | 0 | 55.4 | 47.7 | 0 | 30.7 | 0 |
| 6 | 0.53 | 0.34 | 0.04 | 0.08 | 0 | 0.68 | 0.26 | 0.02 | 0.03 | 0 | 58.3 | 45.2 | 39.1 | 30.7 | 0 |
| 7 | 0.42 | 0.39 | 0.11 | 0.08 | 0 | 0.55 | 0.34 | 0.08 | 0.03 | 0 | 59 | 48 | 45.7 | 30.7 | 0 |
| 10 | 0.17 | 0.32 | 0.2 | 0 | 0.32 | 0.21 | 0.28 | 0.25 | 0 | 0.26 | 57.6 | 48.7 | 58 | 0 | 46.3 |

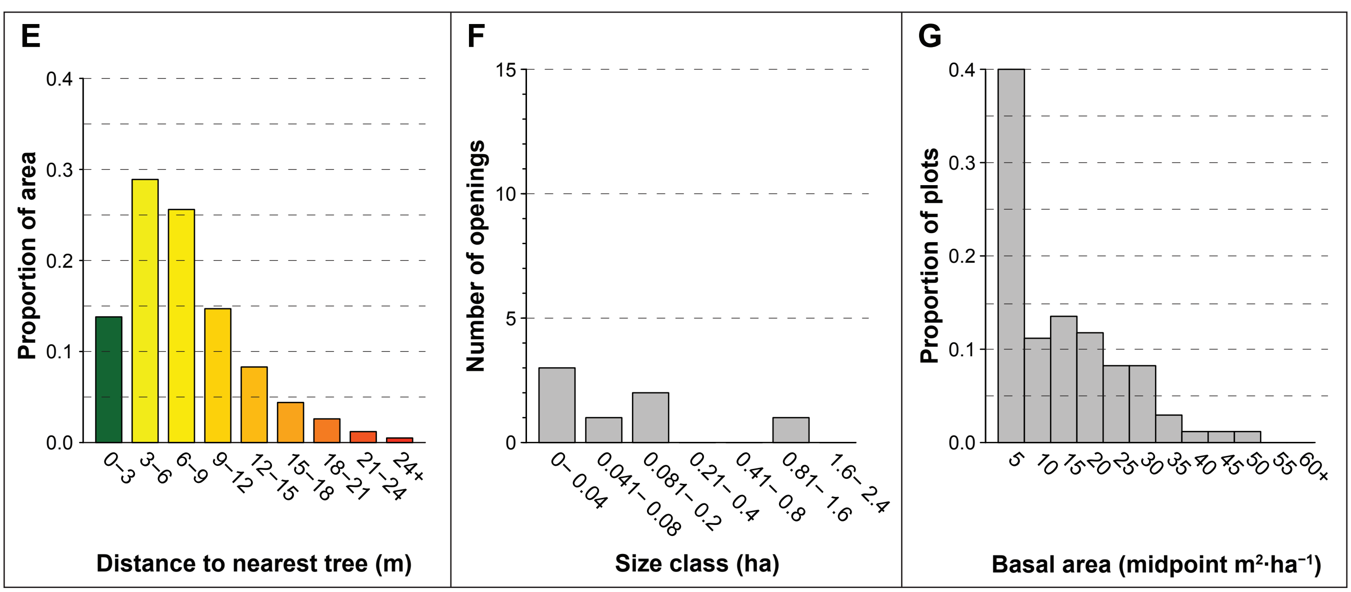

## Grand Fir 4

**Location:** Canyon Creek Research Natural Area

**Plant association:** ABGR/CAGE-VASC

**Topography:** Slope: 5 to 50 percent, mean 15 pecent; aspect: split, E and S; elevation: 5,540-5,685 ft, mean 5,590 ft.

**Description:** This plot straddles a draw running from northwest to southeast. The southern aspect portions contain very large old ponderosa pine with some old grand fir, while the areas across the draw have more medium-size Douglas-fir and grand fir with some lodgepole pine and larch. The understory is covered with grouseberry in shady spots, but grades into elk sedge and pinegrass in drier openings.

### Summary metrics

| Hectares | Basal area | Trees | Avg. d.b.h. | QMD | Max height | Canopy cover | Acres | Basal area | Trees | Avg. d.b.h. | QMD | Max height | SDI |
|---|---|---|---|---|---|---|---|---|---|---|---|---|---|
| | *$m^2 \cdot ha^{-1}$* | *$ha^{-1}$* | | | *m* | *Percent* | | *$ft^2 \cdot ac^{-1}$* | *$ac^{-1}$* | | | *ft* | |
| 4.3 | 20 | 122 | 41.8 | 45.3 | 43 | 25 | 10.7 | 85 | 49 | 16.5 | 17.8 | 142 | 135 |

Avg. = average, d.b.h. = diameter at breast height, OMD = quadratic mean diameter, SDI = standard density index.

### Proportion of basal area

| PIPO | ABGR | PSME | LAOC | JUOC | PICO | CELE3 | Unknown |
|---|---|---|---|---|---|---|---|
| 0.409 | 0.479 | 0.094 | 0.012 | 0 | 0.002 | 0 | 0.003 |

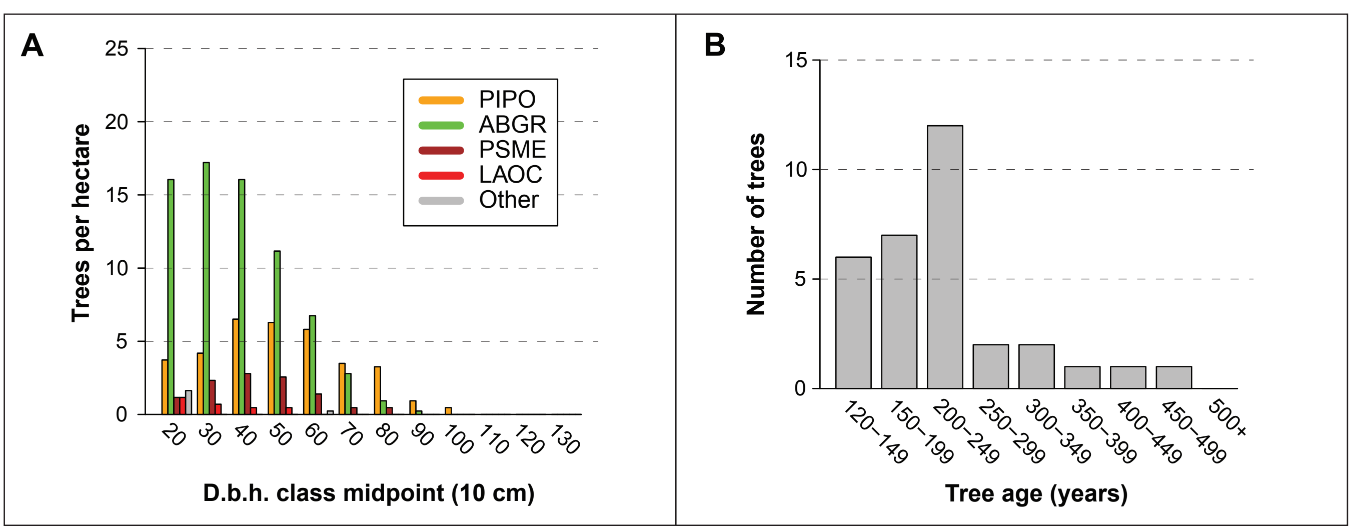

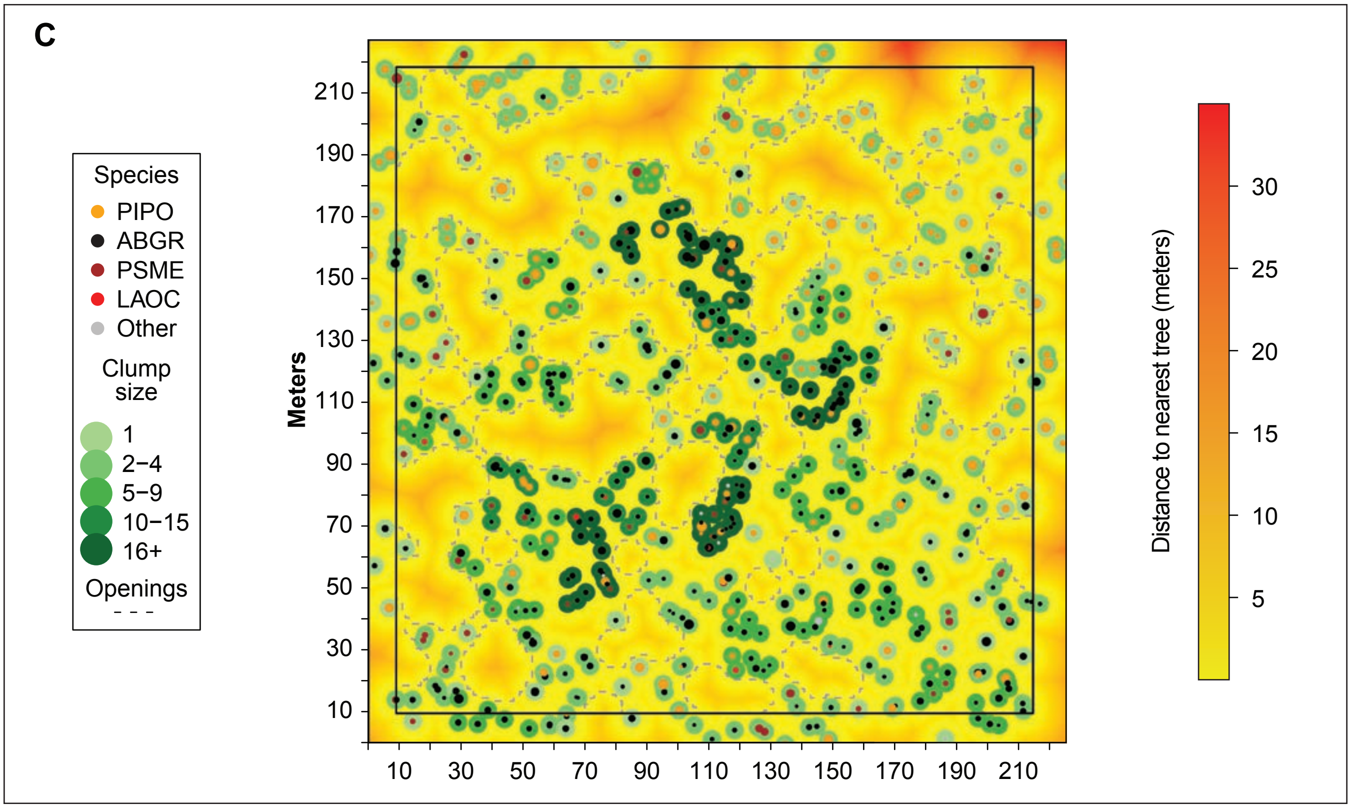


| D<br>Intertree dist. (m) | Clump proportions (trees) | | | | | Clump proportions (basal area) | | | | | Clump quadratic mean diameter (cm) | | | | |
|---|---|---|---|---|---|---|---|---|---|---|---|---|---|---|---|
| | Clump size (No. of trees) | | | | | Clump size (No. of trees) | | | | | Clump size (No. of trees) | | | | |
| | 1 | 2-4 | 5-9 | 10-15 | 16+ | 1 | 2-4 | 5-9 | 10-15 | 16+ | 1 | 2-4 | 5-9 | 10-15 | 16+ |
| 6 | 0.17 | 0.33 | 0.22 | 0.11 | 0.18 | 0.25 | 0.33 | 0.19 | 0.10 | 0.14 | 54.8 | 44.9 | 42.4 | 42.7 | 40.6 |

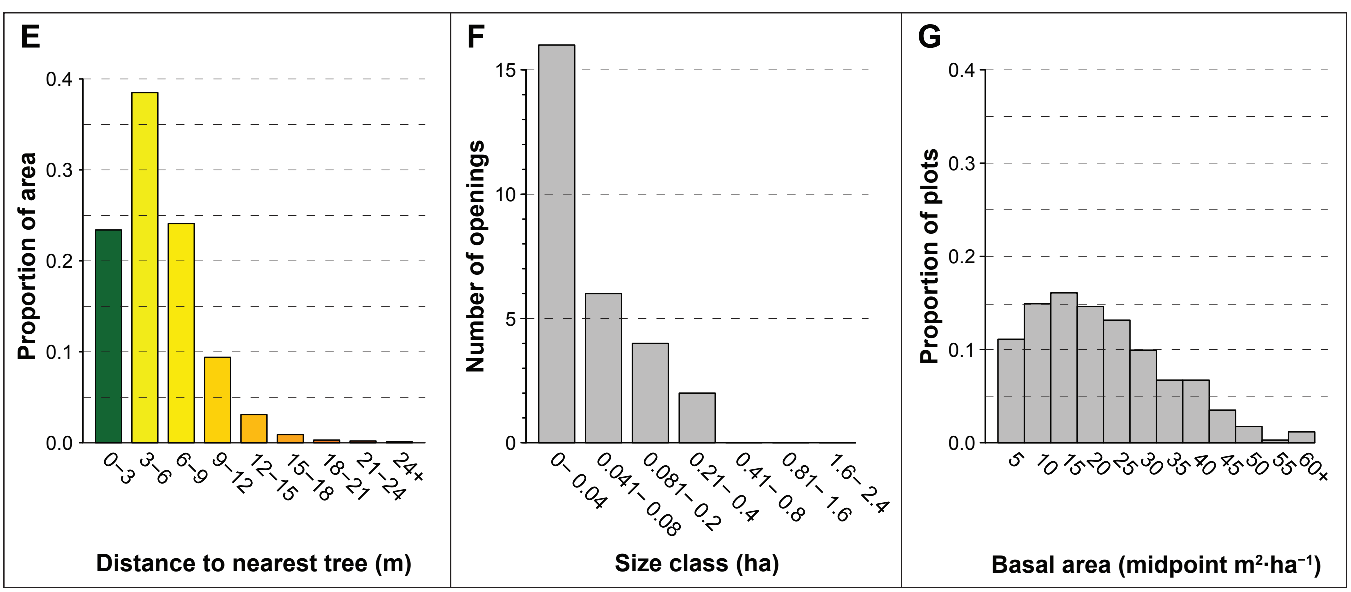

# Chapter 5: Ecological Implications

## Structure, Density, Composition, and Age

The historical stem densities and basal areas found in this reconstruction study are consistent with other reference condition studies in pine and mixed-conifer, frequent-fire forests in the Western United States (Abella and Denton 2009, Clyatt et al. 2016, Fry et al. 2014, Harrod et al. 1999, Larson et al. 2012, Lydersen et al. 2013, Reynolds et al. 2013, Schneider et al. 2015, Taylor 2004, Youngblood et al. 2004). The historical basal areas in this study are generally in the upper $50^{th}$ percentile of those found on ponderosa pine (*Pinus ponderosa* Lawson & C. Lawson) and mixed-conifer forest types on the Klamath and Warm Springs Indian Reservations in 1920s timber inventories (Hagmann et al. 2013, 2014). While direct comparisons among studies are complicated by differences in reconstruction methods (especially lower diameter cutoffs); frequent-fire forests with active fire regimes historically had densities well below maximum carrying capacities (Kaufmann et al. 2007). The dramatic increase in density after fire exclusion is clear evidence of this (Agee 1993). The basal areas and equivalent stand density index (SDI) levels found in this study are in line with this conclusion. Even the higher density grand fir (*Abies grandis* (Douglas ex D. Don) Lindl.) plots were relatively open-canopy forests with reconstructed canopy cover just over 30 percent (table 3.1).

The dominance of ponderosa pine on the pine and Douglas-fir (*Pseudotsuga menziesii* (Mirb.) Franco) series plots is also consistent with other reference condition studies in these forest types in Oregon and Washington (Churchill 2013; Hagmann et al. 2013, 2014; Harrod et al. 1999). The high percentage of grand fir (*Abies grandis* (Douglas ex D. Don) Lindl.) in terms of tree density and basal area on three of the four grand fir plots was surprising, as these sites are on dry grand fir plant associations within a dry forest landscape that had a frequent-fire-regime (Heyerdahl et al. 2001). Data from other sites in central and eastern Oregon indicate that grand and white fir (*Abies concolor* (Gord. & Glend.) Lindl. ex Hildebr, plant associations were historically dominated by ponderosa pine (Hagmann et al. 2014, Merschel et al. 2014). However, the proportion of grand fir is consistent with results from Johnston et al. (2016) who examined historical structure and composition in similar forest types in the same region. Potential reasons for high levels of grand fir are deep, ash-capped soils and longer fire-return intervals than on adjacent plots. An analysis of the relationship between fire-return intervals and density on the plots is underway using fire history data from Heyerdahl et al. (2001). The fact that we found high proportions of grand fir on three of four grand fir plots does not suggest that all grand fir sites in the Blue Mountains were historically similar. The low density and low proportion of grand fir on G3 is evidence of this. We can infer, however, that not all dry grand fir sites were pine-dominated forest similar in structure and density to dry Douglas-fir and ponderosa pine plant associations.

The higher current densities relative to historical conditions is consistent with many other studies that have shown increases in density (Covington and Moore 1994, Hagmann et al. 2013, Harrod et al. 1999, Lydersen et al. 2013, Reynolds et al. 2013, Sánchez Meador et al. 2009, Schneider et al. 2015) The decrease in mean diameter indicates that structure has changed owing to infill of small-diameter trees. While our reconstruction methods likely underestimate small trees and thus overall density, we observed during our sampling an obvious postfire suppression cohort on these sites that was dense in many places. Our sites have never been logged and retain a robust old-tree population; thus density increases can be attributed to a combination of fire exclusion, grazing, and favorable climate for tree establishment in the early part of the 20th century (Merschel et al. 2014, Naficy et al. 2010, Rummel 1951).

## Spatial Pattern

Spatial pattern was also similar to the patterns of individual trees, clumps, and openings found at other dry-forest reference sites (Larson and Churchill 2012). Clump size proportions span the range found at other sites (Churchill 2013, Clyatt et al. 2016, Fry et al. 2014, Larson and Churchill 2012, Lydersen et al. 2013, Schneider et al. 2015). In general, the proportion of individual trees in dry forest reference sites appears to range from around 10 percent in highly clumped plots to around 50 percent in the least clumped plots (at an intertree distance of 6 m). Plots with low clumping often have no large clumps (10+ trees), while highly clumped plots can have 20 to 30+ percent of trees in large clumps (Larson and Churchill 2012). The largest clumps found in most studies are generally 30 to 40 trees (also at an intertree distance of 6 m). The similarity of the range of clump size distributions found in this study to others suggests that these reference sites are a reasonable representation of the envelope of historical patterns in the study domain. Areas with higher and lower levels of clumping were likely present but do not appear to have been very common based on the available data. Our data are from a relatively narrow geographic area, however, and further reconstruction studies would be necessary to have higher confidence that the historical range and distribution of pattern is indeed represented by this dataset.

The shape and amount of open space found on the plots illustrates the discontinuous nature of forest canopy in frequent-fire forests. Even the higher density plots had 5 to 10 percent of their area in open space (F > 9 m) and openings of up to 0.1 ha that are large enough for regeneration and growth of shade-intolerant species. Openings often extended throughout much of the plot in a linear, sinuous fashion. In the lower density plots, openings tended to join together into large interconnected, sinuous openings (e.g., D4). In very few cases were the larger openings (>0.4 ha) circular or compact in shape. Instead, these sinuous openings created multiple breaks in the canopy across each plot that were wide enough to force active crown fire onto the ground in all but the most extreme conditions (Peterson et al. 2005). By reducing canopy bulk density, openings allow for greater release of heat from surface fires, which reduces potential for passive or active crown fire (Graham et al. 2004). We hypothesize that the amount and shape of openings in frequent-fire forests is a major driver of their resistance and resilience to disturbance. Treatments that sought to mimic historical clumped-stand structure with such openings were effective at reducing fire severity and crown scorch in the Wallow fire in Arizona compared to untreated conditions (Kennedy and Johnson 2014).

We found that density, clumping, and openings were unevenly distributed across some of our plots (i.e., nonstationary or inhomogeneous patterns), similar to Fry et al. (2014). Large clumps were often grouped together in areas of a plot and not evenly spread out (e.g., plot D1). Likewise, portions of some plots were much more open than the rest of the plot (e.g., plot G3). This was likely caused by a significant change in the processes creating pattern such as a change in soil conditions (e.g., area of shallow soil) or past disturbance severity (e.g., a large root rot pocket or past torching of a patch of trees) (Fry et al. 2014, Getzin et al. 2008, Perry et al. 2006). The presence of inhomogeneous patterns suggests that spatial pattern of these plots was likely driven by a mix of fine-scale gap-phase processes (<0.2 ha) that maintained the basic pattern of individuals, clumps, and openings and somewhat larger scale variation in soils, solar radiation, topographic position, and disturbance intensities (1~10+ha) that caused higher variation in densities, levels of clumping, and amount of open space.

The variation in density and pattern among the 14 plots also suggests that larger scale variation in topography, climate, and disturbance behavior created varying patterns of structure and composition at larger spatial extents (100s to 1000s of ha) (Cansler 2011, Hessburg et al. 1999, Heyerdahl et al. 2001, Kane et al. 2015, Perry et al. 2011, Taylor and Skinner 2003)

## Relationships Among Pattern, Density and Potential Vegetation Series

The strong relationship between higher stem densities and higher proportions of clumping found in this study has also been found on other dry forest sites (Abella and Denton 2009, Churchill 2013, Clyatt et al. 2016, Fry et al. 2014). As tree density increases, the proportion of trees in individuals and small clumps declines, while the proportion in medium and large clumps increases. Part of this relationship is simply a matter of more trees connecting into larger clumps as the available space is filled with additional trees. However, higher density stands with low levels of clumping have not been found in reference studies even though there is more than enough physical space for trees to be individuals or in small clumps. This suggests that higher densities in dry forests are primarily the result of higher numbers of trees in clumps vs. individual trees. Plot P1, for example, has 65 trees per hectare (tph) and 25 tph as individuals while G1 has 161 tph but only 21 tph as individuals. Under strict uniform spacing, all 161 tph in G1 would be individuals. Also, the denser plots still have open space (F >9 m), which is directly related to high levels of clumping in these plots.

The relationships we found between potential vegetation series and pattern are difficult to disentangle from the underlying relationship of density to pattern. The ponderosa pine, Douglas-fir (*Pseudotsuga menziesii* (Mirb.) Franco), and grand fir plots have similar pair correlation curves and appear to follow the same basic relationships between density, mean clump size, and openings (fig. 3.5). The Douglas-fir plots are not more uniform or less clumped than the pine or grand fir, given that they are lower in density. Furthermore, the two outlier plots suggest that adding more plots from more areas would further weaken the relationship between potential vegetation series and pattern. The Douglas-fir plots are in the middle in terms of productivity, but were statistically less clumped than the other two series.

Given the lack of a clear trend between more productive plant associations and pattern, we thus rejected our hypothesis that density and average clump size would increase with productivity. Plant association classification offers a useful approach to characterize gradients in the biophysical environment (Powell et al. 2007), but there are clearly many other factors that influence structure and composition. Hagmann et al. (2013, 2014) and Merschel et al. (2014) also found that potential vegetation was not a significant predictor of structure in mixed-conifer forests in central and eastern Oregon. Our hypothesis that the historical range, or envelope, of density and spatial pattern in dry forests was partitioned by potential vegetation series was clearly too simplistic.

A more likely hypothesis is that higher productivity plant associations, especially those that had more variable fire regimes (Everett et al. 2000, Heyerdahl et al. 2001), had a wider envelope of structure and composition. More productive sites can support higher tree densities, and thus higher clumping levels, owing to lower levels of moisture stress, presence of shade-tolerant species, and higher overall carrying capacity (Powell 1999). As found in this study, higher productivity sites likely occupied the higher density and higher clumping end of the overall dry forest envelope. However, fire and other disturbances created low density and low clumping patterns on all sites, including the Grand fir series. In contrast, low productivity sites can support fewer trees and so have a narrower potential range of conditions. Other important mechanisms such as seed caching by birds and small mammals, interspecies competition within clumps, soil conditions, and understory composition likely also created variability in clumping and density across different potential vegetation series.

## Forest Development Pathways

The historical forest conditions we reconstructed on these plots have all of the characteristics of frequent-fire, open-canopy, old-growth, pine and mixed-conifer forests described by many researchers (Agee 1993, Cooper 1961, Fry and Stephens 2010, Kaufmann et al. 2007, Keen 1940, Larson and Churchill 2012, Sánchez Meador et al. 2009, Weaver 1961). The strongly clumped spatial patterns, openings, wide distribution of age classes, presence of old trees, and dominance of large-diameter trees are clear evidence of a fine-scale, multicohort, gap-phase replacement system that has persisted through multiple centuries of frequent disturbance and climatic fluctuation (Kaufmann et al. 2007). Relatively few trees appear to have lived past 300 years, however, indicating a dynamic tree population.

Tree recruitment appears to have occurred somewhat continuously over time with some discreet pulses. However, further investigation is needed to explain temporal patterns of tree establishment and potential mechanisms. Also, we did not collect a sufficient number of tree cores to fully determine whether tree establishment occurred primarily in spatially segregated, even-aged clumps or within multiage clumps. Our limited data suggest that many clumps have multi-age cohorts, similar to findings from northern Arizona (White 1985).

# Chapter 6: Management Implications

## Key Functional Components of Reference Conditions

The structure and composition of the historical forests found in this study offer information that can be used to guide restoration efforts. However, managers must first understand the key components of historical patterns from a functional perspective. Quantifying historical structure and composition is only the first step in understanding how these systems function and provide the ecosystem functions and services that humans want. Ultimately, targets for variability should consider the desired functions, current structure, biophysical conditions, and anticipated future disturbances. Determining which components of historical patterns drive key ecosystem functions and services and which components are just natural variations is necessary. Density, composition, and pattern targets from reference forests offer useful guideposts but should not become ends in themselves.

Much progress has been made in understanding how size, density, and composition interact with forest development and disturbance processes in dry forests to drive resilience and ecological function at the stand level (see chapter 1). How some components of pattern affect particular functions is also known. Examples include the effects of gap size on tree regeneration and growth (Bigelow and North 2012, York et al. 2004), and the use of dense patches for nesting or denning by many wildlife species (Lehmkuhl et al. 2006, Long and Smith 2000, Roberts et al. 2008). However, relatively little experimental work has been done to empirically test how different stand-level patterns affect specific processes such as fire behavior or ecosystem functions and services such as snow retention or provision of wildlife habitat. Managing for resilient forests in the face of changing climate will require such knowledge in order to critically evaluate and modify historical reference targets (Joyce et al. 2009, Spies et al. 2010, Stephens et al. 2010). Studies on such topics have been initiated and results are beginning to emerge (e.g., Latif et al. 2015), but it will be some time before we have a robust understanding of the relationships between structure, composition, process, and function.

Below, we describe the key functional components of pattern, based on current scientific understanding, to consider when setting pattern targets. Keep in mind, however, that restoration of the fine-scale, multicohort, gap-phase stand development processes associated with dry forests is as important as restoring historical structure and composition. Frequent fire is of course the key driver of these processes.

- **Openings:** They provide an array of ecological functions and are as important in terms of function as the trees (see Chapter 1). The number and size of openings will depend on overall tree density, but linear, sinuous openings with a wide range of widths have been found in almost all reference studies (Larson and Churchill 2012). In this study, all plots had some openings that were at least 18 m across. The largest openings found were up to 50 m across. Large, circular gaps (>0.4 ha) are not consistent with the shape and size of openings found in this study.
- **Medium and large clumps:** These provide patches of continuous canopy that are large enough to create a shady understory light environment and differences in subcanopy temperatures and soil moisture levels. This creates niches for different understory species and can alter fire behavior. It also provides cover and nesting locations for wildlife species and snag creation through competitive mortality. The largest clumps appear to be around 30 to 40 trees in this dataset (for trees greater than 15 cm diameter at breast height [d.b.h].), but multiple large clumps are sometimes adjacent and form larger patches (e.g., 0.2 to 0.5 ha). Large clumps (10+ trees) were not present on every acre, however, and four of our 4-ha plots did not contain any large clumps.
- **Widely spaced individuals:** Large trees with deep and wide crowns are a defining component of frequent-fire forests. They are fire resistant, provide habitat elements, and eventually become large snags and downed logs. While we define individuals here as trees with no neighbors within 6 m, many individuals in our plots had wider spacing (e.g., 8 to 12 m).
- **Variation in density and clumping within and across treatment units:** The multiscale variation found in this study and others is thought to be an important aspect of resilience, akin to having a diversified investment portfolio. Multiscale variation is thought to impede the spread of high-severity disturbances, perpetuate variable postdisturbance patterns, and facilitate species diversity (Beaty and Taylor 2007, Hessburg et al. 2015, Pimont et al. 2011, Stephens et al. 2008, Virah-Sawmy et al. 2009). Creating the same clump and opening size distribution across a whole treatment unit (10+ ha) or set of units (hundreds of hectares) is not consistent with the multiscale variation found in this study and others. There is no "average" or target level of variability that should be replicated across a whole unit. Although unit-level targets and averages are a necessity for management, the range and distribution of density and clumps are more important.

## Using Reference Data to Set Targets for Density, Composition, and Pattern

As a whole, the 14 plots provide an estimate of the historical range of variation (or envelope) for stand-level density, size, composition, and pattern in dry forests. The pattern envelope found in this study has boundaries that are consistent with other dry-forest reference sites (see citations above). The least variable plots have a maximum of around 50 percent of trees as individuals and have no large clumps (10+ trees greater than 15 cm d.b.h.). The most clumped plots have around 10 percent as individuals and 10 to 30 percent in large clumps. These data suggest minimum and maximum values for treatments that seek to restore patterns that are consistent with the patterns found in historical reference studies. For example, spacing-based thinning and fuel reduction treatments can result in 80 percent or more individual trees, no medium or large clumps, few or no openings, and create different patterns than found in this and other reference studies. (Churchill et al. 2013). However, it is unlikely that this study, along with others, captured the full range of historical variation.

A wide range of pattern and density configurations exists within the historical envelope found in this study that offers flexibility to managers. To determine a target level of variability for a particular treatment unit, managers may wish to first consider the target stem density and species composition appropriate for the site. Many factors will go into this decision, including management objectives, biophysical conditions, carrying capacity, current conditions, future management entries, operational considerations, anticipated future disturbances, and climate change projections. Density management guidelines based on plant associations (Cochran 1994, Powell 1999) are a useful starting point, as are density and composition data from reference sites (Franklin et al. 2013). These may need to be modified, however, based on anticipated climate change. Conditions and planned treatments in surrounding units should also be considered. A landscape prescription can provide guidance for setting unit-level targets based on achieving landscape-level objectives (Hessburg et al. 2015). The overall goal of density and composition targets is to better align the vegetation with the current and future biophysical conditions and disturbance regime of the site.

Once the target stem density and composition have been determined, spatial pattern targets that are appropriate for the site can be selected. Pattern targets based on clumping levels offer a simplified approach (e.g., Low, Mod, or High; table 3.3). Basal area distributions from reference plots can also be used. As our results show considerable variation in the relationship between potential vegetation series and pattern, directly using potential vegetation series to select a clumping level can be challenging. Instead, potential vegetation series or plant association group can be one of the factors considered when selecting target density, which will in turn influence the clumping target. We suggest the following considerations in selecting a clumping level for a particular unit.

- Align clumping levels with target density. Historically, low-density stands (50 to around 100 trees per hectare [tph]) typically had low or moderate clump level, while higher density stands have moderate to high clumping levels.
- Assess the number and clumping levels of live old trees in the stand. If retaining old trees is part of the prescription, the clump percentage targets should accommodate retaining existing old trees to avoid conflicts for the marking crew.
- Assess the extent to which leave trees of the desired species and condition are clumped in the stand. (e.g., healthy foliage, crown ratio greater than 40 percent, wildlife habitat features). If there are not a sufficient number of suitable leave trees in clumps, prescribing higher clumping levels can result in excessive numbers of trees with poor vigor. Some inferior trees can be retained to make up larger clumps and will provide for snag recruitment over time.
- Factor in wildlife habitat requirements and visual considerations. Larger clumps can provide cover for different species and break up siting distances (Franklin et al. 2013).
- Factor in the potential effects of prescribed fire. Some clumps can be intentionally killed or thinned out with prescribed fire to create snag patches and openings.
- Factor in no-cut buffers or larger skips (~0.2+ ha) that will be retained within the unit or on unit edges (Franklin et al. 2013). These dense leave areas will provide many of the functions of large or very large clumps. However, keep in mind that the clumping levels found in this study are from 2.4- to 6-ha reference plots, indicating that clumps were distributed across stands and not packed into riparian areas or other microsites.
- Vary pattern among units. Varying clumping levels for units across a larger project area will avoid creating a similar fine-scale pattern across large areas. Treatments that only achieve one end of the historical envelope (e.g., the more uniform end) will not create the larger scale variability associated with historical forests.

Targets for openings should also be considered. However, because density, clumping level, and openings are closely related, we have found through monitoring that small- to medium-sized openings are created in the course of achieving a particular density and clumping level, and that the resulting openings are within the range of reference conditions. As long as some areas are left without leave trees for 20 to 50 m apart, specific targets for openings may not be necessary. Additionally, most openings found in this study were small (<0.04 ha), and opening size distributions exponentially decreased (fig. 3.5). Also, opening shape was generally linear and sinuous vs large, circular gaps (>0.4 ha). Monitoring or real-time tracking can be done to assess where openings are indeed being created. Guidance as to where to locate openings can also be helpful as soil conditions or disturbance pockets often drive opening locations.

For openings larger than about 0.4 ha, we have found that specific marking guidelines may be needed. Instead of prescribing openings in terms of area, we have found width and linear distance to be easier to implement. Linear, sinuous openings can be laid out prior to general marking with a flag line. Marking crews can then be instructed to space off of the flag line for a certain width (e.g., remove most trees within 9 to 30 m of the flag line).

## Marking Guide Development and Implementation

Translating density, compositional, and clumping targets into an operationally practical marking guide can be done in a number of ways. The Individuals, clumps, and openings (ICO) method (Churchill et al. 2014) is one option. The ICO method was designed to explicitly combine typical dry-forest prescriptions with targets for clumping. Instead of marking for an average or range of basal area, crews are given a target number of individuals, and small, medium, and large clumps to retain across a unit. The use of unit-wide targets instead of per-acre targets provides more flexibility to work with stand conditions.

Basal area or other marking guide approaches can also be used to achieve the target range of variability (e.g., Franklin et al. 2013, Jain et al. 2012, Powell 2014). We have found that individual trees and small clumps are relatively easy to retain with a basal-area marking guide that emphasizes tree selection over strict spacing. Medium and larger clumps, however, generally are more difficult to achieve without specific direction (Churchill et al. 2013). Thus, adding targets for medium and large clumps to a basal area marking guide can provide clear guidance to marking crews and can be easily tracked during marking. A challenge with basal area marking, however, is the tendency to leave the target basal area in the majority of the stand with some variation around the mean (a normal distribution or bell-shaped curve). However, basal area was not normally distributed in most of the reference plots (fig. 3.6), and the mean basal area value was not the dominant condition. Restoring the multiscale variability similar to that of the reference plots may require marking for a wide range of basal area where the mean is not the dominant condition.

Several important factors should be considered for all prescription approaches. The first is to emphasize to marking crews that the goal of these treatments is to create or maintain an overall pattern of individuals, clumps, and openings. The targets should not be applied in a rigid manner, but instead used as "guard rails" to help marking crews know if they are creating too little or too much variability. Second, marking crews can work with existing tree and biophysical conditions to create variable patterns within and across treatment units and avoid trying to force the same density and variability on every acre. For example, medium and large clumps can be concentrated in areas where good leave tree candidates exist. Individuals and openings can be more dominant in other areas. Underlying variation in soils, topography, and disturbance processes can also be used to adjust target density and clumping levels across a stand (e.g., leave more clumps on north-facing slopes and more individuals and openings on patches with shallow soils) (North et al. 2009).

Finally, we have found that real-time tracking of leave tree density, clumps, and openings greatly helps marking crews implement these kinds of prescriptions. Tracking gives crews flexibility to adjust their marking to work with existing tree and biophysical conditions as they move through a unit while knowing where they are relative to the "guard rails." An android app has been developed to facilitate such tracking. Contact the lead author for more information.

## Conclusion

Restoration and sustainable long-term management of dry-forest ecosystems in eastern Oregon requires looking to the past to understand how these forests developed and persisted under intact natural disturbance regimes, as well as anticipating future climate change and disturbance regimes. The historical data for forest ecosystem composition, structure, and spatial pattern we report here can be used to inform the development of prescriptions, and monitoring using the ICO (Churchill et al. 2014) or other methods. These are "historical estimates," but their value lies in showing the range of variability that was present within and across a sample of historical stands. Restoring such variability is a reasonable approach to restoring the functions that historical forests provided and that society desires today. Current conditions, future stand development and disturbance, and anticipated climate change can necessitate deviating from these historical estimates, however. Ultimately, these historical data provide a quantitative baseline for managers and stakeholders to draw upon when developing marking guidelines and interpreting monitoring results in dry forests of the Blue Mountains. Combined with results from similar studies from across the interior West, they can be used to inform restoration of dry forests in similar forest types in other areas as well.

## English Equivalents

| When you know: | Multiply by: | To get: |
|---|---|---|
| Centimeters (cm) | 0.394 | Inches |
| Meters (m) | 3.28 | Feet |
| Hectares (ha) | 2.47 | Acres |

## References

**Abella, S.R.; Denton, C.W. 2009**. Spatial variation in reference conditions: historical tree density and pattern on *Pinus ponderosa* landscape. Canadian Journal of Forest Research. 39: 2391–2403.

**Agee, J.K. 1993.** Fire ecology of Pacific Northwest forests. Washington, DC: Island Press. 493 p.

**Agee, J.K. 2005.** The complex nature of mixed severity fire regimes. In: Lagene, L.; Zelnik, J.; Cadwallader, S.; Hughes, B., eds. Mixed-severity fire regimes: ecology and management. Spokane, WA: Washington State University Cooperative Extension Service/The Association for Fire Ecology: 1–10.

**Agee, J.K.; Skinner, C.N. 2005.** Basic principles of forest fuel reduction treatments. Forest Ecology and Management. 211: 83–96.

**Allen, C.D.; Savage, M.; Falk, D.A.; Suckling, K.F.; Swetnam, T.W.; Schulke, T.; Stacey, P.B.; Morgan, P.; Hoffman, M.; Klingel, J.T. 2002.** Ecological restoration of Southwestern ponderosa pine ecosystems: a broad perspective. Ecological Applications. 12: 1418–1433.

**Anderson, M.J. 2001.** A new method for non-parametric multivariate analysis of variance. Austral Ecology. 26: 32–46.

**Baker, S.C.; Read, S.M. 2011.** Variable retention silviculture in Tasmania's wet forests: ecological rationale, adaptive management and synthesis of biodiversity benefits. Australian Forestry. 74: 218–232.

**Bakker, J.D. 2005.** A new, proportional method for reconstructing historical tree diameters. Canadian Journal of Forest Research. 35: 2515–2520.

**Barth, M.A.; Larson, A.J.; Lutz, J.A. 2015.** A forest reconstruction model to assess changes to Sierra Nevada mixed-conifer forest during the fire suppression era. Forest Ecology and Management. 354: 104–118.

**Beaty, M.R.; Taylor, A.H. 2007.** Fire disturbance and forest structure in old-growth mixed-conifer forests in the northern Sierra Nevada, California. Journal of Vegetation Science. 18: 879–890.

**Belote, R.T.; Larson, A.J.; Dietz, M.S. 2015.** Tree survival scales to community-level effects following mixed-severity fire in a mixed-conifer forest. Forest Ecology and Management. 353: 221–231.

**Bigelow, S.W.; North, M.P. 2012.** Microclimate effects of fuels-reduction and group-selection silviculture: implications for fire behavior in Sierran mixed-conifer forests. Forest Ecology and Management. 264: 51–59.

**Bones, J.T. 1960.** Estimating d.b.h. from stump diameter in the Pacific Northwest. Res. Note PNW-RN-186. Portland, OR: U.S. Department of Agriculture, Forest Service, Pacific Northwest Research Station. 2 p.

**Buchanan, J.B.; Rogers, R.E.; Pierce, J.D.; Jacobson, J.E. 2003.** Nest-site habitat use by white-headed woodpeckers in the eastern Cascade Mountains, Washington. Northwestern Naturalist. 84: 119–128.

**Cansler, C.A. 2011.** Drivers of burn severity in the northern Cascade Range, Washington, USA. University of Washington. Seattle, WA: 128 p. M.S. thesis

**Churchill, D.J. 2013.** Quantifying and restoring stand-level spatial pattern in dry forests of the eastern Washington Cascades. Seattle, WA: University of Washington, School of Environmental and Forest Sciences. 152 p. Dissertation.

**Churchill, D.J.; Dahlgreen, M.C.; Larson, A.J. 2014.** The ICO approach to restoring spatial pattern in dry forests: implementation guide. Version 2.2. Vashon, WA: Stewardship Forestry. 37 p.

**Churchill, D.J.; Larson, A.J.; Dalhgreen, M.C.; Franklin, J.F.; Hessburg, P.F.; Lutz, J.A. 2013.** Restoring forest resilience: from reference spatial patterns to silvicultural prescriptions and monitoring. Forest Ecology and Management. 291: 442–457.

**Cline, S.P.; Berg, A.B.; Wight, H.M. 1980.** Snag characteristics and dynamics in Douglas-fir forests, western Oregon. The Journal of Wildlife Management: 773–786.

**Clyatt, K.A.; Crotteau, J.S.; Schaedel, M.S.; Wiggins, H.L.; Kelley, H.; Churchill, D.C.; Larson A.J. 2016.** Historical spatial patterns and contemporary tree mortality in dry mixed-conifer forests. Forest Ecology and Management. 361: 23-37.

**Cochran, P.H. 1994.** Suggested stocking levels for forest stands in northeastern Oregon and southeastern Washington. Res. Note PNW-RN-513. Portland, OR: U.S. Department of Agriculture, Forest Service, Pacific Northwest Research Station. 21 p.

**Collaborative Forest Landscape Restoration Program [CFLRP]. 2012.** People restoring America's forests: 2012 report on the collaborative forest landscape restoration program. The Nature Conservancy. 38 p.

**Contreras, M.A.; Affleck, D.; Chung, W. 2011.** Evaluating tree competition indices as predictors of basal area increment in western Montana forests. Forest Ecology and Management. 262: 1939–1949.

**Cooper, C.F. 1961.** Pattern in ponderosa pine forests. Ecology. 42: 493–499.

**Covington, W.W.; Moore, M.M. 1994.** Southwestern ponderosa forest structure—changes since Euro-American settlement. Journal of Forestry. 92: 39–47.

**Diggle, P.J. 2003.** Statistical analysis of spatial point patterns. New York: Academic Press. 148 p.

**Dodd, N.L.; Schweinsburg, R.E.; Boe, S. 2006.** Landscape-scale forest habitat relationship to tassel-eared squirrel populations: implications for ponderosa pine forest restoration. Restoration Ecology. 14: 537–547.

**Dodson, E.K.; Peterson, D.W.; Harrod, R.J. 2008.** Understory vegetation response to thinning and burning restoration treatments in dry conifer forests of the eastern Cascades, USA. Forest Ecology and Management. 255: 3130–3140.

**Everett, R.J.; Lehmkuhl, R.; Schellhass, P.; Ohlson, P.; Keenum, D.; Riesterer, H.; Spurbeck, D. 1999.** Snag dynamics in a chronosequence of 26 wildfires on the east slope of the Cascade Range in Washington state, USA. International Journal of Wildland Fire. 9: 223–234.

**Everett, R.L.; Baumgartner, D.; Ohlson, P.; Schellhaas, R.; Harrod, R.J. 2007.** Development of current stand structure in dry fir-pine forests of eastern Washington. Journal of the Torrey Botanical Society. 134: 199–214.

**Everett, R.L.; Schellhaas, R.; Keenum, D.; Spurbeck, D.; Ohlson, P. 2000.** Fire history in the ponderosa pine/Douglas-fir forests on the east slope of the Washington Cascades. Forest Ecology and Management. 129: 207–225.

**Fettig, C.J.; Klepzig, K.D.; Billings, R.F.; Munson, A.S.; Nebeker, T.E.; Negrón, J.F.; Nowak, J.T. 2007.** The effectiveness of vegetation management practices for prevention and control of bark beetle infestations in coniferous forests of the western and southern United States. Forest Ecology and Management. 238: 24–53.

**Fortin, M.J.; Dale, M.R.T. 2005.** Spatial analysis: a guide for ecologists. Cambridge, United Kingdom: Cambridge University Press.

**Franklin, J.F.; Johnson, K.N. 2012.** A restoration framework for federal forests in the Pacific Northwest. Journal of Forestry. 110: 429–439.

**Franklin, J.F.; Johnson, N.K.; Churchill, D.J.; Hagmann, K.; Johnson, D.; Johnston, J. 2013.** Restoration of dry forests in eastern Oregon: a field guide. Portland, OR: The Nature Conservancy of Oregon. 202 p.

**Franklin, J.F.; Spies, T.A.; Pelt, R.V.; Carey, A.B.; Thornburgh, D.A.; Berg, D.R.; Lindenmayer, D.B.; Harmon, M.E.; Keeton, W.S.; Shaw, D.C.; Bible, K.; Chen, J. 2002.** Disturbances and structural development of natural forest ecosystems with silvicultural implications, using Douglas-fir forests as an example. Forest Ecology and Management. 155: 399–423.

**Fry, D.L.; Stephens, S.L. 2010.** Stand-level spatial dependence in an old-growth Jeffrey pine—mixed conifer forest, Sierra San Pedro Martir, Mexico. Canadian Journal of Forest Research. 40: 1803–1814.

**Fry, D.L.; Stephens, S.L.; Collins, B.M.; North, M.P.; Franco-Vizcaíno, E.; Gill, S.J. 2014.** Contrasting spatial patterns in active-fire and fire-suppressed mediterranean climate old-growth mixed conifer forests. PloS one 9:e88985.

**Fule, P.Z. 2008.** Does it make sense to restore wildland fire in changing climate? Restoration Ecology. 16: 526–531.

**Gärnter, S.; Reynolds, K.M.; Hessburg, P.F.; Hummel, S.; Twery, M. 2008.** Decision support for evaluating landscape departure and prioritizing forest management activities in a changing environment. Forest Ecology and Management. 256: 1666–1676.

**Getzin, S.; Wiegand, T.; Wiegand, K.; He, F.L. 2008.** Heterogeneity influences spatial patterns and demographics in forest stands. Journal of Ecology. 96: 807–820.

**Graham, R.; Jain, T.; Sandquist, J. 2007.** Free selection: a silvicultural option. In: Powers, R.F., ed. Restoring fire-adapted ecosystems: proceedings of the 2005 national silviculture workshop. Gen. Tech. Rep. PSW-GTR- 203. Albany, CA: U.S. Department of Agriculture, Forest Service, Pacific Southwest Research Station: 121–156

**Graham, R.; McCaffrey, S.; Jain, T., tech. eds. 2004.** Science basis for changing forest structure to modify wildfire behavior and severity. Gen. Tech. Rep. RMRS-GTR-120. Fort Collins, CO: U.S. Department of Agriculture, Forest Service, Rocky Mountain Research Station. 43 p.

**Gundale, M.J.; Metlen, K.L.; Fiedler, C.E.; DeLuca, T.H. 2006.** Nitrogen spatial heterogeneity influences diversity following restoration in a ponderosa pine forest, Montana. Ecological Applications. 16: 479–489.

**Hagmann, K.; Franklin, J.F.; Johnson, K.N. 2013.** Historical structure and composition of ponderosa pine and mixed-conifer forests in south-central Oregon. Forest Ecology and Management. 304: 492–504.

**Hagmann, R.K.; Franklin, J.F.; Johnson, K.N. 2014.** Historical conditions in mixed-conifer forests on the eastern slopes of the northern Oregon Cascade Range, USA. Forest Ecology and Management. 330: 158–170.

**Hamrick, J.; Blanton, H.; Hamrick, K. 1989.** Genetic-structure of geographically marginal populations of ponderosa pine. American Journal of Botany. 76: 1559–1568.

**Harrod, R.J.; McRae, B.H.; Hartl, W.E. 1999.** Historical stand reconstruction in ponderosa pine forests to guide silvicultural prescriptions. Forest Ecology and Management. 114: 433–446.

**Hessburg, P.F.; Agee, J.K.; Franklin, J.F. 2005.** Dry forests and wildland fires of the inland Northwest USA: contrasting the landscape ecology of the pre-settlement and modem eras. Forest Ecology and Management. 211: 117–139.

**Hessburg, P.F.; Churchill, D.J.; Larson, A.J.; Haugo, R.D.; Miller, C.; Spies, T. A.; North, M.P.; Povak, N.A.; Belote, R.T.; Singleton, P.H.; Gaines, W.L.; Keane, R.E.; Aplet, G.H.; Stephens, S.L.; Morgan, P.; Bisson, P.A.; Rieman, B.E.; Salter, R.B.; Reeves, G.H. 2015.** Restoring fire-prone landscapes: seven core principles. Landscape Ecology. DOI 10.1007/s10980-015-0218-0.

**Hessburg, P.F.; Reynolds, K.M.; Salter, R.B.; Dickinson, J.D.; Gaines, W.L.; Harrod, R.J. 2013.** Landscape evaluation for restoration planning on the Okanogan-Wenatchee national forest, USA. Sustainability. 5: 805–840.

**Hessburg, P.F.; Smith, B.G.; Kreiter, S.D.; Miller, C.A.; Salter, R.B.; McNicoll, C.H.; Hann, W.J. 1999.** Historical and current forest and range landscapes in the interior Columbia River basin and portions of the Klamath and Great Basins. Part 1: Linking vegetation patterns and landscape vulnerability to potential insect and pathogen disturbances. Gen. Tech. Rep. PNW-GTR-458. Portland, OR: U.S. Department of Agriculture, Forest Service, Pacific Northwest Research Station. 357 p. (Quigley, Thomas, M., ed., Interior Columbia Basin Ecosystem Management Project: scientific assessment).

**Heyerdahl, E.K.; Brubaker, L.B.; Agee, J.K. 2001.** Spatial controls of historical fire regimes: a multiscale example from the interior West, USA. Ecology. 82: 660–678.

**Hiers, J.K.; O'Brien, J.J.; Mitchell, R.J.; Grego, J.M.; Loudermilk, E.L. 2009.** The wildland fuel cell concept: an approach to characterize fine-scale variation in fuels and fire in frequently burned longleaf pine forests. International Journal of Wildland Fire. 18: 315–325.

**Hopkins, T.; Larson, A.J.; Belote, R.T. 2014.** Contrasting effects of wildfire and ecological restoration in old-growth western larch forests. Forest Science. 60(5): 1005–1013

**Jackson, S.T.; Hobbs, R.J. 2009.** Ecological restoration in the light of ecological history. Science. 325: 567–569.

**Jain, T.B.; Battaglia, M.A.; Han, H.-S.; Graham, R.T.; Keyes, C.R.; Fried, J.S.; Sandquist, J.E. 2012.** A comprehensive guide to fuel management practices for dry mixed conifer forests in the northwestern United States. Gen. Tech. Rep. RMRS-GTR-292. Fort Collins, CO: U.S. Department of Agriculture, Forest Service, Rocky Mountain Research Station. 331 p.

**Jain, T.B.; Graham, R.T.; Sandquist, J.; Butler, M.; Brockus, K.; Frigard, D.; Cobb, D.; Sup-Han, H.; Halbrook, J.; Denner, R.; Evans, J.S. 2008.** Restoration of northern Rocky Mountain moist forests: integrating fuel treatments from the site to the landscape. In: Deal, R.L., ed. Integrated restoration of forested ecosystems to achieve multiple resource benefits: proceedings of the 2007 national silviculture workshop. Gen. Tech. Rep. PNW-GTR-733. Portland, OR: U.S. Department of Agriculture, Forest Service, Pacific Northwest Research Station: 147–172

**Johnson, C.G.; Clausnitzer, R.R. 1992.** Plant associations of the Blue and Ochoco Mountains. R6-ERW-TP-036-92. Portland, OR: U.S. Department of Agriculture, Forest Service, Pacific Northwest Region, Wallowa-Whitman National Forest. 207 p.

**Johnston, J.D.; Bailey, J.D.; Dunn, C.J. 2016.** Influence of fire disturbance and biophysical heterogeneity on pre-settlement ponderosa pine and mixed conifer forests. Ecosphere 7:11.

**Joyce, L.A.; Blate, G.M.; McNulty, S.; Millar, C.I.; Moser, S.; Neilson, R.P.; Peterson, D.L. 2009.** Managing for multiple resources under climate change: national forests. Environmental Management. 44: 1022–1032.

**Kane, V.R.; Lutz, J.A.; Cansler, A.; Povak, N.A.; Churchill, D.J.; Smith, D.; Kane, J.T.; North, M.P. 2015.** Water balance and topography predict fire and forest structure patterns. Forest Ecology and Management. 338: 1–13.

**Kaufmann, M.R.; Binkley, D.; Fule, P.Z.; Johnson, M.; Stephens, S.L.; Swetnam, T.W. 2007.** Defining old growth for fire-adapted forests of the Western United States. Ecology and Society 12.

**Keane, R.E.; Hessburg, P.F.; Landres, P.B.; Swanson, F.J. 2009.** The use of historical range and variability (HRV) in landscape management. Forest Ecology and Management. 258: 1025–1037.

**Keen, F.P. 1940.** Longevity of ponderosa pine. Journal of Forestry. 38: 597–598.

**Kennedy, M.C.; Johnson, M.C. 2014.** Fuel treatment prescriptions alter spatial patterns of fire severity around the wildland-urban interface during the Wallow Fire, Arizona, USA. Forest Ecology and Management. 318: 122–132.

**King, K.J.; Bradstock, R.A.; Cary, G.J.; Chapman, J.; Marsden-Smedley, J.B. 2008.** The relative importance of fine-scale fuel mosaics on reducing fire risk in south-west Tasmania, Australia. International Journal of Wildland Fire. 17: 421–430.

**Knapp, E.E.; North, M.P.; Benech, M.; Estes, B. 2012.** The variable-density thinning study at Stanislaus-Tuolumne Experimental Forest. In: North, M.P., ed. Managing Sierra Nevada forests. Gen. Tech. Rep. PSW-GTR-237. Albany, CA: U.S. Department of Agriculture, Forest Service, Pacific Southwest Research Station: 127–140

**Larson, A.J.; Belote, R.T.; Cansler, C.A.; Parks, S.A.; Dietz, M.S. 2013.** Latent resilience in ponderosa pine forest: effects of resumed frequent fire. Ecological Applications. 23: 1243–1249.

**Larson, A.J.; Churchill, D.J. 2012.** Tree spatial patterns in fire-frequent forests of western North America, including mechanisms of pattern formation and implications for designing fuel reduction and restoration treatments. Forest Ecology and Management. 267: 74–92.

**Larson, A.J.; Stover, K.C.; Keyes, C.R. 2012.** Effects of restoration thinning on spatial heterogeneity in mixed conifer forest. Canadian Journal of Forest Research. 42: 1505–1517.

**Larsson, L.A. 2003.** CDendro: Cybis Dendro Dating Program. Saltsjöbaden, Sweden: Cybis Elektronik & Data AB.

**Latif, Q.S.; Saab, V.A.; Mellen-Mclean, K.; Dudley, J.G. 2015.** Evaluating habitat suitability models for nesting white-headed woodpeckers in unburned forest. The Journal of Wildlife Management. 79: 263–273.

**Lehmkuhl, J.F.; Kistler, K.D.; Begley, J.S.; Boulanger, J. 2006.** Demography of northern flying squirrels informs ecosystem management of western interior forests. Ecological Applications. 16: 584–600.

**Linhart, Y.; Mitton, J.; Sturgeon, K.; Davis, M. 1981.** Genetic-variation in space and time in a population of ponderosa pine. Heredity. 46: 407–426.

**Long, J.N.; Smith, F.W. 2000.** Restructuring the forest, goshawks and restoration of southwestern ponderosa pine. Journal of Forestry. 98: 25–30.

**Loosmore, N.B.; Ford, E.D. 2006.** Statistical inference using the G or K point pattern spatial statistics. Ecology. 87: 1925–1931.

**Lutz, J.A.; Larson, A.J.; Swanson, M.E.; Freund J.A. 2012.** Ecological importance of large-diameter trees in a temperate mixed-conifer forest. PloS one. 7: e36131.

**Lydersen, J.M.; North, M.P.; Knapp, E.E.; Collins, B.M. 2013.** Quantifying spatial patterns of tree groups and gaps in mixed-conifer forests: reference conditions and long-term changes following fire suppression and logging. Forest Ecology and Management. 304: 370–382.

**McCune, B.; Grace, J. 2002.** Analysis of ecological communities. Gleneden Beach, OR: MjM Software Design.

**Merschel, A.; Spies, T.A.; Heyerdahl, E.K. 2014.** Mixed-conifer forests of central Oregon: effects of logging and fire exclusion vary with environment. Ecological Applications. 24: 1670–1688.

**Moore, M.M.; Casey, C.A.; Bakker, J.D.; Springer, J.D.; Fule, P.Z.; Covington, W.W.; Laughlin, D.C. 2006.** Herbaceous vegetation responses (1992-2004) to restoration treatments in a ponderosa pine forest. Rangeland Ecology and Management. 59: 135–144.

**Moore, M.M.; Covington, W.W.; Fule, P.Z. 1999.** Reference conditions and ecological restoration: a southwestern ponderosa pine perspective. Ecological Applications. 9: 1266–1277.

**Naficy, C.; Sala, A.; Keeling, E.G.; Graham, J.; DeLuca, T.H. 2010.** Interactive effects of historical logging and fire exclusion on ponderosa pine forest structure in the northern Rockies. Ecological Applications. 20: 1851–1864.

**Nathanson, J.; Lanzafama, M.T.; Kissam, P. 2006.** Surveying fundamentals and practices. Upper Saddle River, NJ: Prentice Hall.

**North, M.; Innes, J.; Zald, H. 2007.** Comparison of thinning and prescribed fire restoration treatments to Sierran mixed-conifer historic conditions. Canadian Journal of Forest Research. 37: 331–342.

**North, M.; Oakley, B.; Fiegener, R.; Gray, A.; Barbour, M. 2005.** Influence of light and soil moisture on Sierran mixed-conifer understory communities. Plant Ecology. 177: 13–24.

**North, M.P.; Sherlock, J.W. 2012.** Marking and assessing forest heterogeneity. In: North, M.P., ed. Managing Sierra Nevada forests. Gen. Tech. Rep. PSW-GTR-237. Albany, CA: U.S. Department of Agriculture, Forest Service, Pacific Southwest Research Station: 95–105

**North, M.P.; Stine, P.; O'Hara, K.L.; Zielinski, W.J.; Stephens, S. 2009.** An ecosystem management strategy for Sierran mixed-conifer forests. Gen. Tech. Rep. PSW-GTR-220. Albany, CA: U.S. Department of Agriculture, Forest Service, Pacific Southwest Research Station. 49 p.

**Noss, R.F.; Beier, P.; Covington, W.W.; Grumbine, R.E.; Lindenmayer, D.B.; Prather, J.W.; Schmiegelow, F.; Sisk, T.D.; Vosick, D.J. 2006.** Recommendations for integrating restoration ecology and conservation biology in ponderosa pine forests of the southwestern United States. Restoration Ecology. 14: 4–10.

**Parisien, M.A.; Miller, C.; Ager, A.A.; Finney, M.A. 2010.** Use of artificial landscapes to isolate controls on burn probability. Landscape Ecology. 25: 79–93.

**Perry, D.A.; Hessburg, P.F.; Skinner, C.N.; Spies, T.A.; Stephens, S.L.; Taylor, A.H.; Franklin, J.F.; McComb, B.; Riegel, G.M. 2011.** The ecology of mixed severity fire regimes in Washington, Oregon, and Northern California. Forest Ecology and Management. 262: 703–717.

**Perry, G.L.W.; Miller, B.P.; Enright, N.J. 2006.** A comparison of methods for the statistical analysis of spatial point patterns in plant ecology. Plant Ecology. 187: 59–82.

**Peterson, D.L.; Halofsky, J.S.; Johnson, M.C. 2011.** Managing and adapting to changing fire regimes in a warmer climate. In: McKenzie, D.; Miller, C.; Falk, D.A., eds. The landscape ecology of fire. New York: Springer: 249–268

**Peterson, D.L.; Johnson, M.C. 2007.** Science-based strategic planning for hazardous fuel treatment. Fire Management Today. 67: 13–17.

**Peterson, D.L.; Johnson, M.C.; McKenzie, D.; Agee, J.K.; Jain, T.B.; Reinhardt, E.D. 2005.** Forest structure and fire hazard in dry forests of the Western United States. Gen. Tech. Rep. PNW-GTR-628. Portland, OR: U.S. Department of Agriculture, Forest Service, Pacific Northwest Research Station. 30 p.

**Pimont, F.; Dupuy, J.L.; Linn, R.R.; Dupont, S. 2011**. Impacts of tree canopy structure on wind flows and fire propagation simulated with FIRETEC. Annals of Forest Science. 68: 523–530.

**Plotkin, J.B.; Chave, J.M.; Ashton, P.S. 2002.** Cluster analysis of spatial patterns in Malaysian tree species. American Naturalist. 160: 629–644.

**Powell, D.C. 1999.** Suggested stocking levels for forest stands in northeastern Oregon and southeastern Washington: an implementation guide for the Umatilla National Forest. F14-SO-TP-03-99. [Portland, OR]: U.S. Department of Agriculture, Forest Service, Pacific Northwest Region, Umatilla National Forest. 89 p.

**Powell, D.C. 2010.** Estimating crown fire susceptibility for project planning. Fire Management Today. 70: 8–15.

**Powell, D.C. 2014.** Active management of dry forests in the Blue Mountains: silvicultural considerations. Umatilla National Forest White Paper F14- SO-WP-Silv-4. [Portland, OR]: U.S. Department of Agriculture, Forest Service, Pacific Northwest Region. 436 p.

**Powell, D.C.; Johnson, C.G.; Crowe, E.A.; Wells, A.; Swanson, D.K. 2007.** Potential vegetation hierarchy for the Blue Mountains section of northeastern Oregon, southeastern Washington, and west-central Idaho. Gen. Tech. Rep. PNW-GTR-709. Portland, OR: U.S. Department of Agriculture, Forest Service, Pacific Northwest Research Station. 87 p.

**Reynolds, R.T.; Meador, A.J.S.; Youtz, J.A.; Nicolet, T.M.; Matonis, S.; Jackson, P.L.; DeLorenzo, D.G.; Graves, A.D. 2013.** Restoring composition and structure in southwestern frequent-fire forests: a science-based framework for improving ecosystem resiliency. Gen. Tech. Rep. RMRS-GTR-310. Fort Collins, CO: U.S. Department of Agriculture, Forest Service, Rocky Mountain Research Station. 76 p.

**Ripley, B.D. 1988.** Statistical inference for spatial processes. Cambridge, United Kingdom: Cambridge University Press. 148 p.

**Roberts, S.L.; van Wagtendonk, J.W.; Miles, A.K.; Kelt, D.A.; Lutz, J.A. 2008.** Modeling the effects of fire severity and spatial complexity on small mammals in Yosemite National Park, California. Fire Ecology. 4(2): 83–104. Fire Ecology Special Issue. 4: 84.

**Rummel, R.S. 1951.** Some effects of livestock grazing on ponderosa pine forest and range in central Washington. Ecology. 32: 594–607.

**Sánchez Meador, A.J.; Moore, M.M.; Bakker, J.D.; Parysow, P.F. 2009.** 108 years of change in spatial pattern following selective harvest of a *Pinus ponderosa* stand in northern Arizona, USA. Journal of Vegetation Science. 20: 79–90.

**Sánchez Meador, A.J.; Parysow, P.F.; Moore, M.M. 2011.** A new method for delineating tree patches and assessing spatial reference conditions of ponderosa pine forests in northern Arizona. Restoration Ecology. 19: 490–499.

**Schneider, E.E.; Sánchez Meador, A.J.; Covington, W.W. 2015.** Reference conditions and historical changes in an unharvested ponderosa pine stand on sedimentary soil. Restoration Ecology. 24(2): 212–221.

**Seidl, R.; Spies, T.A.; Peterson, D.L.; Stephens, S.L.; Hicke, J.A. 2015.** Searching for resilience: addressing the impacts of changing disturbance regimes on forest ecosystem services. Journal of Applied Ecology. 53(1): 120-129.

**Simard, S.W.; Beiler, K.J.; Bingham, M.A.; Deslippe, J.R.; Philip, L.J.; Teste, F.P. 2012.** Mycorrhizal networks: mechanisms, ecology and modelling. Fungal Biology Reviews. 26: 39–60.

**Spada, B. 1960.** Estimating past diameters of several species in the ponderosa pine subregion of Oregon and Washington. Res. Note RN-181. Portland, OR: U.S. Department of Agriculture, Forest Service, Pacific Northwest Forest and Range Experiment Station. 4 p.

**Spies, T.A.; Giesen, T.W.; Swanson, F.J.; Franklin, J.F.; Lach, D.; Johnson, K.N. 2010.** Climate change adaptation strategies for federal forests of the Pacific Northwest, USA: ecological, policy, and socio-economic perspectives. Landscape Ecology. 25: 1185–1199.

**Stephens, S.L.; Fry, D.L.; Franco-Vizcaino, E. 2008.** Wildfire and spatial patterns in forests in northwestern Mexico: the United States wishes it had similar fire problems. Ecology and Society. 13(2): 10.

**Stephens, S.L.; Millar, C.I.; Collins, B.M. 2010.** Operational approaches to managing forests of the future in Mediterranean regions within a context of changing climates. Environmental Research Letters. 5: 1–9.

**Stine, P.; Hessburg, P.F.; Spies, T.A.; Kramer, M.G.; Fettig, C.J.; Hansen, A.J.; Lehmkuhl, J.F.; O'Hara, K.L.; Polivka, K.; Singleton, P.H.; Charnley, S.; Merschel, A.; White R. 2014.** The ecology and management of moist mixed-conifer forests in eastern Oregon and Washington: a synthesis of the relevant biophysical science and implications for future land management. Gen. Tech. Rep. PNW-GTR-897. Portland, OR: U.S. Department of Agriculture, Forest Service, Pacific Northwest Research Station. 254 p.

**Swetnam, T.W.; Allen, C.D.; Betancourt, J.L. 1999.** Applied historical ecology: using the past to manage for the future. Ecological Applications. 9: 1189–1206.

**Taylor, A.H. 2004.** Identifying forest reference conditions on early cut-over lands, Lake Tahoe Basin, USA. Ecological Applications. 14: 1903–1920.

**Taylor, A.H.; Skinner, C.N. 2003.** Spatial patterns and controls on historical fire regimes and forest structure in the Klamath Mountains. Ecological Applications. 13: 704–719.

**Thaxton, J.M.; Platt, W.J. 2006.** Small-scale fuel variation alters fire intensity and shrub abundance in a pine savanna. Ecology. 87: 1331–1337.

**U.S. Department of Agriculture, Forest Service [USDA FS]. 2012.** The Okanogan-Wenatchee National Forest Restoration Strategy: adaptive ecosystem management to restore landscape resiliency. Okanogan-Wenatchee National Forest. [Portland, OR]. 118 p.

**U.S. Department of Agriculture, Forest Service [USDA FS]. 2014.** Draft environmental impact statement: proposed revised land management for the Malheur, Umatilla, and Wallowa-Whitman National Forests. [Portland, OR]. 3 vol.

**Van Pelt, R.V. 2008.** Identifying old trees and forests in eastern Washington. Olympia, WA: Washington Department of Natural Resources. 166 p.

**Virah-Sawmy, M.; Gillson, L.; Willis, K.J. 2009.** How does spatial heterogeneity influence resilience to climatic changes? Ecological dynamics in southeast Madagascar. Ecological Monographs. 79: 557–574.

**Weaver, H. 1961.** Ecological changes in the ponderosa pine forest of cedar valley in southern Washington. Ecology. 42: 416–420.

**White, A.S. 1985.** Presettlement regeneration patterns in a southwestern ponderosa pine stand. Ecology. 66: 589–594.

**Williams, M.A.; Baker, W.L. 2012.** Spatially extensive reconstructions show variable-severity fire and heterogeneous structure in historical Western United States dry forests. Global Ecology and Biogeography. 21: 1042–1052.

**York, R.A.; Heald, R.C.; Battles, J.J.; York, J.D. 2004.** Group selection management in conifer forests: relationships between opening size and tree growth. Canadian Journal of Forest Research. 34: 630–641.

**Youngblood, A.; Max, T.; Coe, K. 2004.** Stand structure in eastside old-growth ponderosa pine forests of Oregon and northern California. Forest Ecology and Management. 199: 191–217.

# Appendix 1: Methods to Reconstruct Diameters in 1890

We followed methods used by North et al. (2007) and Bakker (2005) to reconstruct outside bark diameter at breast height (d.b.h.) in 1890 for all live trees on each plot. A regression model was built using the live measure trees to predict total inside bark basal area increment from 1890 to 2013, which was then used to estimate 1890 d.b.h. for all live trees. Predictor variables that were tested to develop the best model included 2013 inside bark d.b.h., species, potential vegetation series, location, vigor class, age class, and a neighborhood competition index using 2013 diameters from Contreras et al. (2011). Numeric values for Van Pelt rating and vigor rating were used vs. categorical values. This model was then used to derive 1890 inside bark d.b.h. for the rest of the live trees by subtracting the predicted basal area increment from 1890 to 2013 from the 2013 inside bark basal area (derived from field-measured outside bark d.b.h.). Inside bark d.b.h. in 1890 was then converted to outside bark d.b.h. All conversions between inside and outside bark diameters were done using bark thickness equations from Spada (1960).

For snags and downed logs that were believed to be alive in 1890, diameter in 1890 was established using the following approach. First, diameters taken at stump height were converted to breast height diameters using regression equations developed from the live measure trees and from Bones (1960). Year of death was then estimated from species and decay class using equations from Everett et al. (1999) and rounded to the nearest 5$^{th}$ year. Regression models from the live measure trees were then developed to predict basal area increment from 1890 to year of death. These models were then used to "grow" all structures back to 1890.

Model form, predictors, and parameters are provided below for regression models used to reconstruct 1890 d.b.h. for live trees that were not cored. Models were based on 940 cores from live trees: *Pinus ponderosa* (PIPO) 667 trees, *Abies grandis* (ABGR) 176 trees, *Pseudotsuga menziesii* (PSME) 71 trees, *Larix occidentalis* (LAOC) 26 trees. Separate models for snags and downed logs were created owing to the fact that ratings for vigor and Van Pelt age could not be made for dead structures.

## Live Tree Model

Model form:

$$BAE = e^{a + b \times ln(DIA) + c \times NI + d \times VPR + h \times VIG}$$

**Parameters and $R^2$ (all parameters were significant: $p < 0.05$):**

| a | b | c | d | h | $r^2$ |
|---|---|---|---|---|---|
| 2.2122 | 1.4801 | -0.0068 | -0.2913 | -0.1289 | 0.7953 |

Predictor variables:

- BAI: Basal area increment in cubic centimeters from 2013 to 1890.
- *DIA* is inside bark d.b.h. in 2013.
- VPR is the Van Pelt (2008) age rating as a continuous variable:
  - 1: young (<80 years); 2: mature (80 to 150); 3: old (15 to 250); 4: very old (>250).
- VIG: is Van Pelt (2008) vigor rating as a continuous variable:
  - 1: A (very high vigor); 2: B (high vigor); 3: C (moderate vigor); 4: D (low vigor).
- NI is a neighborhood index from Contreras et al. (2011) that measures the competitive environment of the tree using an 11-m radius. Values were calculated using 2013 diameters of neighboring trees. Values for dead neighbors were weighted by the number of years they were alive from 1890 to 2013 (e.g., the index value for a neighbor that died in 1980 was weighted by a value of (1980 to 1890)/123 = 0.73. The index is calculated using the following formula:

$$\sum_{i=1}^{n}(d_i/d) \times \text{arctan}\ (d_i/\text{dist}_i)$$

Where

*d* is the diameter of the subject tree.

*n* is the number of trees within a 8-m radius of the subject tree.

$d_i$ is the diameters of $i^{th}$ neighbor.

$\text{dist}_i$ is the distance from the $i^{th}$ neighbor to the subject tree.

Diameter in 2013 (DIA) was the most important predictor, followed by NI, VPR, and VIG. Potential vegetation series, tree species, and plot location (e.g., Dugout Research Natural Area [RNA] vs. Canyon Creek RNA), were not significant predictors.

## Dead Structure Model

### Model form:

$$BAE = e^{\mathrm{a} + \mathrm{b} \times \ln(DIA) + \mathrm{c} \times NI + d \times PVGF + h \times PVPP}$$

**Parameters (all parameters were significant: $p < 0.05$):**

| a | b | c | d | h | r2 | Year of death |
|---|---|---|---|---|---|---|
| 2.7065 | 1.1161 | -0.0153 | 0.1676 | -0.0776 | 0.7182 | 2010 |
| 2.7711 | 1.0950 | -0.0160 | 0.1611 | -0.0825 | 0.7160 | 2005 |
| 2.8311 | 1.0749 | -0.0167 | 0.1570 | -0.0880 | 0.7145 | 2000 |
| 2.8995 | 1.0507 | -0.0175 | 0.1570 | -0.0907 | 0.7118 | 1995 |
| 2.9456 | 1.0334 | -0.0181 | 0.1577 | -0.0940 | 0.7090 | 1990 |
| 3.0133 | 1.0092 | -0.0190 | 0.1604 | -0.0971 | 0.7053 | 1985 |
| 3.0817 | 0.9824 | -0.0200 | 0.1587 | -0.1038 | 0.7039 | 1980 |
| 3.1276 | 0.9618 | -0.0208 | 0.1548 | -0.1088 | 0.7029 | 1975 |
| 3.1592 | 0.9439 | -0.0216 | 0.1515 | -0.1107 | 0.7020 | 1970 |
| 3.1819 | 0.9263 | -0.0223 | 0.1476 | -0.1151 | 0.7001 | 1965 |
| 3.2024 | 0.9077 | -0.0230 | 0.1432 | -0.1183 | 0.6971 | 1960 |
| 3.2225 | 0.8866 | -0.0239 | 0.1366 | -0.1208 | 0.6942 | 1955 |
| 3.2354 | 0.8645 | -0.0247 | 0.1275 | -0.1213 | 0.6917 | 1950 |
| 3.2270 | 0.8450 | -0.0255 | 0.1160 | -0.1270 | 0.6914 | 1945 |
| 3.1580 | 0.8386 | -0.0256 | 0.0977 | -0.1298 | 0.6926 | 1940 |
| 3.0893 | 0.8365 | -0.0256 | 0.0796 | -0.1315 | 0.6946 | 1935 |
| 3.0248 | 0.8304 | -0.0255 | 0.0683 | -0.1277 | 0.6931 | 1930 |
| 2.9792 | 0.8147 | -0.0258 | 0.0629 | -0.1207 | 0.6893 | 1925 |
| 2.8774 | 0.8081 | -0.0263 | 0.0654 | -0.1177 | 0.6871 | 1920 |
| 2.2218 | 0.9334 | -0.0219 | 0.0948 | -0.1168 | 0.6947 | 1915 |
| 2.2466 | 0.8705 | -0.0228 | 0.0355 | -0.1387 | 0.6906 | 1910 |
| 1.7821 | 0.9157 | -0.0191 | 0.0151 | -0.1332 | 0.6824 | 1905 |
| 2.1247 | 0.7193 | -0.0254 | -0.0358 | -0.1407 | 0.6642 | 1900 |
| 1.5301 | 0.6982 | -0.0256 | -0.0428 | -0.1667 | 0.6593 | 1895 |

### Variables:

- BAI: Basal area increment in cubic centimeters from year of death to 1890.
- *DIA* is inside bark diameter as derived from field measurement
    - NI is a neighborhood index (see explanation above)
    - PV: Potential vegetation series as a categorical variable:
      - PVGF: 1 value for plots in grand fir series. 0 values for other series.
      - PVPP: 1 value for plots in ponderosa pine series. 0 values for other series.

## Bark thickness equation to derive diameter outside bark (DOB) from diameter inside bark (DIB) at breast height:

Equation form:

$$DOB = a = b \times DIB$$

**Parameters:**

| Species | a | b |
|---|---|---|
| PSME | 0.079782 | 1.133273 |
| PIPO | 0.616246 | 1.108156 |
| ABGR | 0 | 1.10673 |
| Other | 0.079782 | 1.133273 |

This equation is used in reverse to derive diameter inside bark from diameter outside bark. Equations are from Spada (1960)

# Appendix 2: Crown Radius Models

The following models were used to derive crown radii from diameter at breast height (d.b.h.) to project crowns and estimate canopy cover. Data are from U.S. Forest Service Current Vegetation Survey plots from the Blue Mountains and eastern Washington.

## Model form:

$$CR = e^{a+b\times \ln(DBH)}$$

**Model information and parameters:**

| Species | a | b | r2 | No. of trees |
|---|---|---|---|---|
| ABGR | -0.8822 | 0.5261 | 0.79 | 11,732 |
| PIPO | -1.4210 | 0.6462 | 0.82 | 9,900 |
| PSME | -0.9025 | 0.5420 | 0.83 | 43,113 |
| LAOC | -1.3965 | 0.6322 | 0.77 | 8,991 |

Variables

- CR: Crown radius in meters
- DBH: diameter at breast height in cubic centimeters.

# Appendix 3: Clump Size Proportions for All Trees >10 cm

**Table 3A.1—Clump size distributions for Malheur National Forest reference plots ordered by the proportion of trees that are individuals (clump size = 1)**

| | | | Proportion of trees | | | | | Proportion of basal area | | | | |
|---|---|---|---|---|---|---|---|---|---|---|---|---|
| | | | Clump size (No. of trees) | | | | | Clump size (No. of trees) | | | | |
| Plot | Series[b] | Clumping level | 1 | 2-4 | 5-9 | 10-15 | 16-30+ | 1 | 2-4 | 5-9 | 10-15 | 16-30+ |
| G3 | ABGR | Low | 0.41 | 0.45 | 0.08 | 0.07 | 0.00 | 0.66 | 0.28 | 0.03 | 0.03 | 0.00 |
| P1 | PIPO | Low | 0.38 | 0.48 | 0.11 | 0.04 | 0.00 | 0.45 | 0.47 | 0.06 | 0.01 | 0.00 |
| D2 | PSME | Low | 0.35 | 0.36 | 0.19 | 0.09 | 0.00 | 0.52 | 0.32 | 0.12 | 0.04 | 0.00 |
| D1 | PSME | Low | 0.36 | 0.43 | 0.11 | 0.11 | 0.00 | 0.49 | 0.39 | 0.06 | 0.06 | 0.00 |
| D4 | PSME | Low | 0.31 | 0.42 | 0.20 | 0.07 | 0.00 | 0.42 | 0.39 | 0.17 | 0.02 | 0.00 |
| D3 | PSME | Low | 0.32 | 0.37 | 0.31 | 0.00 | 0.00 | 0.35 | 0.40 | 0.25 | 0.00 | 0.00 |
| D5 | PSME | Low | 0.33 | 0.56 | 0.08 | 0.03 | 0.00 | 0.45 | 0.48 | 0.07 | 0.00 | 0.00 |
| P5 | PIPO | Mod | 0.20 | 0.38 | 0.38 | 0.05 | 0.00 | 0.27 | 0.37 | 0.31 | 0.05 | 0.00 |
| P4 | PIPO | Mod | 0.21 | 0.39 | 0.28 | 0.11 | 0.00 | 0.26 | 0.38 | 0.28 | 0.08 | 0.00 |
| P2 | PIPO | Mod | 0.20 | 0.27 | 0.23 | 0.20 | 0.11 | 0.31 | 0.30 | 0.19 | 0.11 | 0.09 |
| P3 | PIPO | Mod | 0.16 | 0.37 | 0.34 | 0.07 | 0.05 | 0.21 | 0.40 | 0.32 | 0.04 | 0.03 |
| G4 | ABGR | High | 0.15 | 0.33 | 0.24 | 0.10 | 0.17 | 0.24 | 0.32 | 0.20 | 0.09 | 0.14 |
| G1 | ABGR | High | 0.11 | 0.27 | 0.26 | 0.10 | 0.24 | 0.17 | 0.31 | 0.23 | 0.07 | 0.22 |
| G2 | ABGR | High | 0.07 | 0.16 | 0.18 | 0.18 | 0.41 | 0.11 | 0.19 | 0.19 | 0.18 | 0.33 |

[a] The clump size distribution is the proportion of trees or basal area by clump size. Clump size is the number of trees in a clump. Clumps are defined as trees within at least 6.1 ha of another tree in the clump. Plots are grouped by plant series and clumping level.
[b]ABGR = *Abies grandis*, PIPO = *Pinus ponderosa*, PSME = *Pseudotsuga menziesii*.

**Table 3A.2—Clump size distributions from table 3A.1 summarized by clumping level and plant association group[a]**

| | Proportion of trees | | | | | Proportion of basal area | | | | |
|---|---|---|---|---|---|---|---|---|---|---|
| | Clump size (No. of trees) | | | | | Clump size (No. of trees) | | | | |
| Clumping level | 1 | 2-4 | 5-9 | 10-15 | 16-30+ | 1 | 2-4 | 5-9 | 10-15 | 16-30+ |
| Low | 0.35 | 0.44 | 0.15 | 0.06 | 0.00 | 0.48 | 0.39 | 0.11 | 0.02 | 0.00 |
| Mod | 0.19 | 0.35 | 0.31 | 0.11 | 0.04 | 0.26 | 0.36 | 0.28 | 0.07 | 0.03 |
| High | 0.11 | 0.25 | 0.23 | 0.13 | 0.28 | 0.17 | 0.27 | 0.21 | 0.12 | 0.23 |
| **Series** | | | | | | | | | | |
| PIPO | 0.23 | 0.38 | 0.27 | 0.09 | 0.03 | 0.30 | 0.38 | 0.23 | 0.06 | 0.02 |
| PSME | 0.33 | 0.43 | 0.18 | 0.06 | 0.00 | 0.45 | 0.40 | 0.13 | 0.02 | 0.00 |
| ABGR | 0.19 | 0.30 | 0.19 | 0.11 | 0.21 | 0.30 | 0.27 | 0.16 | 0.09 | 0.17 |

[a] Values are averages for that group.
[b] ABGR = *Abies grandis*, PIPO = *Pinus ponderosa*, PSME = *Pseudotsuga menziesii*.

# Appendix 4: Distribution of Basal Area

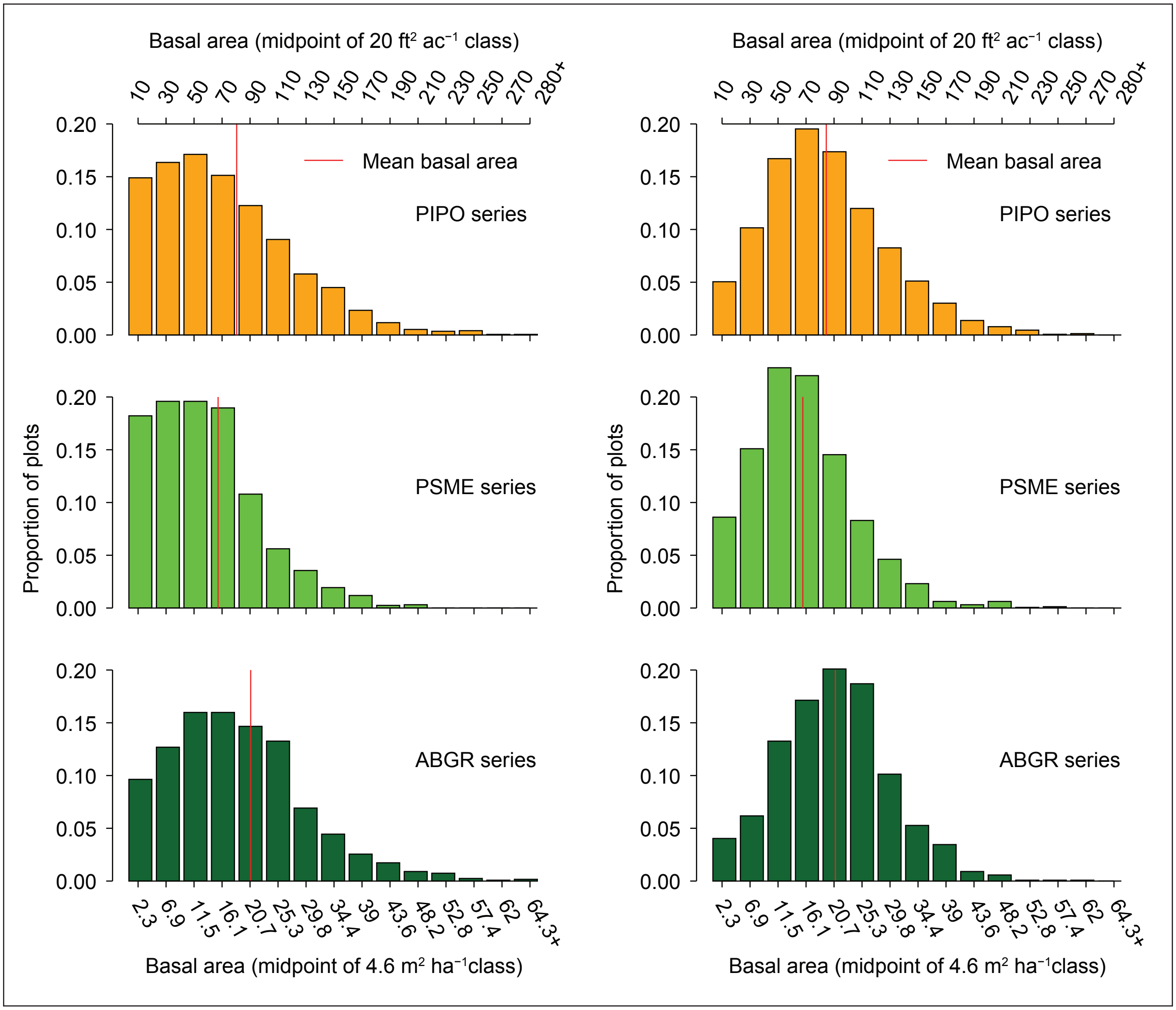


Figure 4A.1—Frequency distribution of historical basal area pooled by potential vegetation series. Left panel displays basal area calculated using variable radius plots with a 4.6-basal area factor (20 English basal area factor) on a 20-m grid across each of the 14 stem map reference plots. The right panel displays results from 0.08-ha fixed area plots. See figure 3.5 for results from 0.04-ha fixed area plots. Orange bars show the pooled results for the five ponderosa pine plots, green bars show results for the five Douglas-fir plots, and the dark green bars show results for the four grand-fir plots. Red lines are means for the respective series. All plots were simulated.

# Appendix 5: Pair Correlation Plots for 14 Reference Plots

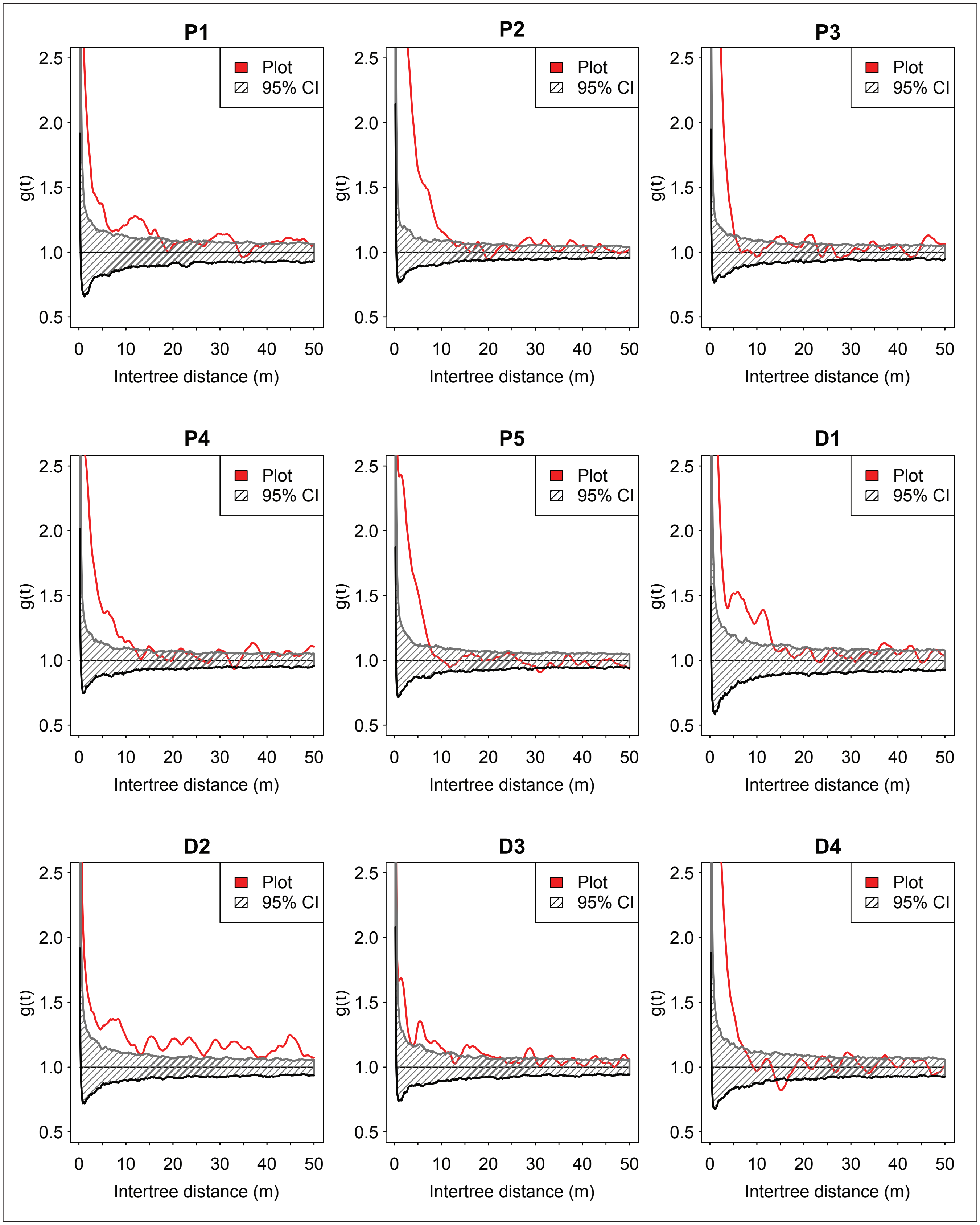

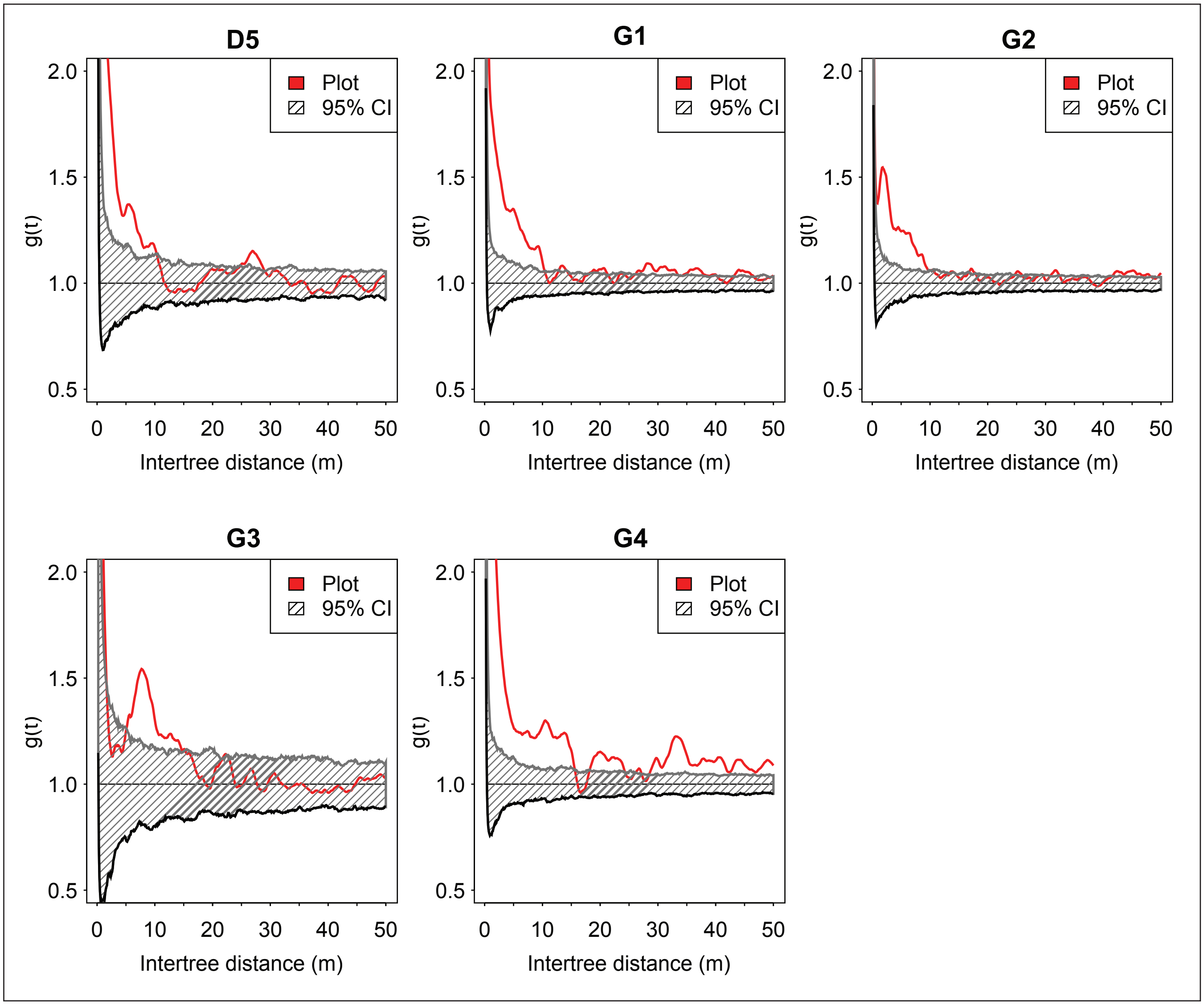


Figure A5.1—Plots of pair correlation function, g(*t*), for 14 reference plots. Red lines display the g(*t*) values from 0.1 to 30 m intertree distance for each plot. The hatched envelopes are the 95 percent confidence intervals (CI) from 1,000 simulated random patterns (complete spatial randomness [CSR]). Tree patterns are clustered when the red lines above the 95 percent CSR confidence interval, random when inside the envelope, and uniform when below the envelope.

**Pacific Northwest Research Station**

| | |
|---|---|
| **Website** | http://www.fs.fed.us/pnw/ |
| **Telephone** | (503) 808–2592 |
| **Publication requests** | (503) 808–2138 |
| **FAX** | (503) 808–2130 |
| **E-mail** | pnw_pnwpubs@fs.fed.us |
| **Mailing address** | Publications Distribution<br>Pacific Northwest Research Station<br>P.O. Box 3890<br>Portland, OR 97208–3890 |

U.S. Department of Agriculture
Pacific Northwest Research Station
1220 SW 3rd Ave., Suite 1400
P.O. Box 3890
Portland, OR 97208–3890